The functional role of dystrophin in the heart: implications for inherited and non-inherited heart disease

by

Matthew Scott Barnabei

A dissertation submitted in partial fulfillment
of the requirements for the degree of
Doctor of Philosophy
(Molecular and Integrative Physiology)
in The University of Michigan
2012

Doctoral Committee:

Professor Joseph M. Metzger, Co-Chair
Associate Professor Daniel E. Michele, Co-Chair
Professor Linda C. Samuelson
Associate Professor Mark W. Russell

Acknowledgements

Pursuing graduate studies has been a long and challenging road. If I've accomplished anything during this time, it is only because I've had the good fortune to be surrounded by great people who deserve my thanks. I would first like to thank my mentor, Dr. Joseph Metzger, for continuous support of my scientific development throughout my time in the Metzger lab. I would also like to thank each member of my committee, whose thoughtful advice and feedback were key to my progress. I'd especially like to thank Dr. Dan Michele, whose friendship and extensive knowledge of the muscular dystrophies continues to be invaluable to me. My sincerest gratitude goes out to the members, past and present, of the Metzger lab, whose friendship and scientific expertise was critical to me during my graduate career. Finally, I'd like to thank my family and friends for their unwavering friendship, support, and love.

Table of Contents

List of Figures

List of Tables

Chapter 1

Introduction

Overview

The central focus of this thesis is the pathogenesis of cardiomyopathy caused by loss of dystrophin, and how this may be a unifying mechanism for cardiac dysfunction in inherited and non-inherited heart disease. Dystrophin is most notable for being identified as the cause of Duchenne muscular dystrophy (DMD), a lethal disease of muscle wasting first described in the mid-1800's [1,2,3,4]. Historically, the majority of basic and clinical research on DMD has been focused on skeletal muscle. However, DMD also causes a significant cardiomyopathy which causes ~20% of deaths in DMD [5,6]. More recently, dystrophin has also been implicated in non-dystrophic heart failure due to a variety of causes (Table 1-1). The purpose of this chapter is to introduce and describe dystrophin, the inherited and non-inherited diseases it is associated with, and to point out gaps in our knowledge of dystrophin's physiological function which are addressed in the later chapters of this thesis.

Clinical description of Duchenne muscular dystrophy

DMD is the most common inherited muscular dystrophy, occurring in approximately 1 in 3500 males [7]. DMD affects patients very early in life, presenting as general weakness within the first few years, particularly within the lower limbs and postural muscles. Young patients with DMD will typically display a characteristic method of righting themselves from a supine position by using their limb muscles to bring the torso to an upright position. This behavior, called Gowers' sign, was first described by William Richard Gowers in 1865 [8]. In the modern clinical setting, a diagnosis of DMD is also accompanied by muscle biopsy and/or genetic testing to confirm lack of dystrophin protein and the presence of a mutation in dystrophin, respectively [9]. Affected muscles of DMD patients also show enlargement of certain muscle groups, particularly in the calves, despite muscle weakness [2,3,4]. Microscopic analysis of muscles from DMD patients reveals that this enlargement is not hypertrophy, but is due to massive replacement of muscle with fat and fibrotic tissue, a pseudohypertrophy [3]. The presence in the serum of cytoplasmic muscle enzymes such as muscle creatine kinase, a marker of muscle damage, is also a hallmark of DMD [10,11,12]. In the years following initial diagnosis, DMD patients experience progressive declines in strength and mobility accompanied by joint contractures [13,14,15]. Patients typically lose the ability to ambulate at approximately 10 years of age [16]. Death typically occurs in the second decade of life, the most common cause of which is respiratory failure brought on by severe wasting of the diaphragm [6,17,18].

In addition to skeletal muscle disease, DMD patients also have a pronounced dystrophic cardiomyopathy, which has been noted in DMD patients since the very first descriptions of the disease by Conte and Gioia [1]. Much like skeletal muscle, cardiac involvement is progressive in DMD, but generally proceeds at a slower rate when compared with skeletal muscle [19]. Subclinical cardiomyopathy is nearly universal in DMD patients over 6 years of age [19]. Specifically, diastolic dysfunction, tachycardia and ECG abnormalities, most commonly prominent R waves in the precordial leads, are common in the early (ambulatory) stage of the disease [20,21,22,23]. Subsequent study of autopsy specimens from DMD patients has linked these ECG defects with dystrophic replacement of the posterobasal portion of the left ventricle with fibrotic tissue, similar to the processes occurring in skeletal muscle [21]. As disease progresses, DMD patients develop clinical cardiomyopathy, which is in most cases a dilated cardiomyopathy [5,19]. The incidence of dilated cardiomyopathy increases dramatically after age 10, having a prevalence of approximately 25% between ages 10-14, 50% between ages 14 and 18, and over 70% in patients over 18 years of age [19]. This cardiomyopathy often develops into frank heart failure and accounts for 20% of deaths in DMD patients [5,6]. Interestingly, there is a disconnect between the number of patients with diagnostically determined DCM and those with symptomatic cardiac involvement. Less than 50% of DMD patients with DCM report having any symptoms of cardiac involvement [19]. This surprising observation is likely due to the reduced sensitivity of wheelchair-bound

DMD patients to exercise intolerance brought on by severe skeletal muscle wasting which masks the significance of cardiomyopathy in DMD.

Identification of the DMD gene

Despite the careful and discriminating characterization of the clinical presentation of DMD dating back through the mid-19th century [1,2,3,24], the genetic foundation of this debilitating disease remained unknown through most of the 20th century. The clinical manifestations of DMD did, however, provide some clues about its genetic underpinnings. The documentation of families with DMD clearly established it as a heritable disease [2,3]. Additionally, DMD affected males almost exclusively and was inherited maternally, suggesting an X-linked recessive mode of inheritance [1,2,3]. Also, the frequency of DMD is relatively high [7,24], suggesting that the DMD gene may be very large or perhaps prone to mutation. Armed with this knowledge and aided by advances in molecular genetics, the genetic cause of DMD began to emerge in the 1980's. Interestingly, some of the most important studies leading to the identification of the DMD gene focused on females. These cases are exceptionally rare, but in each case patients were found to have chromosomal translocations between the X chromosome and various other autosomes [25,26,27,28]. Specifically, these translocations all occurred on the short arm of the X chromosome at Xp21 [25,26,27,28]. A series of genetic linkage studies utilizing known DMD mutations identified a particular locus, DXS164, on the X chromosome [29,30,31,32,33]. A group led by Dr. Louis Kunkel then used probes generated from this locus to

screen a fetal muscle cDNA library and identified a large (14 kb) cDNA [34]. Sequence fragments of this cDNA were found to detect deletions in the DMD gene at a high rate in DMD patients, supporting its identity as the cDNA of the DMD gene [34]. Antibodies created by immunization of animals with peptides derived from this cDNA detected a ~400 kDa protein in muscle, which was not detected in DMD patients [35]. This provided strong evidence that the gene residing at the DXS164 locus was the DMD gene. Further characterization of the DMD gene showed it to be massive, spanning over 2 million base pairs, containing over 75 distinct exons and multiple independent promoters [36,37,38,39,40]. To this day, the DMD gene is the largest known gene in the human genome. There are numerous isoforms and splice variants of the DMD gene expressed in various tissues throughout the body (Figure 1-1) [38,41,42,43]. The dominant isoform expressed in striated muscle is a 427 kDa protein which was given the name dystrophin [35].

It should also be mentioned that mutations in the DMD gene also cause Becker muscular dystrophy (BMD) and X-linked dilated cardiomyopathy, allelic variants of DMD [44]. BMD is a mild form of muscular dystrophy compared with DMD, with patients maintaining ambulation through 15 years of age [13]. There is significant variation in the onset in severity of symptoms, with some BMD patients maintaining ambulation through the sixth decade [45]. The discrepancy in severity between DMD and BMD can, in general, be explained by the “reading frame rule”. In short, mutations which disrupt the reading frame and cause protein truncation will result in DMD [46,47]. Mutations which do not disrupt

dystrophin's reading frame, including deletions and insertions, which can be quite large, tend to cause BMD [45,46,47]. These are general rules, to which there are numerous exceptions including DMD-causing missense mutations and in-frame deletions that cause DMD. A more detailed discussion is included in this chapter under the heading, "Physiological role of dystrophin in striated muscle".

X-linked dilated cardiomyopathy is also caused by mutations in the dystrophin gene [48], but in this case significant cardiomyopathy is present with little to no wasting of skeletal muscle [49]. The onset of clinical cardiac involvement occurs at approximately 15-20 years of age and is followed by a precipitous decline in cardiac function and often death within one year of diagnosis [48,49]. Although the genetic mutations which cause X-linked dilated cardiomyopathy have been determined in numerous families, the mechanisms by which these mutations cause heart disease vary. Previous reports have documented X-linked dilated cardiomyopathy families in which dystrophin content from the heart is drastically reduced due to mutations which cause aberrant exon skipping [50,51], missense mutations [52], insertions within the 5' untranslated region of the DMD gene [53,54,55], and in-frame deletions [51,56,57]. In some cases dystrophin content is reduced specifically in the heart but in other cases normal levels of protein are detected in both skeletal and cardiac muscle. It is unclear why some mutations specifically affect expression of dystrophin in the heart. However, in some cases, it has been shown that mutations which prevent expression of the muscle isoform of dystrophin are compensated for by expression of the similar cortical and Purkinjie isoforms of dystrophin (Dp427c

and Dp427p, respectively) in skeletal muscle but not in cardiac muscle (Figure 1-1) [53,54,55]. The reasons for this lack of compensation in cardiac muscle is not fully understood but may involve dystrophin muscle enhancer-1, which resides downstream from dystrophin's muscle promoter [58]. This genetic element has been shown to enhance expression of the cortical and Purkinjie promoters in skeletal muscle, but not in the heart [59].

Biochemical and molecular characterization of dystrophin

Analysis of the primary amino acid sequence of dystrophin was first carried out by Dr. Louis Kunkel, whose research team described a 3685 amino acids protein that was predominantly hydrophilic and rod-shaped [60]. The predicted rod shaped structure of dystrophin has been verified by electron microscopy [61,62]. Structurally, the dystrophin protein is divided into 4 major domains: an N-terminal actin binding domain, a large central rod domain, a cysteine-rich domain, and a C-terminal domain (Figure 1-2a). The N-terminal 250 amino acids of dystrophin contain two anti-parallel calponin homology domains that show significant homology with the actin-binding domain of α-actinin [63,64]. Truncated recombinant proteins containing this N-terminal portion of dystrophin have been shown to bind actin, confirming dystrophin's actin binding activity [65,66,67,68]. The next ~3000 amino acids constitute the central rod domain of dystrophin, which contains 24 triple helical homologous repeats. These repeats have homology to α-actinin and spectrin, which contribute to dystrophin's rod-like structure. Additionally, before repeat 1 and after repeats 3,

19, and 24 are 4 hinge regions [69]. Numerous proline residues within these hinge regions disrupt the helical rod domain of dystrophin and promote flexibility within the protein [69]. Additionally, spectrin-like repeats 11-17 contain numerous basic residues which constitute a second actin binding domain and contributes significantly to the dystrophin's actin binding activity [68,70]. The next section of ~400 amino acids is known as the cysteine-rich domain, due to its relative abundance of cysteine residues compared to the rest of dystrophin [60]. This domain contains a WW motif, 2 EF hand motifs, and ZZ motif [60,71,72]. Finally, the most C-terminal ~300 amino acids are important for dystrophin's interaction with other proteins and will be discussed in detail below.

Dystrophin's place in muscle: subcellular localization and the dystrophin-glycoprotein complex

The identification of the DMD gene and creation of antibodies against the dystrophin protein allowed for the characterization of dystrophin's subcellular localization and provided clues to its physiological function. Dystrophin is localized to the periphery of striated muscle, specifically located on the cytoplasmic face of the sarcolemma [73,74,75,76,77,78,79]. Further studies reveal that when longitudinal sections of skeletal muscle fibers are visualized, dystrophin shows a striated pattern and colocalizes with the costameres, the subsarcolemmal protein assembly which links the sarcomeres with the sarcolemma [76,77,80]. In cardiac myocytes, dystrophin also appears to localize at the t-tubules [75]. This finding was particularly informative with regards to

dystrophin's acting binding function and suggested that dystrophin interacted with cytoplasmic actins (β or γ) rather than with sarcomeric α-cardiac or α-skeletal muscle actin. Experiments in peeled muscle fibers suggest that dystrophin interacts with γ-cytoplasmic actin in skeletal muscle [81]. Complimentary studies have yet to be carried out in cardiac myocytes.

Dystrophin's interaction with the sarcolemma remained somewhat of an enigma, especially given dystrophin's nature as a hydrophilic rod shaped protein [60]. The first clues into the nature of dystrophin's interaction with the sarcolemma were provided by a group led by Kevin Campbell, who showed that dystrophin could be detected in by wheat-germ agglutinin chromatography of digitonin-solubilized muscle extracts [82], suggesting that dystrophin was associated with a glycosylated integral membrane protein. Subsequent analysis showed that dystrophin was part of a large, oligomeric complex containing numerous glycoproteins [83,84]. Due to dystrophin's prominent role in its discovery and the numerous glycoproteins present, this complex was given the name dystrophin-glycoprotein complex, or DGC (Figure 1-2b) [83,84].

The DGC is composed of several membrane-spanning and membrane-associated proteins including the dystroglycans, sarcoglycans, dystrobrevins, the syntrophins, and sarcospan. The dystroglycans, α and β, are discreet proteins derived from a common gene via post-translational polypeptide cleavage [85,86,87]. β-dystroglycan is a transmembrane protein which binds to the C-terminal end of dystrophin [88,89,90]. Specifically, dystrophin interacts with β-dystroglycan via the WW, EF hand, and ZZ motifs in the cysteine-rich domain

[91,92,93]. α-dystroglycan is an extracellular protein that interacts with β-dystroglycan [85,86,87]. The core α-dystroglycan protein is 75 kDa but is highly glycosylated with the mature protein appearing at ~156 kDa by gel electrophoresis [85]. α-dystroglycan binds the extracellular matrix protein laminin, and proper glycosylation of α-dystroglycan is crucial for its laminin binding function [85,94,95]. Proper glycosylation of α-dystroglycan is mediated enzymatically by glycosyltransferases, mutations in which alter normal glycosylation, disrupt laminin binding, and cause several forms of so called glycosylation-deficient muscular dystrophy [94,96]. Collectively, the interactions of dystrophin and the dystroglycans with actin and laminin, respectively, form a mechanical linkage between the cytoskeleton and the extracellular matrix (Figure 1-2) [95].

In addition to dystrophin and the dystroglycans, the DGC also contains the sarcoglycan complex. In striated muscle, the sarcoglycan complex is composed of α, β, γ, and δ sarcoglycan [97]. The sarcoglycans are transmembrane proteins expressed from discreet genes [98,99,100,101,102]. The sarcoglycans do not directly participate in the mechanical tether formed by dystrophin and the dystroglycans, but clearly play an important role in striated muscle as evidenced by the limb-girdle muscular dystrophies (types 2C, 2D, 2E, and 2F) caused by mutations in these genes [98,103,104,105,106,107].

The transmembrane protein sarcospan is also a part of the DGC [108]. Sarcospan appears to be dispensable for muscle function since it has not been associated with any known diseases and knockout mice show no signs of

dystrophy [109,110]. However, transgenic overexpression of sarcospan ameliorates muscular dystrophy in dystrophin-deficient mice associated with increased expression of DGC proteins, suggesting a role in stabilizing the DGC [111].

In addition to dystrophin, the DGC also contains other cytoplasmic proteins, the dystrobrevins and syntrophins. The dystrobrevins share significant homology with coiled coil domains within dystrophin's C-terminus [112,113]. Dystrobrevins interact with dystrophin and its homolog utrophin through these homologous coiled coil domains [114]. In skeletal muscle, α-dystrobrevin-2 is the primary dystrobrevin isoform associated with the DGC, with α-dystrobrevin-1 associating primarily with utrophin at the neuromuscular junction [115,116]. Genetic ablation of α-dystrobrevin causes mild muscle wasting but, curiously, does not cause defects in muscle function [117,118]. In addition to dystrophin, dystrobrevin also interacts with the syntrophins. Syntrophins are cytoskeletal proteins which interact with dystrobrevin via a pleckstrin homology domain [119,120,121,122]. In skeletal muscle, the α1- and β1- isoforms interact with the DGC at the sarcolemma, whereas in cardiac muscle the β2 isoform is also found at the sarcolemma [116,123]. In addition to dystrobrevin, syntrophins also bind to homologous sequences in the C-terminal domain of dystrophin [116,120,124] and thus each DGC complex is associated with 2 syntrophin proteins. Syntrophins also contain a PDZ domain within the most N-terminal PH domain which recruits other proteins to the DGC including, nNOS, aquaporin-4, diacylglycerol kinase-ζ, and ion channels [125,126,127,128,129,130,131].

Genetic ablation of α1-syntrophin does not cause muscle defects, suggesting that it is not essential for muscle function [130].

Although not technically a part of the DGC, the dystrophin homolog utrophin plays an important role in the pathogenesis of DMD. Utrophin shares significant homology with dystrophin and has a similar 4 domain structure [132]. Utrophin binds cytoskeletal actin and β-dystroglycan as well, although with biochemically distinct modes of interaction [133,134,135]. Utrophin is highly expressed in developing muscle but largely restricted to the neuromuscular junction in adult muscle [136,137]. Expression of utrophin is enhanced in the absence of dystrophin in some models of DMD, being found at the sarcolemma in the niche typically occupied by dystrophin (see discussion on mdx mice below) [138,139,140]. These observations have led to the hypothesis that utrophin plays a role in DMD pathogenesis and may be a therapeutic candidate for gene delivery.

On the whole, the DGC is a multimeric, membrane spanning protein complex, the constituents of which can be biochemically co-purified and are expressed in stoichiometric ratios [83,84,141]. Biochemically, titration with the detergent n-octyl beta-D-glucoside further resolves the DGC into 3 subcomplexes: Dystrophin/dystrobrevin/syntrophins, the dystroglycans, and the sarcoglycans [142]. Aside from being a purely biochemical distinction, the interaction of proteins within these subcomplexes affect the stability of the DGC. For instance, loss of a sarcoglycan from the DGC typically causes a drastic reduction in the membrane expression of the other sarcoglycans while having a

much less dramatic effect on the other components of the DGC [101,103,105,143,144]. Dystrophin plays a crucial role in the stability of the DGC in skeletal muscle, the lack of which causes a dramatic reduction in all DGC components [145]. This is not the case in cardiac muscle, however, where DGC expression is largely unaffected by loss of dystrophin [146]. The reason for this discrepancy between skeletal and cardiac muscle is not known.

Physiological role of dystrophin in striated muscle

Mdx Mouse. Before discussing the function of dystrophin in striated muscle, it is first necessary to introduce the primary animal model used to carry out these physiological studies, the X chromosome-linked muscular dystrophy (mdx) mouse. The mdx mouse was identified in a screen for glycolytic enzyme mutants due to the presence in the serum of muscle pyruvate kinase [147,148]. The mdx mouse harbors a spontaneous point mutation in exon 23 of the DMD gene which causes truncation of the dystrophin protein at spectrin-like repeat 7 within the N-terminal portion of the rod domain [149]. This truncated protein is degraded by the proteasome, resulting in a functional loss of dystrophin in striated muscle [150]. The mdx mouse displays many of the hallmarks of DMD, including muscle wasting, cardiomyopathy, fibrotic replacement of muscle, and the presence of muscle specific enzymes in the serum [147,151,152]. One significant difference between mdx mice and DMD patients is the severity of muscle wasting. DMD is characterized by severe muscle wasting and premature death, whereas the mdx mouse has only ~20% reduced lifespan and, with the

exception of the diaphragm, mild muscle wasting [17,147,152,153]. The reason for this discrepancy in disease severity between mdx mice and DMD patients is not fully understood, but may be due to compensatory expression of utrophin (to ~5% molar equivalent of normal dystrophin expression) in mdx mice [134,154]. Dystrophin/utrophin double knockout mice have a much more severe dystrophic phenotype than mdx mice and expression of full length or engineered micro-utrophins can potently prevent dystrophy in mdx mice [155,156,157,158,159]. Additionally, a recent study has identified a gene, cytidine monophosphate–sialic acid hydroxylase (CMAH), involved in modifying extracellular sugar moieties that is active in mice but not in humans due to genetic divergence [160]. Knockin mice expressing the human form of the CMAH gene on a mdx background have a more severe phenotype than normal mdx mice [160]. Alternatively, previous reports have shown that the dystrophic phenotype of mdx and other dystrophic mice can be significantly altered by crossing them onto discrete inbred mouse strains, suggesting that genetic background is an important determinant of disease severity in dystrophic mice [161,162,163]. To determine the influence of genetic background on cardiac function in inbred mice, in Chapter 2 of this dissertation I quantitatively assessed cardiac function in several commonly used strains of inbred mice. Despite the mild phenotype of mdx mice, the vast majority of studies on dystrophin's physiological function have been carried out in this model.

GRMD dog. In addition to mdx mouse, the golden retriever muscular dystrophy (GRMD) dog has also served as a model for physiological studies on

DMD. This model harbors a spontaneous mutation within the splice acceptor site of intron 6 of the DMD gene [164] which is expected to cause a premature stop codon within exon 8 and lead to the production of a drastically truncated protein. Interestingly, in this model a small amount of nearly complete dystrophin (~390 kDa) is expressed due to splicing adaptations which are not currently understood [165]. GRMD dogs have a severe dystrophic phenotype in skeletal muscle as characterized by profound muscle wasting, fibrosis, and elevation of serum creatine kinase [166,167,168]. Additionally, GRMD dogs show a pronounced cardiomyopathy characterized by myocardial wasting and fibrosis [169], contractile dysfunction [170], and dilated cardiomyopathy [171]. Because the severity of muscle wasting in the skeletal and cardiac muscle of GRMD dog is so similar to DMD patients, this animal model is considered the “gold standard” for large animal DMD research.

Dystrophin as a mechanical stabilizer of the sarcolemma. As described above, the DGC provides a mechanical linkage between the cytoskeletal and the extracellular matrix localized to the costamere (Figure 1-2) [95]. Previous studies suggest that the costamere is a conduit for the lateral transmission of force generated in the sarcomeres to the extracellular matrix [172,173]. These findings along with the findings that dystrophin contains flexible hinge regions have led to the hypothesis that dystrophin acts to transmit force generated by the sarcomeres and also as a molecular shock absorber, stabilizing the membrane during the rigors of contraction and relaxation. This hypothesis is in line with the findings of increased levels of muscle cytoplasmic enzymes in the serum and the

findings that mdx skeletal muscle is highly susceptible to injury brought on by mechanical stresses including hypo-osmotic stress, lengthening contractions, and exercise [10,11,12,174,175,176,177]. Increased susceptibility to injury in mdx mice is associated with decreased force production, decreased lateral force transmission, and increased membrane permeability, but not with reductions in the force generating capacity of the sarcomeres, suggesting that the primary defect resides in the sarcolemma [174,177,178,179,180]. The role of dystrophin appears to be similar in cardiac muscle, where isolated mdx cardiac myocytes are more susceptible to membrane damage due to passive stretch or hypo-osmotic stress [181,182]. This mechanical injury is associated with increased membrane permeability in the absence of change in sarcomeric force production [181,182] (Metzger, J.M., unpublished observations). Interestingly, when the tensile strength of the sarcolemma is tested directly there is no significant deficit in mdx mice [183]. Mdx muscle does, however, show aberrant reductions in sarcolemma folding [184]. The apparent excess of sarcolemma due to folding is necessary to mitigate the forces of mechanical stretch in normal muscle, suggesting that the mechanical instability of the membrane in mdx mice is due to lack of available membrane surface area during stretch [185].

The theory that dystrophin acts primarily as a tether to mechanically stabilize the sarcolemma suggests that its actin- and dystroglycan-binding properties are the most critical for its function. Given the structural complexity and numerous interacting partners of dystrophin, a precise determination of the structural domains necessary for dystrophin's physiological function can be

challenging. Analysis of the mutations in dystrophin which cause DMD and BMD has revealed some clues regarding the regions of dystrophin most essential to its function. In-frame deletions encompassing both actin-binding domains typically cause DMD [34,37,46,186,187]. DMD-causing missense mutations also cluster in this region, further emphasizing the importance of the actin binding domains for dystrophin's function [188]. Nonsense mutations resulting in protein truncation cause DMD invariably, with the exception of truncations occurring distal to the cysteine-rich domain (which may cause BMD), establishing this as the distal edge of essential domains for dystrophin function [46,189,190]. Patients with in-frame deletions of the cysteine-rich domain invariably develop DMD [46,190], implicating this region as essential for dystrophin function. With regard to the importance of the rod domain, a particularly informative patient study on the structural basis for dystrophin function was carried out by England and colleagues who described a BMD family which included an ambulatory 61 year old man harboring an in-frame deletion of exons 17-48 in the DMD gene, resulting in loss in nearly 50% of the coding sequence of dystrophin [45]. This deletion was contained entirely within the rod domain, sparing the N-terminal, cysteine-rich and C-terminal portions of dystrophin [45]. Collectively, these findings in DMD and BMD patients suggest that the actin- and dystroglycan-binding domains are absolutely essential for dystrophin function, with loss of the rod and C-terminal domains having a lesser impact. A group led by Dr. Jeffrey Chamberlain undertook the rational design of truncated mini- and micro-dystrophin constructs based on the BMD mutation identified by England et al

[191,192]. The impetus for these studies was to design functional dystrophin constructs compact enough to be packaged into adeno-associated virus (AAV) vectors, but also enhanced our understanding of the structural basis for dystrophin function. In these studies, similar to DMD/BMD patients, it was found that truncated dystrophin constructs containing dystrophin's N-terminal actin binding domain and cysteine-rich domains can prevent dystrophy in mdx mice despite lacking the C-terminal domain and the vast majority of the rod domain [191]. Numerous studies have shown these truncated dystrophin constructs to be very effective in preventing dystrophy in skeletal and cardiac muscle, suggesting that dystrophin's primary physiological role is related to its function as a mechanical tether between actin and β-dystroglycan [146,191,192,193,194,195,196,197].

In addition to engineered dystrophin constructs, several studies have also tested the effects of expressing truncated, but naturally occurring dystrophin isoforms on skeletal muscle function. Expression of the dystrophin isoforms Dp116 and Dp71 (which contain the cysteine-rich domain, the C-terminal domain and part of the rod domain, and named as Dystrophin protein, molecular weight in kDa) did not prevent dystrophy in mdx mice and, in some cases, exacerbated muscular dystrophy by displacing utrophin at the sarcolemma [198,199,200,201,202]. Expression of Dp260, which retains the rod domain actin binding region of dystrophin, partially corrected dystrophy in mdx mice [199]. Additionally, expression of Dp71 and a truncated dystrophin construct lacking only the cysteine-rich domain (and thus expressing the actin binding and

dystroglycan binding segments of dystrophin *in trans*) did not correct dystrophy in mdx mice [203]. Collectively, these findings suggest that the ability of dystrophin to prevent is directly dependent on its ability to mechanical tether cytoskeletal actin to β-dystroglycan.

In addition to studies in mdx mice, expression of short dystrophin isoforms was also investigated in mice on a wild-type background. Interestingly, expression of short isoforms of dystrophin in wild-type mice caused a dystrophy-like myopathy [199,201,204]. This was true even for Dp260, which partially corrected the phenotype of mdx mice [199]. Additionally, in each case transgenic mice showed dystrophic myopathy despite increasing expression of the remaining DGC proteins. This pathological change was associated with loss of endogenous dystrophin from the sarcolemma, suggesting that truncated dystrophin isoforms can cause dystrophy by exerting dominant negative effect on DGC function [199].

Dystrophin and the DGC as scaffolds and mediators for cell signaling. As mentioned above, the DGC is associated with numerous proteins involved in cell signaling through interactions with dystrobrevin and the syntrophins. Recently, it has also been shown that neuronal nitric oxide synthase (nNOS) can interaction directly with dystrophin at spectrin-like repeats 16-17 [205]. Collectively, this has led to the hypothesis that dystrophin and the DGC play an important role as scaffolds for cell signaling proteins. A large portion of the research carried out on dystrophin's role in cell signaling has focused on nNOS. Transgenic overexpression of nNOS corrects many histological aspects of dystrophy in mdx

mice and reduces serum creatine kinase through mechanisms that are not totally clear but may involve suppression of macrophage-mediated inflammation or enhanced blood flow to muscle during exercise [206,207]. Additionally, nNOS-null mice show exaggerated fatigue following exercise and inclusion of the nNOS binding domain of dystrophin in micro-dystrophin constructs correct muscle circulation and exercise performance in mdx mice [205,208]. However, nNOS-null mice show no evidence of muscle wasting or sarcolemma permeability and crossing these mice onto an mdx background does not enhance muscle wasting or sarcolemmal fragility [208,209]. As mentioned above, numerous studies have shown that micro-dystrophin proteins lacking the C-terminal domain, which therefore cannot recruit dystrobrevin and syntrophins to the sarcolemma, are highly effective in preventing muscular dystrophy in mdx mice [146,191,192,193,194,195,196,197]. Therefore, whereas the signaling functions of the DGC appear to play a role in certain aspects of muscle function, most notably exercise capacity and fatigue, they are not necessary for correcting muscle wasting, the primary defect of DMD.

Development of dilated cardiomyopathy associated with DMD

As discussed above, thorough clinical research has led to a clear description of the progressive cardiomyopathy which frequently leads to dilated cardiomyopathy in DMD patients [19]. Studies by the Metzger lab and others have provided strong evidence that the primary cellular defect leading to necrotic cardiac myocyte death and cardiomyopathy in DMD is mechanical destabilization

of the membrane in the absence of dystrophin [181,182]. Muscular dystrophy caused by loss of other DGC proteins also causes mechanical instability, though in some cases it has been shown that apoptosis also contributes to muscle wasting [103,105,143,210,211,212]. Although it is tempting to hypothesize that necrotic loss of myocytes leads to weakness and dilation of the ventricular wall in DMD, it is also important to consider the limitations of studying intact cells and the physiological complexities of intact organs. A gap in knowledge regarding DMD cardiomyopathy is a more detailed description of how mechanical instability in individual myocytes manifests as dilated cardiomyopathy in DMD patients. To this end, chapter 3 of this thesis investigates the effects of dystrophin loss on the mechanical properties of intact hearts to gain a better understanding of the mechanisms by which dilated cardiomyopathy develops in DMD patients.

Dystrophin in the pathogenesis of non-inherited heart disease

In addition to its involvement in the inherited dystrophinopathies, there is also a sizable and expanding body of research to suggest that dystrophin expression is significantly altered in various forms of inherited heart disease (Table 1-1). Studies in our laboratory have shown that expression of dystrophin declines significantly in aging mice [213]. Additionally, dystrophin expression is altered following acute ischemia, enteroviral infection, and isoproterenol-induced cardiomyopathy [214,215,216,217,218,219]. In human patients, altered dystrophin expression is associated with viral myocarditis, atrial fibrillation, and heart failure [220,221,222,223]. Specifically, in these studies, dystrophin is often

truncated into smaller fragments as observed by Western blot [215,219,220]. Additionally, these studies show mislocalization or loss of dystrophin from the sarcolemma following injury [214,216,217,218,219,220,221]. Two particularly interesting studies carried out by Campos and colleagues and Rodriguez and colleagues compared dystrophin to integrins, DGC components, and other myocardial proteins following isoproterenol toxicity and ischemia [216,224]. These studies found dystrophin to have enhanced susceptibility to degradation when compared to these other proteins [216,224]. Mechanistically, the manner in which dystrophin expressed is diminished in these disease states is not totally clear. There is evidence of age-related declines in dystrophin transcription [225]. Additionally, dystrophin is a substrate of the calpain proteases [226]. Calpains are calcium-dependent cysteine proteases which are aberrantly activated in disease processes including DMD and heart failure [124,227,228]. Expression of the endogenous calpain inhibitor calpistatin and other calpain inhibitors is therapeutic in DMD and heart failure, confirming the maladaptive role of the calpains in these disease states [227,229]. However, since the calpains cleave numerous substrates the specific effects of dystrophin cleavage remains unknown. Dystrophin is also cleaved by the 2A protease expressed by cardiotropic enteroviruses [230]. A detailed discussion of this topic is included below in the section entitled, "Dystrophin cleavage and cardiac enteroviral infection".

The observation that dystrophin expression is altered in non-inherited heart disease has led to the provocative hypothesis that dystrophin loss is a

common link between inherited and non-inherited heart disease (Table 1-1). The importance of cytoskeletal proteins in heart disease is not without precedence. A growing body of research pioneered by Dr. Jeffrey Towbin suggests that numerous disease processes converge on disruption of the sarcolemma, constituting a “Final Common Pathway” for cardiovascular disease [219,231,232,233]. The prospect of dystrophin and other cytoskeletal proteins being critical components in non-inherited heart disease pathology is of particular relevance given the prevalence of heart disease in the United States. An age-related and progressive disease, over 5.5 million Americans suffer from heart disease [234]. Additionally, heart failure is the leading cause of death in the elderly and the size of the 65+ population is predicted to double in size within the next 30 years. During this time, the total population is predicted to increase by only ~30%, suggesting that heart failure will remain at the forefront of clinical relevance well into the future (2011 census data).

Dystrophin cleavage and cardiac enteroviral infection

Enteroviruses, including the Coxsackie B viruses, are the most common cause of viral myocarditis [235]. Cardiac enteroviral infection is a clinically relevant condition which is highly variable in its presentation. Autopsy samples taken from apparently healthy individuals show ~5% rate of subclinical myocarditis and ~5-10% rate of subclinical enterovirus infection, suggesting undiagnosed, asymptomatic viral infection in otherwise healthy individuals [236,237,238,239]. Alternatively, patients who succumb to sudden cardiac death

show ~20% rate of previously undiagnosed viral infection [240,241]. Similarly, ~40% of patients with idiopathic dilated cardiomyopathy and those who die suddenly following acute myocardial infarction show evidence of undiagnosed viral infection [236,242,243,244,245,246,247,248,249]. Acute myocarditis brought on by fulminant viral infection clearly plays a role in the pathogenesis of many patients [235]. Interestingly, however, it has recently been shown that 5' terminal deletions within the coxsackievirus genome can promote stability of the viral genome and persistent expression of viral genes within the myocardium [250,251]. Collectively, this suggests an insidious mode of cardiomyopathy through viral infection and persistent expression of viral genes which promotes chronic cardiac disease and development of DCM.

Using a computer algorithm, it was found that dystrophin was a predicted substrate for cleavage by the 2A protease expressed by enteroviruses ($2A^{pro}$) [252]. A group led by Dr. Kirk Knowlton showed that dystrophin is cleaved by $2A^{pro}$ *in vitro* and that fragmentation of dystrophin was observed following viral infection *in vivo* [230,253]. Importantly, enterovirus infection is also associated with increased Evans blue dye uptake, showing membrane permeability and suggesting a dystrophic cardiomyopathy [230]. Transgenic expression of $2A^{pro}$ in the heart causes sarcolemmal fragility and the development of dilated cardiomyopathy [254]. It has been hypothesized that the ability for $2A^{pro}$ to cleave dystrophin has evolved to increase viral propagation through destabilization of the sarcolemma. This is supported by the finding that mdx mice are highly susceptible to enterovirus infection compared to wild-type mice

[255]. However, $2A^{pro}$ also cleaves factors involved in host translation such as poly-A binding protein and elongation-initiation factor 4 [230,256,257]. Studies to dissect the substrate-specific effects of $2A^{pro}$ activity in the heart have yet to be carried out.

As mentioned above, the presence of truncated dystrophin isoforms containing dystrophin's dystroglycan-binding function but lacking its actin-binding function cause a dystrophic phenotype in skeletal muscle by exerting a dominant effect on DGC function [198,199,200,201,202]. Cleavage of dystrophin by $2A^{pro}$ is predicted to result in 2 fragments: an N-terminal fragment containing both of dystrophin's actin-binding domains and the majority of the rod domain, and a C-terminal fragment containing the remainder of the rod domain, the cysteine-rich domain, and the C-terminal domain. Previous studies of dystrophin fragments containing dystrophin's actin binding domain have shown that, surprisingly, these fragments localize to the sarcolemma, possibly through direct interactions between spectrin-like repeat 2 and membrane phospholipids [258,259,260,261]. Although these N-terminal dystrophin fragments localized to the sarcolemma, expression does not exacerbate (or improve) the dystrophic phenotype in mdx [260]. This supports the hypothesis that the dominant negative effects of short dystrophin isoforms is due to displacement of dystrophin at the DGC through competition for β-dystroglycan binding sites. The putative C-terminal fragment is very similar to previously tested short dystrophin isoforms and therefore may also exert dominant negative effects when expressed in the heart. Studies investigating the effects of a putative dominant negative dystrophin protein on the

heart are lacking, and this would represent a novel mechanism for the progression of a clinically relevant disease process. A characterization of cardiac function in transgenic mice expressing the putative products of $2A^{pro}$-mediated cleavage of dystrophin is the subject of chapter 4 of this thesis.

Major objectives and specific aims

The preceding introduction reviews some of the major gaps in knowledge regarding the effects of dystrophin deficiency on cardiac function in inherited and non-inherited heart disease. The overarching questions to be answered by this work are: (1) How does genetic background affect cardiac function at baseline and during physiologically relevant stress in commonly used inbred mouse strains?; (2) How does loss of dystrophin affect left ventricular myocardial compliance and susceptibility to mechanical injury?; (3) Is expression of the C-terminal product of dystrophin cleavage by $2A^{pro}$ sufficient to cause dystrophic cardiomyopathy by exerting a dominant negative effect on DGC function? The following specific aims were used to answer these questions.

Specific aim 1: To determine the effect of genetic background on cardiac function in several commonly used inbred mouse strains at baseline and during stress. Inbred mouse strains are among the most widely used animal models for biomedical research. Chapter 2 characterizes baseline cardiac function of 8 commonly used inbred mouse strains using the *ex vivo* isolated heart preparation and *in vivo* conductance micromanometry. Inbred strains were also subjected to cardiac stressors: *ex vivo* ischemia and reperfusion for isolated hearts, and

esmolol treatment and acute hypoxia while simultaneously recording *in vivo* cardiac function.

Specific aim 2: To determine the effects of dystrophin deficiency on the mechanical properties of the intact left ventricle. Previous studies have shown that loss of dystrophin affects the mechanical compliance of individual cardiac myocytes. Chapter 3 builds on these studies and characterizes the compliance of isolated dystrophin-deficient hearts subjected to mechanical stretch of the left ventricle. Sarcomere length during stretch is also recorded to determine the effects of whole-heart stretch on individual cardiac myocytes. Additional studies in other models of inherited muscular dystrophy are also performed to broaden the scope of this chapter and identify similarities between discrete forms of muscular dystrophy.

Specific aim 3: To determine if transgenic expression of the C-terminal product of dystrophin cleavage by $2A^{pro}$ is sufficient to cause dystrophic cardiomyopathy. During enterovirus infection, dystrophin is cleaved by $2A^{pro}$ into a fragment that is structurally similar to non-muscle dystrophin isoforms shown to cause dystrophic myopathy by exerting a dominant negative effect on DGC function. Chapter 4 of this thesis characterizes the effects of transgenically expressing the products of $2A^{pro}$-mediated dystrophin cleavage in the heart. The biochemical and physiological effects of transgene expression on DGC function are explored in this chapter. Dystrophic cardiomyopathy is assessed by membrane stability, development of cardiac fibrosis, and susceptibility to

ischemic injury. The results of this study shed light on DGC function in the heart and the mechanisms of enterovirus-mediated cardiomyopathy.

Tables

Disease process	Proposed Mechanism	References
Aging	Reduced transcription	Townsend et al, 2011
Acute ischemia	Calpain cleavage	Armstrong et al, 2001 Rodriguez et al, 2005 Kyoi et al, 2006
Isoproterenol toxicity	Calpain cleavage	Xi et al, 2000 Miyazato et al, 1997 Toyo-oka et al, 2004
Enterovirus infection	$2A^{pro}$ cleavage	Badorff et al, 1999
Myocarditis	Calpain/$2A^{pro}$ cleavage	Badorff et al, 1999
Heart failure	Calpain/$2A^{pro}$ cleavage	Toyo-oka et al, 2004 Vatta et al, 2002 Vatta et al, 2004

Table 1-1. Proposed mechanisms for non-inherited loss of dystrophin.

Figures

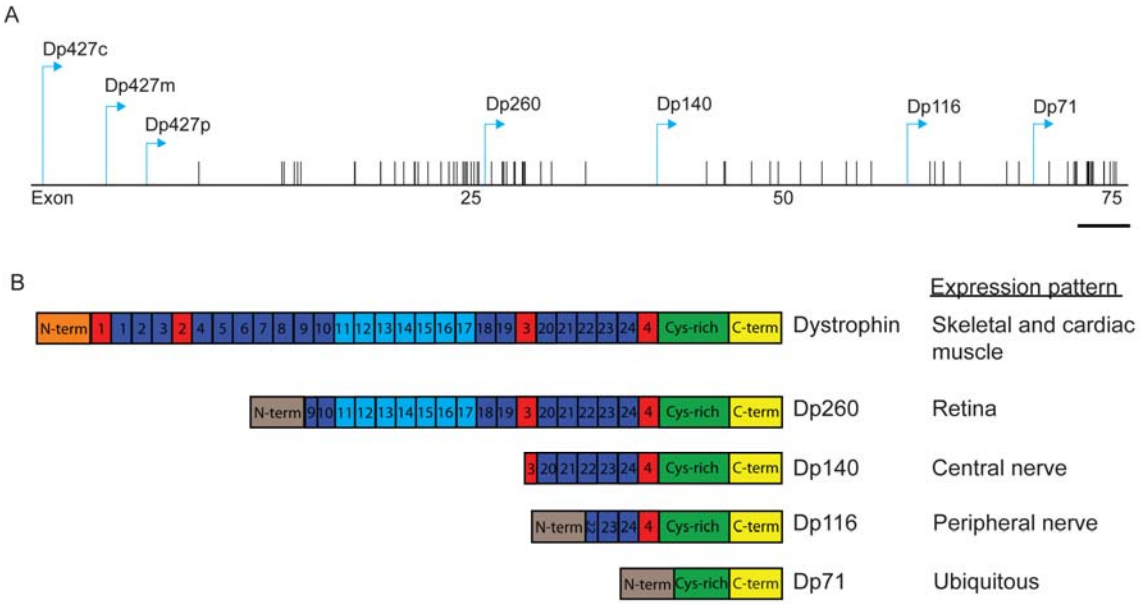

Figure 1-1. The DMD gene and its protein products. A) Schematic of the DMD gene. Promoters and first introns (with the exception of Dp140, which does not have a unique first exon) are indicated by light blue lines and arrows. Exons are indicated by black lines and numbers beneath the gene. Scale bar – 100 kbp. B) Protein products of the DMD gene and their expression. N-term, N-terminal domain. Orange N-terminal domains containing actin binding sites. Gray N-terminal domains do not contain actin-binding sites. Hinge domains are indicated by red boxes. Spectrin-like repeats are indicated by blue boxes. Light blue boxes are repeats which participate in actin binding. Cys-rich, cysteine-rich domain. C-term, C-terminal domain. Isoforms of DMD named as dystrophin protein (Dp) and distinguished from each other by listing the molecular weight (in kDa).

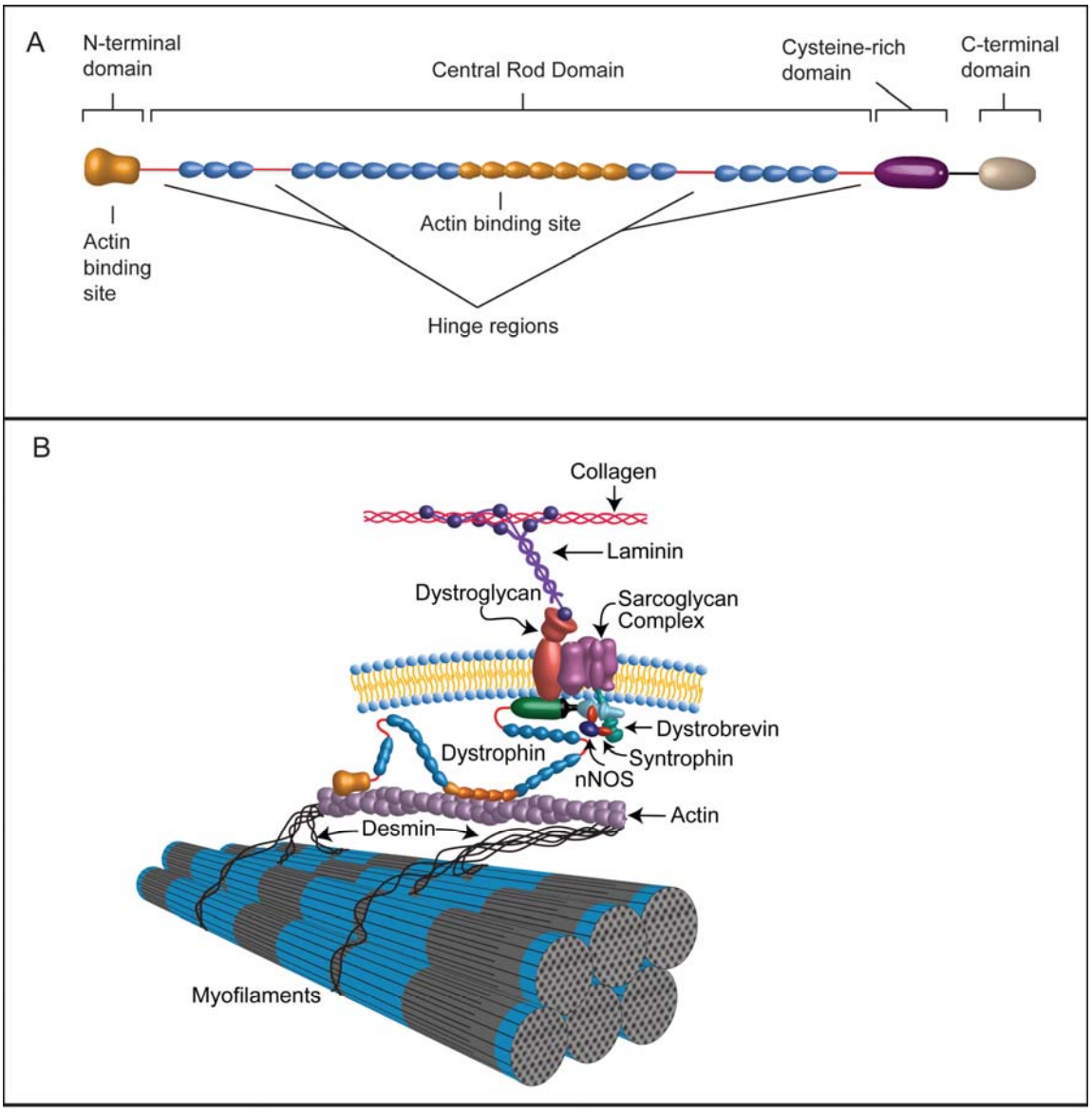

Figure 1-2. Schematic of dystrophin and the dystrophin-glycoprotein complex (DGC). Functional domains of dystrophin (A) and the DGC (B). Adapted from Barnabei and colleagues [262] with permission from John Wiley and Sons.

Literature cited

1. Conte G, Gioia L (1836) Scrofola del sistema muscolare. Annali Clinici dell'Ospedale degli Incurabili 66.

2. Duchenne GBA (1868) Recherches sur la paralysie musculaire pseudo-hypertrophique ou paralysie myosclerosique. Arch Gen Med 11: 5, 178, 305, 421, 552.

3. Meryon E (1852) On granular and fatty degeneration of the voluntary muscles. Medico-Chirurgical Trans (London) 35: 73.

4. Tyler KL (2003) Origins and early descriptions of "Duchenne muscular dystrophy". Muscle Nerve 28: 402-422.

5. Cox GF, Kunkel LM (1997) Dystrophies and heart disease. Curr Opin Cardiol 12: 329-343.

6. Gulati S, Saxena A, Kumar V, Kalra V (2005) Duchenne muscular dystrophy: prevalence and patterns of cardiac involvement. Indian J Pediatr 72: 389-393.

7. Emery AE (1991) Population frequencies of inherited neuromuscular diseases--a world survey. Neuromuscul Disord 1: 19-29.

8. Gowers WR (1895) A manual of the nervous system. Philadelphia: Blakiston.

9. Bushby K, Finkel R, Birnkrant DJ, Case LE, Clemens PR, et al. Diagnosis and management of Duchenne muscular dystrophy, part 1: diagnosis, and pharmacological and psychosocial management. Lancet Neurol 9: 77-93.

10. Somer H, Donner M, Murros J, Konttinen A (1973) A serum isozyme study in muscular dystrophy. Particular reference to creatine kinase, aspartate aminotransferase, and lactic acid dehydrogenase isozymes. Arch Neurol 29: 343-345.

11. Dreyfus JC, Schapira G, Schapira F (1954) Biochemical study of muscle in progressive muscular dystrophy. J Clin Invest 33: 794-797.

12. Munsat TL, Baloh R, Pearson CM, Fowler W, Jr. (1973) Serum enzyme alterations in neuromuscular disorders. JAMA 226: 1536-1543.

13. Chamberlain JS, Rando TA (2006) Duchenne muscular dystrophy : advances in therapeutics. New York: Taylor & Francis. xxii, 461 p. p.

14. Spencer GE, Jr. (1967) Orthopaedic care of progressive muscular dystrophy. J Bone Joint Surg Am 49: 1201-1204.

15. Vignos PJ, Jr., Archibald KC (1960) Maintenance of ambulation in childhood muscular dystrophy. J Chronic Dis 12: 273-290.

16. Kohler M, Clarenbach CF, Bahler C, Brack T, Russi EW, et al. (2009) Disability and survival in Duchenne muscular dystrophy. J Neurol Neurosurg Psychiatry 80: 320-325.

17. Eagle M, Baudouin SV, Chandler C, Giddings DR, Bullock R, et al. (2002) Survival in Duchenne muscular dystrophy: improvements in life expectancy since 1967 and the impact of home nocturnal ventilation. Neuromuscul Disord 12: 926-929.

18. Finsterer J, Stollberger C (2003) The heart in human dystrophinopathies. Cardiology 99: 1-19.

19. Nigro G, Comi LI, Politano L, Bain RJ (1990) The incidence and evolution of cardiomyopathy in Duchenne muscular dystrophy. Int J Cardiol 26: 271-277.

20. D'Orsogna L, O'Shea JP, Miller G (1988) Cardiomyopathy of Duchenne muscular dystrophy. Pediatr Cardiol 9: 205-213.

21. Perloff JK, Roberts WC, de Leon AC, Jr., O'Doherty D (1967) The distinctive electrocardiogram of Duchenne's progressive muscular dystrophy. An electrocardiographic-pathologic correlative study. Am J Med 42: 179-188.

22. Manning GW, Cropp GJ (1958) The electrocardiogram in progressive muscular dystrophy. Br Heart J 20: 416-420.

23. Markham LW, Michelfelder EC, Border WL, Khoury PR, Spicer RL, et al. (2006) Abnormalities of diastolic function precede dilated cardiomyopathy associated with Duchenne muscular dystrophy. J Am Soc Echocardiogr 19: 865-871.

24. Moser H (1984) Duchenne muscular dystrophy: pathogenetic aspects and genetic prevention. Hum Genet 66: 17-40.

25. de Martinville B, Kunkel LM, Bruns G, Morle F, Koenig M, et al. (1985) Localization of DNA sequences in region Xp21 of the human X chromosome: search for molecular markers close to the Duchenne muscular dystrophy locus. Am J Hum Genet 37: 235-249.

26. Worton RG, Duff C, Sylvester JE, Schmickel RD, Willard HF (1984) Duchenne muscular dystrophy involving translocation of the dmd gene next to ribosomal RNA genes. Science 224: 1447-1449.

27. Jacobs PA, Hunt PA, Mayer M, Bart RD (1981) Duchenne muscular dystrophy (DMD) in a female with an X/autosome translocation: further evidence that the DMD locus is at Xp21. Am J Hum Genet 33: 513-518.

28. Ray PN, Belfall B, Duff C, Logan C, Kean V, et al. (1985) Cloning of the breakpoint of an X;21 translocation associated with Duchenne muscular dystrophy. Nature 318: 672-675.

29. Francke U, Ochs HD, de Martinville B, Giacalone J, Lindgren V, et al. (1985) Minor Xp21 chromosome deletion in a male associated with expression of Duchenne muscular dystrophy, chronic granulomatous disease, retinitis pigmentosa, and McLeod syndrome. Am J Hum Genet 37: 250-267.

30. Kunkel LM, Hejtmancik JF, Caskey CT, Speer A, Monaco AP, et al. (1986) Analysis of deletions in DNA from patients with Becker and Duchenne muscular dystrophy. Nature 322: 73-77.

31. Davies KE, Pearson PL, Harper PS, Murray JM, O'Brien T, et al. (1983) Linkage analysis of two cloned DNA sequences flanking the Duchenne muscular dystrophy locus on the short arm of the human X chromosome. Nucleic Acids Res 11: 2303-2312.

32. Thompson MW, Ray PN, Belfall B, Duff C, Logan C, et al. (1986) Linkage analysis of polymorphisms within the DNA fragment XJ cloned from the breakpoint of an X;21 translocation associated with X linked muscular dystrophy. J Med Genet 23: 548-555.

33. Monaco AP, Bertelson CJ, Middlesworth W, Colletti CA, Aldridge J, et al. (1985) Detection of deletions spanning the Duchenne muscular dystrophy locus using a tightly linked DNA segment. Nature 316: 842-845.

34. Koenig M, Hoffman EP, Bertelson CJ, Monaco AP, Feener C, et al. (1987) Complete cloning of the Duchenne muscular dystrophy (DMD) cDNA and preliminary genomic organization of the DMD gene in normal and affected individuals. Cell 50: 509-517.

35. Hoffman EP, Brown RH, Jr., Kunkel LM (1987) Dystrophin: the protein product of the Duchenne muscular dystrophy locus. Cell 51: 919-928.

36. Roberts RG, Coffey AJ, Bobrow M, Bentley DR (1993) Exon structure of the human dystrophin gene. Genomics 16: 536-538.

37. Den Dunnen JT, Grootscholten PM, Bakker E, Blonden LA, Ginjaar HB, et al. (1989) Topography of the Duchenne muscular dystrophy (DMD) gene: FIGE and cDNA analysis of 194 cases reveals 115 deletions and 13 duplications. Am J Hum Genet 45: 835-847.

38. Feener CA, Koenig M, Kunkel LM (1989) Alternative splicing of human dystrophin mRNA generates isoforms at the carboxy terminus. Nature 338: 509-511.

39. Roberts RG, Coffey AJ, Bobrow M, Bentley DR (1992) Determination of the exon structure of the distal portion of the dystrophin gene by vectorette PCR. Genomics 13: 942-950.

40. Bies RD, Phelps SF, Cortez MD, Roberts R, Caskey CT, et al. (1992) Human and murine dystrophin mRNA transcripts are differentially expressed during skeletal muscle, heart, and brain development. Nucleic Acids Res 20: 1725-1731.

41. Gorecki DC, Monaco AP, Derry JM, Walker AP, Barnard EA, et al. (1992) Expression of four alternative dystrophin transcripts in brain regions regulated by different promoters. Hum Mol Genet 1: 505-510.

42. Holder E, Maeda M, Bies RD (1996) Expression and regulation of the dystrophin Purkinje promoter in human skeletal muscle, heart, and brain. Hum Genet 97: 232-239.

43. D'Souza VN, Nguyen TM, Morris GE, Karges W, Pillers DA, et al. (1995) A novel dystrophin isoform is required for normal retinal electrophysiology. Hum Mol Genet 4: 837-842.

44. Kingston HM, Harper PS, Pearson PL, Davies KE, Williamson R, et al. (1983) Localisation of gene for Becker muscular dystrophy. Lancet 2: 1200.

45. England SB, Nicholson LV, Johnson MA, Forrest SM, Love DR, et al. (1990) Very mild muscular dystrophy associated with the deletion of 46% of dystrophin. Nature 343: 180-182.

46. Aartsma-Rus A, Van Deutekom JC, Fokkema IF, Van Ommen GJ, Den Dunnen JT (2006) Entries in the Leiden Duchenne muscular dystrophy mutation database: an overview of mutation types and paradoxical cases that confirm the reading-frame rule. Muscle Nerve 34: 135-144.

47. Koenig M, Beggs AH, Moyer M, Scherpf S, Heindrich K, et al. (1989) The molecular basis for Duchenne versus Becker muscular dystrophy: correlation of severity with type of deletion. Am J Hum Genet 45: 498-506.

48. Towbin JA, Hejtmancik JF, Brink P, Gelb B, Zhu XM, et al. (1993) X-linked dilated cardiomyopathy. Molecular genetic evidence of linkage to the Duchenne muscular dystrophy (dystrophin) gene at the Xp21 locus. Circulation 87: 1854-1865.

49. Berko BA, Swift M (1987) X-linked dilated cardiomyopathy. N Engl J Med 316: 1186-1191.

50. Bies RD, Maeda M, Roberds SL, Holder E, Bohlmeyer T, et al. (1997) A 5' dystrophin duplication mutation causes membrane deficiency of alpha-dystroglycan in a family with X-linked cardiomyopathy. J Mol Cell Cardiol 29: 3175-3188.

51. Franz WM, Muller M, Muller OJ, Herrmann R, Rothmann T, et al. (2000) Association of nonsense mutation of dystrophin gene with disruption of sarcoglycan complex in X-linked dilated cardiomyopathy. Lancet 355: 1781-1785.

52. Feng J, Yan JY, Buzin CH, Sommer SS, Towbin JA (2002) Comprehensive mutation scanning of the dystrophin gene in patients with nonsyndromic X-linked dilated cardiomyopathy. J Am Coll Cardiol 40: 1120-1124.

53. Milasin J, Muntoni F, Severini GM, Bartoloni L, Vatta M, et al. (1996) A point mutation in the 5' splice site of the dystrophin gene first intron responsible for X-linked dilated cardiomyopathy. Hum Mol Genet 5: 73-79.

54. Yoshida K, Nakamura A, Yazaki M, Ikeda S, Takeda S (1998) Insertional mutation by transposable element, L1, in the DMD gene results in X-linked dilated cardiomyopathy. Hum Mol Genet 7: 1129-1132.

55. Muntoni F, Melis MA, Ganau A, Dubowitz V (1995) Transcription of the dystrophin gene in normal tissues and in skeletal muscle of a family with X-linked dilated cardiomyopathy. Am J Hum Genet 56: 151-157.

56. Muntoni F, Di Lenarda A, Porcu M, Sinagra G, Mateddu A, et al. (1997) Dystrophin gene abnormalities in two patients with idiopathic dilated cardiomyopathy. Heart 78: 608-612.

57. Arbustini E, Diegoli M, Morbini P, Dal Bello B, Banchieri N, et al. (2000) Prevalence and characteristics of dystrophin defects in adult male patients with dilated cardiomyopathy. J Am Coll Cardiol 35: 1760-1768.

58. Klamut HJ, Bosnoyan-Collins LO, Worton RG, Ray PN, Davis HL (1996) Identification of a transcriptional enhancer within muscle intron 1 of the human dystrophin gene. Hum Mol Genet 5: 1599-1606.

59. De Repentigny Y, Marshall P, Worton RG, Kothary R (2004) The mouse dystrophin muscle enhancer-1 imparts skeletal muscle, but not cardiac muscle, expression onto the dystrophin Purkinje promoter in transgenic mice. Hum Mol Genet 13: 2853-2862.

60. Koenig M, Monaco AP, Kunkel LM (1988) The complete sequence of dystrophin predicts a rod-shaped cytoskeletal protein. Cell 53: 219-228.

61. Sato O, Nonomura Y, Kimura S, Maruyama K (1992) Molecular shape of dystrophin. J Biochem 112: 631-636.

62. Pons F, Augier N, Heilig R, Leger J, Mornet D, et al. (1990) Isolated dystrophin molecules as seen by electron microscopy. Proc Natl Acad Sci U S A 87: 7851-7855.

63. Norwood FL, Sutherland-Smith AJ, Keep NH, Kendrick-Jones J (2000) The structure of the N-terminal actin-binding domain of human dystrophin and how mutations in this domain may cause Duchenne or Becker muscular dystrophy. Structure 8: 481-491.

64. Castresana J, Saraste M (1995) Does Vav bind to F-actin through a CH domain? FEBS Lett 374: 149-151.

65. Hemmings L, Kuhlman PA, Critchley DR (1992) Analysis of the actin-binding domain of alpha-actinin by mutagenesis and demonstration that dystrophin contains a functionally homologous domain. J Cell Biol 116: 1369-1380.

66. Way M, Pope B, Cross RA, Kendrick-Jones J, Weeds AG (1992) Expression of the N-terminal domain of dystrophin in E. coli and demonstration of binding to F-actin. FEBS Lett 301: 243-245.

67. Corrado K, Mills PL, Chamberlain JS (1994) Deletion analysis of the dystrophin-actin binding domain. FEBS Lett 344: 255-260.

68. Rybakova IN, Amann KJ, Ervasti JM (1996) A new model for the interaction of dystrophin with F-actin. J Cell Biol 135: 661-672.

69. Koenig M, Kunkel LM (1990) Detailed analysis of the repeat domain of dystrophin reveals four potential hinge segments that may confer flexibility. J Biol Chem 265: 4560-4566.

70. Amann KJ, Renley BA, Ervasti JM (1998) A cluster of basic repeats in the dystrophin rod domain binds F-actin through an electrostatic interaction. J Biol Chem 273: 28419-28423.

71. Ponting CP, Blake DJ, Davies KE, Kendrick-Jones J, Winder SJ (1996) ZZ and TAZ: new putative zinc fingers in dystrophin and other proteins. Trends Biochem Sci 21: 11-13.

72. Bork P, Sudol M (1994) The WW domain: a signalling site in dystrophin? Trends Biochem Sci 19: 531-533.

73. Watkins SC, Hoffman EP, Slayter HS, Kunkel LM (1988) Immunoelectron microscopic localization of dystrophin in myofibres. Nature 333: 863-866.

74. Bonilla E, Samitt CE, Miranda AF, Hays AP, Salviati G, et al. (1988) Duchenne muscular dystrophy: deficiency of dystrophin at the muscle cell surface. Cell 54: 447-452.

75. Klietsch R, Ervasti JM, Arnold W, Campbell KP, Jorgensen AO (1993) Dystrophin-glycoprotein complex and laminin colocalize to the sarcolemma and transverse tubules of cardiac muscle. Circ Res 72: 349-360.

76. Porter GA, Dmytrenko GM, Winkelmann JC, Bloch RJ (1992) Dystrophin colocalizes with beta-spectrin in distinct subsarcolemmal domains in mammalian skeletal muscle. J Cell Biol 117: 997-1005.

77. Straub V, Bittner RE, Leger JJ, Voit T (1992) Direct visualization of the dystrophin network on skeletal muscle fiber membrane. J Cell Biol 119: 1183-1191.

78. Arahata K, Ishiura S, Ishiguro T, Tsukahara T, Suhara Y, et al. (1988) Immunostaining of skeletal and cardiac muscle surface membrane with antibody against Duchenne muscular dystrophy peptide. Nature 333: 861-863.

79. Zubrzycka-Gaarn EE, Bulman DE, Karpati G, Burghes AH, Belfall B, et al. (1988) The Duchenne muscular dystrophy gene product is localized in sarcolemma of human skeletal muscle. Nature 333: 466-469.

80. Ervasti JM (2003) Costameres: the Achilles' heel of Herculean muscle. J Biol Chem 278: 13591-13594.

81. Rybakova IN, Patel JR, Ervasti JM (2000) The dystrophin complex forms a mechanically strong link between the sarcolemma and costameric actin. J Cell Biol 150: 1209-1214.

82. Campbell KP, Kahl SD (1989) Association of dystrophin and an integral membrane glycoprotein. Nature 338: 259-262.

83. Ervasti JM, Ohlendieck K, Kahl SD, Gaver MG, Campbell KP (1990) Deficiency of a glycoprotein component of the dystrophin complex in dystrophic muscle. Nature 345: 315-319.

84. Yoshida M, Ozawa E (1990) Glycoprotein complex anchoring dystrophin to sarcolemma. J Biochem 108: 748-752.

85. Ibraghimov-Beskrovnaya O, Ervasti JM, Leveille CJ, Slaughter CA, Sernett SW, et al. (1992) Primary structure of dystrophin-associated glycoproteins linking dystrophin to the extracellular matrix. Nature 355: 696-702.

86. Holt KH, Crosbie RH, Venzke DP, Campbell KP (2000) Biosynthesis of dystroglycan: processing of a precursor propeptide. FEBS Lett 468: 79-83.

87. Esapa CT, Bentham GR, Schroder JE, Kroger S, Blake DJ (2003) The effects of post-translational processing on dystroglycan synthesis and trafficking. FEBS Lett 555: 209-216.

88. Suzuki A, Yoshida M, Hayashi K, Mizuno Y, Hagiwara Y, et al. (1994) Molecular organization at the glycoprotein-complex-binding site of dystrophin. Three dystrophin-associated proteins bind directly to the carboxy-terminal portion of dystrophin. Eur J Biochem 220: 283-292.

89. Suzuki A, Yoshida M, Yamamoto H, Ozawa E (1992) Glycoprotein-binding site of dystrophin is confined to the cysteine-rich domain and the first half of the carboxy-terminal domain. FEBS Lett 308: 154-160.

90. Rosa G, Ceccarini M, Cavaldesi M, Zini M, Petrucci TC (1996) Localization of the dystrophin binding site at the carboxyl terminus of beta-dystroglycan. Biochem Biophys Res Commun 223: 272-277.

91. Rentschler S, Linn H, Deininger K, Bedford MT, Espanel X, et al. (1999) The WW domain of dystrophin requires EF-hands region to interact with beta-dystroglycan. Biol Chem 380: 431-442.

92. Ishikawa-Sakurai M, Yoshida M, Imamura M, Davies KE, Ozawa E (2004) ZZ domain is essentially required for the physiological binding of dystrophin and utrophin to beta-dystroglycan. Hum Mol Genet 13: 693-702.

93. Chung W, Campanelli JT (1999) WW and EF hand domains of dystrophin-family proteins mediate dystroglycan binding. Mol Cell Biol Res Commun 2: 162-171.

94. Michele DE, Barresi R, Kanagawa M, Saito F, Cohn RD, et al. (2002) Post-translational disruption of dystroglycan-ligand interactions in congenital muscular dystrophies. Nature 418: 417-422.

95. Ervasti JM, Campbell KP (1993) A role for the dystrophin-glycoprotein complex as a transmembrane linker between laminin and actin. J Cell Biol 122: 809-823.

96. van Reeuwijk J, Janssen M, van den Elzen C, Beltran-Valero de Bernabe D, Sabatelli P, et al. (2005) POMT2 mutations cause alpha-dystroglycan hypoglycosylation and Walker-Warburg syndrome. J Med Genet 42: 907-912.

97. Ervasti JM, Sonnemann KJ (2008) Biology of the striated muscle dystrophin-glycoprotein complex. Int Rev Cytol 265: 191-225.

98. Roberds SL, Leturcq F, Allamand V, Piccolo F, Jeanpierre M, et al. (1994) Missense mutations in the adhalin gene linked to autosomal recessive muscular dystrophy. Cell 78: 625-633.

99. Roberds SL, Ervasti JM, Anderson RD, Ohlendieck K, Kahl SD, et al. (1993) Disruption of the dystrophin-glycoprotein complex in the cardiomyopathic hamster. J Biol Chem 268: 11496-11499.

100. Lim LE, Duclos F, Broux O, Bourg N, Sunada Y, et al. (1995) Beta-sarcoglycan: characterization and role in limb-girdle muscular dystrophy linked to 4q12. Nat Genet 11: 257-265.

101. Noguchi S, McNally EM, Ben Othmane K, Hagiwara Y, Mizuno Y, et al. (1995) Mutations in the dystrophin-associated protein gamma-sarcoglycan in chromosome 13 muscular dystrophy. Science 270: 819-822.

102. Nigro V, de Sa Moreira E, Piluso G, Vainzof M, Belsito A, et al. (1996) Autosomal recessive limb-girdle muscular dystrophy, LGMD2F, is caused by a mutation in the delta-sarcoglycan gene. Nat Genet 14: 195-198.

103. Duclos F, Straub V, Moore SA, Venzke DP, Hrstka RF, et al. (1998) Progressive muscular dystrophy in alpha-sarcoglycan-deficient mice. J Cell Biol 142: 1461-1471.

104. Bonnemann CG, Modi R, Noguchi S, Mizuno Y, Yoshida M, et al. (1995) Beta-sarcoglycan (A3b) mutations cause autosomal recessive muscular dystrophy with loss of the sarcoglycan complex. Nat Genet 11: 266-273.

105. Durbeej M, Cohn RD, Hrstka RF, Moore SA, Allamand V, et al. (2000) Disruption of the beta-sarcoglycan gene reveals pathogenetic complexity of limb-girdle muscular dystrophy type 2E. Mol Cell 5: 141-151.

106. McNally EM, Passos-Bueno MR, Bonnemann CG, Vainzof M, de Sa Moreira E, et al. (1996) Mild and severe muscular dystrophy caused by a single gamma-sarcoglycan mutation. Am J Hum Genet 59: 1040-1047.

107. Coral-Vazquez R, Cohn RD, Moore SA, Hill JA, Weiss RM, et al. (1999) Disruption of the sarcoglycan-sarcospan complex in vascular smooth muscle: a novel mechanism for cardiomyopathy and muscular dystrophy. Cell 98: 465-474.

108. Crosbie RH, Heighway J, Venzke DP, Lee JC, Campbell KP (1997) Sarcospan, the 25-kDa transmembrane component of the dystrophin-glycoprotein complex. J Biol Chem 272: 31221-31224.

109. O'Brien KF, Engle EC, Kunkel LM (2001) Analysis of human sarcospan as a candidate gene for CFEOM1. BMC Genet 2: 3.

110. Lebakken CS, Venzke DP, Hrstka RF, Consolino CM, Faulkner JA, et al. (2000) Sarcospan-deficient mice maintain normal muscle function. Mol Cell Biol 20: 1669-1677.

111. Peter AK, Marshall JL, Crosbie RH (2008) Sarcospan reduces dystrophic pathology: stabilization of the utrophin-glycoprotein complex. J Cell Biol 183: 419-427.

112. Wagner KR, Cohen JB, Huganir RL (1993) The 87K postsynaptic membrane protein from Torpedo is a protein-tyrosine kinase substrate homologous to dystrophin. Neuron 10: 511-522.

113. Yoshida M, Yamamoto H, Noguchi S, Mizuno Y, Hagiwara Y, et al. (1995) Dystrophin-associated protein A0 is a homologue of the Torpedo 87K protein. FEBS Lett 367: 311-314.

114. Sadoulet-Puccio HM, Rajala M, Kunkel LM (1997) Dystrobrevin and dystrophin: an interaction through coiled-coil motifs. Proc Natl Acad Sci U S A 94: 12413-12418.

115. Nawrotzki R, Loh NY, Ruegg MA, Davies KE, Blake DJ (1998) Characterisation of alpha-dystrobrevin in muscle. J Cell Sci 111 (Pt 17): 2595-2605.

116. Peters MF, Sadoulet-Puccio HM, Grady MR, Kramarcy NR, Kunkel LM, et al. (1998) Differential membrane localization and intermolecular associations of alpha-dystrobrevin isoforms in skeletal muscle. J Cell Biol 142: 1269-1278.

117. Grady RM, Grange RW, Lau KS, Maimone MM, Nichol MC, et al. (1999) Role for alpha-dystrobrevin in the pathogenesis of dystrophin-dependent muscular dystrophies. Nat Cell Biol 1: 215-220.

118. Bunnell TM, Jaeger MA, Fitzsimons DP, Prins KW, Ervasti JM (2008) Destabilization of the dystrophin-glycoprotein complex without functional deficits in alpha-dystrobrevin null muscle. PLoS One 3: e2604.

119. Dwyer TM, Froehner SC (1995) Direct binding of Torpedo syntrophin to dystrophin and the 87 kDa dystrophin homologue. FEBS Lett 375: 91-94.

120. Butler MH, Douville K, Murnane AA, Kramarcy NR, Cohen JB, et al. (1992) Association of the Mr 58,000 postsynaptic protein of electric tissue with Torpedo dystrophin and the Mr 87,000 postsynaptic protein. J Biol Chem 267: 6213-6218.

121. Adams ME, Dwyer TM, Dowler LL, White RA, Froehner SC (1995) Mouse alpha 1- and beta 2-syntrophin gene structure, chromosome localization, and homology with a discs large domain. J Biol Chem 270: 25859-25865.

122. Gibson TJ, Hyvonen M, Musacchio A, Saraste M, Birney E (1994) PH domain: the first anniversary. Trends Biochem Sci 19: 349-353.

123. Iwata Y, Shigekawa M, Wakabayashi S (2005) Cardiac syntrophin isoforms: species-dependent expression, association with dystrophin complex and subcellular localization. Mol Cell Biochem 268: 59-66.

124. Suzuki A, Yoshida M, Ozawa E (1995) Mammalian alpha 1- and beta 1-syntrophin bind to the alternative splice-prone region of the dystrophin COOH terminus. J Cell Biol 128: 373-381.

125. Adams ME, Mueller HA, Froehner SC (2001) In vivo requirement of the alpha-syntrophin PDZ domain for the sarcolemmal localization of nNOS and aquaporin-4. J Cell Biol 155: 113-122.

126. Gee SH, Madhavan R, Levinson SR, Caldwell JH, Sealock R, et al. (1998) Interaction of muscle and brain sodium channels with multiple members of the syntrophin family of dystrophin-associated proteins. J Neurosci 18: 128-137.

127. Brenman JE, Chao DS, Gee SH, McGee AW, Craven SE, et al. (1996) Interaction of nitric oxide synthase with the postsynaptic density protein PSD-95 and alpha1-syntrophin mediated by PDZ domains. Cell 84: 757-767.

128. Abramovici H, Hogan AB, Obagi C, Topham MK, Gee SH (2003) Diacylglycerol kinase-zeta localization in skeletal muscle is regulated by phosphorylation and interaction with syntrophins. Mol Biol Cell 14: 4499-4511.

129. Hogan A, Shepherd L, Chabot J, Quenneville S, Prescott SM, et al. (2001) Interaction of gamma 1-syntrophin with diacylglycerol kinase-zeta. Regulation of nuclear localization by PDZ interactions. J Biol Chem 276: 26526-26533.

130. Kameya S, Miyagoe Y, Nonaka I, Ikemoto T, Endo M, et al. (1999) alpha1-syntrophin gene disruption results in the absence of neuronal-type nitric-oxide synthase at the sarcolemma but does not induce muscle degeneration. J Biol Chem 274: 2193-2200.

131. Sabourin J, Lamiche C, Vandebrouck A, Magaud C, Rivet J, et al. (2009) Regulation of TRPC1 and TRPC4 cation channels requires an alpha1-syntrophin-dependent complex in skeletal mouse myotubes. J Biol Chem 284: 36248-36261.

132. Tinsley JM, Blake DJ, Roche A, Fairbrother U, Riss J, et al. (1992) Primary structure of dystrophin-related protein. Nature 360: 591-593.

133. Galkin VE, Orlova A, VanLoock MS, Rybakova IN, Ervasti JM, et al. (2002) The utrophin actin-binding domain binds F-actin in two different modes:

implications for the spectrin superfamily of proteins. J Cell Biol 157: 243-251.

134. Rybakova IN, Humston JL, Sonnemann KJ, Ervasti JM (2006) Dystrophin and utrophin bind actin through distinct modes of contact. J Biol Chem 281: 9996-10001.

135. Amann KJ, Guo AW, Ervasti JM (1999) Utrophin lacks the rod domain actin binding activity of dystrophin. J Biol Chem 274: 35375-35380.

136. Ohlendieck K, Ervasti JM, Matsumura K, Kahl SD, Leveille CJ, et al. (1991) Dystrophin-related protein is localized to neuromuscular junctions of adult skeletal muscle. Neuron 7: 499-508.

137. Schofield J, Houzelstein D, Davies K, Buckingham M, Edwards YH (1993) Expression of the dystrophin-related protein (utrophin) gene during mouse embryogenesis. Dev Dyn 198: 254-264.

138. Pons F, Robert A, Fabbrizio E, Hugon G, Califano JC, et al. (1994) Utrophin localization in normal and dystrophin-deficient heart. Circulation 90: 369-374.

139. Nguyen TM, Ellis JM, Love DR, Davies KE, Gatter KC, et al. (1991) Localization of the DMDL gene-encoded dystrophin-related protein using a panel of nineteen monoclonal antibodies: presence at neuromuscular junctions, in the sarcolemma of dystrophic skeletal muscle, in vascular and other smooth muscles, and in proliferating brain cell lines. J Cell Biol 115: 1695-1700.

140. Mizuno Y, Nonaka I, Hirai S, Ozawa E (1993) Reciprocal expression of dystrophin and utrophin in muscles of Duchenne muscular dystrophy patients, female DMD-carriers and control subjects. J Neurol Sci 119: 43-52.

141. Ervasti JM, Campbell KP (1991) Membrane organization of the dystrophin-glycoprotein complex. Cell 66: 1121-1131.

142. Yoshida M, Suzuki A, Yamamoto H, Noguchi S, Mizuno Y, et al. (1994) Dissociation of the complex of dystrophin and its associated proteins into several unique groups by n-octyl beta-D-glucoside. Eur J Biochem 222: 1055-1061.

143. Hack AA, Ly CT, Jiang F, Clendenin CJ, Sigrist KS, et al. (1998) Gamma-sarcoglycan deficiency leads to muscle membrane defects and apoptosis independent of dystrophin. J Cell Biol 142: 1279-1287.

144. Araishi K, Sasaoka T, Imamura M, Noguchi S, Hama H, et al. (1999) Loss of the sarcoglycan complex and sarcospan leads to muscular dystrophy in beta-sarcoglycan-deficient mice. Hum Mol Genet 8: 1589-1598.

145. Ohlendieck K, Campbell KP (1991) Dystrophin-associated proteins are greatly reduced in skeletal muscle from mdx mice. J Cell Biol 115: 1685-1694.

146. Townsend D, Blankinship MJ, Allen JM, Gregorevic P, Chamberlain JS, et al. (2007) Systemic administration of micro-dystrophin restores cardiac geometry and prevents dobutamine-induced cardiac pump failure. Mol Ther 15: 1086-1092.

147. Bulfield G, Siller WG, Wight PA, Moore KJ (1984) X chromosome-linked muscular dystrophy (mdx) in the mouse. Proc Natl Acad Sci U S A 81: 1189-1192.

148. Bulfield G, Moore EA, Kacser H (1978) Genetic variation in activity of the enzymes of glycolysis and gluconeogenesis between inbred strains of mice. Genetics 89: 551-561.

149. Sicinski P, Geng Y, Ryder-Cook AS, Barnard EA, Darlison MG, et al. (1989) The molecular basis of muscular dystrophy in the mdx mouse: a point mutation. Science 244: 1578-1580.

150. Bonuccelli G, Sotgia F, Schubert W, Park DS, Frank PG, et al. (2003) Proteasome inhibitor (MG-132) treatment of mdx mice rescues the expression and membrane localization of dystrophin and dystrophin-associated proteins. Am J Pathol 163: 1663-1675.

151. Quinlan JG, Hahn HS, Wong BL, Lorenz JN, Wenisch AS, et al. (2004) Evolution of the mdx mouse cardiomyopathy: physiological and morphological findings. Neuromuscul Disord 14: 491-496.

152. Stedman HH, Sweeney HL, Shrager JB, Maguire HC, Panettieri RA, et al. (1991) The mdx mouse diaphragm reproduces the degenerative changes of Duchenne muscular dystrophy. Nature 352: 536-539.

153. Chamberlain JS, Metzger J, Reyes M, Townsend D, Faulkner JA (2007) Dystrophin-deficient mdx mice display a reduced life span and are susceptible to spontaneous rhabdomyosarcoma. FASEB J 21: 2195-2204.

154. Matsumura K, Ervasti JM, Ohlendieck K, Kahl SD, Campbell KP (1992) Association of dystrophin-related protein with dystrophin-associated proteins in mdx mouse muscle. Nature 360: 588-591.

155. Deconinck AE, Rafael JA, Skinner JA, Brown SC, Potter AC, et al. (1997) Utrophin-dystrophin-deficient mice as a model for Duchenne muscular dystrophy. Cell 90: 717-727.

156. Call JA, Ervasti JM, Lowe DA TAT-muUtrophin mitigates the pathophysiology of dystrophin and utrophin double-knockout mice. J Appl Physiol 111: 200-205.

157. Tinsley J, Deconinck N, Fisher R, Kahn D, Phelps S, et al. (1998) Expression of full-length utrophin prevents muscular dystrophy in mdx mice. Nat Med 4: 1441-1444.

158. Odom GL, Gregorevic P, Allen JM, Finn E, Chamberlain JS (2008) Microutrophin delivery through rAAV6 increases lifespan and improves muscle function in dystrophic dystrophin/utrophin-deficient mice. Mol Ther 16: 1539-1545.

159. Sonnemann KJ, Heun-Johnson H, Turner AJ, Baltgalvis KA, Lowe DA, et al. (2009) Functional substitution by TAT-utrophin in dystrophin-deficient mice. PLoS Med 6: e1000083.

160. Chandrasekharan K, Yoon JH, Xu Y, deVries S, Camboni M, et al. A human-specific deletion in mouse Cmah increases disease severity in the mdx model of Duchenne muscular dystrophy. Sci Transl Med 2: 42ra54.

161. Beastrom N, Lu H, Macke A, Canan BD, Johnson EK, et al. mdx(5cv) Mice Manifest More Severe Muscle Dysfunction and Diaphragm Force Deficits than Do mdx Mice. Am J Pathol 179: 2464-2474.

162. Heydemann A, Ceco E, Lim JE, Hadhazy M, Ryder P, et al. (2009) Latent TGF-beta-binding protein 4 modifies muscular dystrophy in mice. J Clin Invest 119: 3703-3712.

163. Heydemann A, Huber JM, Demonbreun A, Hadhazy M, McNally EM (2005) Genetic background influences muscular dystrophy. Neuromuscul Disord 15: 601-609.

164. Sharp NJ, Kornegay JN, Van Camp SD, Herbstreith MH, Secore SL, et al. (1992) An error in dystrophin mRNA processing in golden retriever muscular dystrophy, an animal homologue of Duchenne muscular dystrophy. Genomics 13: 115-121.

165. Schatzberg SJ, Anderson LV, Wilton SD, Kornegay JN, Mann CJ, et al. (1998) Alternative dystrophin gene transcripts in golden retriever muscular dystrophy. Muscle Nerve 21: 991-998.

166. Valentine BA, Cooper BJ, de Lahunta A, O'Quinn R, Blue JT (1988) Canine X-linked muscular dystrophy. An animal model of Duchenne muscular dystrophy: clinical studies. J Neurol Sci 88: 69-81.

167. Kornegay JN, Tuler SM, Miller DM, Levesque DC (1988) Muscular dystrophy in a litter of golden retriever dogs. Muscle Nerve 11: 1056-1064.

168. Valentine BA, Cooper BJ, Cummings JF, deLahunta A (1986) Progressive muscular dystrophy in a golden retriever dog: light microscope and ultrastructural features at 4 and 8 months. Acta Neuropathol 71: 301-310.

169. Valentine BA, Cummings JF, Cooper BJ (1989) Development of Duchenne-type cardiomyopathy. Morphologic studies in a canine model. Am J Pathol 135: 671-678.

170. Devaux JY, Cabane L, Esler M, Flaouters H, Duboc D (1993) Non-invasive evaluation of the cardiac function in golden retriever dogs by radionuclide angiography. Neuromuscul Disord 3: 429-432.

171. Townsend D, Turner I, Yasuda S, Martindale J, Davis J, et al. Chronic administration of membrane sealant prevents severe cardiac injury and ventricular dilatation in dystrophic dogs. J Clin Invest 120: 1140-1150.

172. Street SF (1983) Lateral transmission of tension in frog myofibers: a myofibrillar network and transverse cytoskeletal connections are possible transmitters. J Cell Physiol 114: 346-364.

173. Danowski BA, Imanaka-Yoshida K, Sanger JM, Sanger JW (1992) Costameres are sites of force transmission to the substratum in adult rat cardiomyocytes. J Cell Biol 118: 1411-1420.

174. Clarke MS, Khakee R, McNeil PL (1993) Loss of cytoplasmic basic fibroblast growth factor from physiologically wounded myofibers of normal and dystrophic muscle. J Cell Sci 106 (Pt 1): 121-133.

175. Menke A, Jockusch H (1991) Decreased osmotic stability of dystrophin-less muscle cells from the mdx mouse. Nature 349: 69-71.

176. Weller B, Karpati G, Carpenter S (1990) Dystrophin-deficient mdx muscle fibers are preferentially vulnerable to necrosis induced by experimental lengthening contractions. J Neurol Sci 100: 9-13.

177. Vilquin JT, Brussee V, Asselin I, Kinoshita I, Gingras M, et al. (1998) Evidence of mdx mouse skeletal muscle fragility in vivo by eccentric running exercise. Muscle Nerve 21: 567-576.

178. Cox GA, Cole NM, Matsumura K, Phelps SF, Hauschka SD, et al. (1993) Overexpression of dystrophin in transgenic mdx mice eliminates dystrophic symptoms without toxicity. Nature 364: 725-729.

179. Lowe DA, Williams BO, Thomas DD, Grange RW (2006) Molecular and cellular contractile dysfunction of dystrophic muscle from young mice. Muscle Nerve 34: 92-100.

180. Ramaswamy KS, Palmer ML, van der Meulen JH, Renoux A, Kostrominova TY, et al. Lateral transmission of force is impaired in skeletal muscles of dystrophic mice and very old rats. J Physiol 589: 1195-1208.

181. Yasuda S, Townsend D, Michele DE, Favre EG, Day SM, et al. (2005) Dystrophic heart failure blocked by membrane sealant poloxamer. Nature 436: 1025-1029.

182. Fanchaouy M, Polakova E, Jung C, Ogrodnik J, Shirokova N, et al. (2009) Pathways of abnormal stress-induced Ca2+ influx into dystrophic mdx cardiomyocytes. Cell Calcium 46: 114-121.

183. Hutter OF, Burton FL, Bovell DL (1991) Mechanical properties of normal and mdx mouse sarcolemma: bearing on function of dystrophin. J Muscle Res Cell Motil 12: 585-589.

184. Delaporte C, Dautreaux B, Rouche A, Fardeau M (1990) Changes in surface morphology and basal lamina of cultured muscle cells from Duchenne muscular dystrophy patients. J Neurol Sci 95: 77-88.

185. Dulhunty AF, Franzini-Armstrong C (1975) The relative contributions of the folds and caveolae to the surface membrane of frog skeletal muscle fibres at different sarcomere lengths. J Physiol 250: 513-539.

186. Wapenaar MC, Kievits T, Hart KA, Abbs S, Blonden LA, et al. (1988) A deletion hot spot in the Duchenne muscular dystrophy gene. Genomics 2: 101-108.

187. den Dunnen JT, Bakker E, Breteler EG, Pearson PL, van Ommen GJ (1987) Direct detection of more than 50% of the Duchenne muscular dystrophy mutations by field inversion gels. Nature 329: 640-642.

188. Henderson DM, Lee A, Ervasti JM Disease-causing missense mutations in actin binding domain 1 of dystrophin induce thermodynamic instability and protein aggregation. Proc Natl Acad Sci U S A 107: 9632-9637.

189. Kerr TP, Sewry CA, Robb SA, Roberts RG (2001) Long mutant dystrophins and variable phenotypes: evasion of nonsense-mediated decay? Hum Genet 109: 402-407.

190. Bies RD, Caskey CT, Fenwick R (1992) An intact cysteine-rich domain is required for dystrophin function. J Clin Invest 90: 666-672.

191. Harper SQ, Hauser MA, DelloRusso C, Duan D, Crawford RW, et al. (2002) Modular flexibility of dystrophin: implications for gene therapy of Duchenne muscular dystrophy. Nat Med 8: 253-261.

192. Phelps SF, Hauser MA, Cole NM, Rafael JA, Hinkle RT, et al. (1995) Expression of full-length and truncated dystrophin mini-genes in transgenic mdx mice. Hum Mol Genet 4: 1251-1258.

193. Gregorevic P, Blankinship MJ, Allen JM, Crawford RW, Meuse L, et al. (2004) Systemic delivery of genes to striated muscles using adeno-associated viral vectors. Nat Med 10: 828-834.

194. Yue Y, Li Z, Harper SQ, Davisson RL, Chamberlain JS, et al. (2003) Microdystrophin gene therapy of cardiomyopathy restores dystrophin-glycoprotein complex and improves sarcolemma integrity in the mdx mouse heart. Circulation 108: 1626-1632.

195. Liu M, Yue Y, Harper SQ, Grange RW, Chamberlain JS, et al. (2005) Adeno-associated virus-mediated microdystrophin expression protects young mdx muscle from contraction-induced injury. Mol Ther 11: 245-256.

196. Gregorevic P, Allen JM, Minami E, Blankinship MJ, Haraguchi M, et al. (2006) rAAV6-microdystrophin preserves muscle function and extends lifespan in severely dystrophic mice. Nat Med 12: 787-789.

197. Gregorevic P, Blankinship MJ, Allen JM, Chamberlain JS (2008) Systemic microdystrophin gene delivery improves skeletal muscle structure and function in old dystrophic mdx mice. Mol Ther 16: 657-664.

198. Cox GA, Sunada Y, Campbell KP, Chamberlain JS (1994) Dp71 can restore the dystrophin-associated glycoprotein complex in muscle but fails to prevent dystrophy. Nat Genet 8: 333-339.

199. Warner LE, DelloRusso C, Crawford RW, Rybakova IN, Patel JR, et al. (2002) Expression of Dp260 in muscle tethers the actin cytoskeleton to the dystrophin-glycoprotein complex and partially prevents dystrophy. Hum Mol Genet 11: 1095-1105.

200. Judge LM, Haraguchiln M, Chamberlain JS (2006) Dissecting the signaling and mechanical functions of the dystrophin-glycoprotein complex. J Cell Sci 119: 1537-1546.

201. Wieneke S, Heimann P, Leibovitz S, Nudel U, Jockusch H (2003) Acute pathophysiological effects of muscle-expressed Dp71 transgene on normal and dystrophic mouse muscle. J Appl Physiol 95: 1861-1866.

202. Greenberg DS, Sunada Y, Campbell KP, Yaffe D, Nudel U (1994) Exogenous Dp71 restores the levels of dystrophin associated proteins but does not alleviate muscle damage in mdx mice. Nat Genet 8: 340-344.

203. Gardner KL, Kearney JA, Edwards JD, Rafael-Fortney JA (2006) Restoration of all dystrophin protein interactions by functional domains in trans does not rescue dystrophy. Gene Ther 13: 744-751.

204. Leibovitz S, Meshorer A, Fridman Y, Wieneke S, Jockusch H, et al. (2002) Exogenous Dp71 is a dominant negative competitor of dystrophin in skeletal muscle. Neuromuscul Disord 12: 836-844.

205. Lai Y, Thomas GD, Yue Y, Yang HT, Li D, et al. (2009) Dystrophins carrying spectrin-like repeats 16 and 17 anchor nNOS to the sarcolemma and enhance exercise performance in a mouse model of muscular dystrophy. J Clin Invest 119: 624-635.

206. Tidball JG, Wehling-Henricks M (2004) Expression of a NOS transgene in dystrophin-deficient muscle reduces muscle membrane damage without increasing the expression of membrane-associated cytoskeletal proteins. Mol Genet Metab 82: 312-320.

207. Wehling M, Spencer MJ, Tidball JG (2001) A nitric oxide synthase transgene ameliorates muscular dystrophy in mdx mice. J Cell Biol 155: 123-131.

208. Kobayashi YM, Rader EP, Crawford RW, Iyengar NK, Thedens DR, et al. (2008) Sarcolemma-localized nNOS is required to maintain activity after mild exercise. Nature 456: 511-515.

209. Crosbie RH, Straub V, Yun HY, Lee JC, Rafael JA, et al. (1998) mdx muscle pathology is independent of nNOS perturbation. Hum Mol Genet 7: 823-829.

210. Holzfeind PJ, Grewal PK, Reitsamer HA, Kechvar J, Lassmann H, et al. (2002) Skeletal, cardiac and tongue muscle pathology, defective retinal transmission, and neuronal migration defects in the Large(myd) mouse defines a natural model for glycosylation-deficient muscle - eye - brain disorders. Hum Mol Genet 11: 2673-2687.

211. Michele DE, Kabaeva Z, Davis SL, Weiss RM, Campbell KP (2009) Dystroglycan matrix receptor function in cardiac myocytes is important for limiting activity-induced myocardial damage. Circ Res 105: 984-993.

212. Hack AA, Cordier L, Shoturma DI, Lam MY, Sweeney HL, et al. (1999) Muscle degeneration without mechanical injury in sarcoglycan deficiency. Proc Natl Acad Sci U S A 96: 10723-10728.

213. Townsend D, Daly M, Chamberlain JS, Metzger JM Age-dependent Dystrophin Loss and Genetic Reconstitution Establish a Molecular Link Between Dystrophin and Heart Performance During Aging. Mol Ther.

214. Armstrong SC, Latham CA, Shivell CL, Ganote CE (2001) Ischemic loss of sarcolemmal dystrophin and spectrin: correlation with myocardial injury. J Mol Cell Cardiol 33: 1165-1179.

215. Xi H, Shin WS, Suzuki J, Nakajima T, Kawada T, et al. (2000) Dystrophin disruption might be related to myocardial cell apoptosis caused by isoproterenol. J Cardiovasc Pharmacol 36 Suppl 2: S25-29.

216. Rodriguez M, Cai WJ, Kostin S, Lucchesi BR, Schaper J (2005) Ischemia depletes dystrophin and inhibits protein synthesis in the canine heart: mechanisms of myocardial ischemic injury. J Mol Cell Cardiol 38: 723-733.

217. Kyoi S, Otani H, Hamano A, Matsuhisa S, Akita Y, et al. (2006) Dystrophin is a possible end-target of ischemic preconditioning against cardiomyocyte oncosis during the early phase of reperfusion. Cardiovasc Res 70: 354-363.

218. Miyazato H, Biro S, Setoguchi M, Maeda M, Tashiro T, et al. (1997) Abnormal immunostaining for dystrophin in isoproterenol-induced acute myocardial injury in rats: evidence for change in dystrophin in the absence of genetic defect. J Mol Cell Cardiol 29: 1217-1223.

219. Toyo-Oka T, Kawada T, Nakata J, Xie H, Urabe M, et al. (2004) Translocation and cleavage of myocardial dystrophin as a common pathway to advanced heart failure: a scheme for the progression of cardiac dysfunction. Proc Natl Acad Sci U S A 101: 7381-7385.

220. Vatta M, Stetson SJ, Jimenez S, Entman ML, Noon GP, et al. (2004) Molecular normalization of dystrophin in the failing left and right ventricle of patients treated with either pulsatile or continuous flow-type ventricular assist devices. J Am Coll Cardiol 43: 811-817.

221. Vatta M, Stetson SJ, Perez-Verdia A, Entman ML, Noon GP, et al. (2002) Molecular remodelling of dystrophin in patients with end-stage cardiomyopathies and reversal in patients on assistance-device therapy. Lancet 359: 936-941.

222. Badorff C, Knowlton KU (2004) Dystrophin disruption in enterovirus-induced myocarditis and dilated cardiomyopathy: from bench to bedside. Med Microbiol Immunol 193: 121-126.

223. McMahon CJ, Vatta M, Fraser CD, Jr., Towbin JA, Chang AC (2004) Altered dystrophin expression in the right atrium of a patient after Fontan procedure with atrial flutter. Heart 90: e65.

224. Campos EC, Romano MM, Prado CM, Rossi MA (2008) Isoproterenol induces primary loss of dystrophin in rat hearts: correlation with myocardial injury. Int J Exp Pathol 89: 367-381.

225. Bodyak N, Kang PM, Hiromura M, Sulijoadikusumo I, Horikoshi N, et al. (2002) Gene expression profiling of the aging mouse cardiac myocytes. Nucleic Acids Res 30: 3788-3794.

226. Cottin P, Poussard S, Mornet D, Brustis JJ, Mohammadpour M, et al. (1992) In vitro digestion of dystrophin by calcium-dependent proteases, calpains I and II. Biochimie 74: 565-570.

227. Takahashi M, Tanonaka K, Yoshida H, Koshimizu M, Daicho T, et al. (2006) Possible involvement of calpain activation in pathogenesis of chronic heart failure after acute myocardial infarction. J Cardiovasc Pharmacol 47: 413-421.

228. Zatz M, Starling A (2005) Calpains and disease. N Engl J Med 352: 2413-2423.

229. Spencer MJ, Mellgren RL (2002) Overexpression of a calpastatin transgene in mdx muscle reduces dystrophic pathology. Hum Mol Genet 11: 2645-2655.

230. Badorff C, Lee GH, Lamphear BJ, Martone ME, Campbell KP, et al. (1999) Enteroviral protease 2A cleaves dystrophin: evidence of cytoskeletal disruption in an acquired cardiomyopathy. Nat Med 5: 320-326.

231. Towbin JA, Vatta M (2007) Myocardial infarction, viral infection, and the cytoskeleton final common pathways of a common disease? J Am Coll Cardiol 50: 2215-2217.

232. Bowles NE, Bowles KR, Towbin JA (2000) The "final common pathway" hypothesis and inherited cardiovascular disease. The role of cytoskeletal proteins in dilated cardiomyopathy. Herz 25: 168-175.

233. Towbin JA, Bowles NE (2002) The failing heart. Nature 415: 227-233.

234. Roger VL, Go AS, Lloyd-Jones DM, Adams RJ, Berry JD, et al. Heart disease and stroke statistics--2011 update: a report from the American Heart Association. Circulation 123: e18-e209.

235. Woodruff JF (1980) Viral myocarditis. A review. Am J Pathol 101: 425-484.

236. Andreoletti L, Venteo L, Douche-Aourik F, Canas F, Lorin de la Grandmaison G, et al. (2007) Active Coxsackieviral B infection is associated with disruption of dystrophin in endomyocardial tissue of

patients who died suddenly of acute myocardial infarction. J Am Coll Cardiol 50: 2207-2214.

237. Gore I, Saphir O (1947) Myocarditis; a classification of 1402 cases. Am Heart J 34: 827-830.

238. Stevens PJ, Ground KE (1970) Occurrence and significance of myocarditis in trauma. Aerosp Med 41: 776-780.

239. Bandt CM, Staley NA, Noren GR (1979) Acute viral myocarditis. Clinical and histologic changes. Minn Med 62: 234-237.

240. Okuni M, Yamada T, Mochizuki S, Sakurai I (1975) Studies on myocarditis in childhood, with special reference to the possible role of immunological process and the thymus in the chronicity of the disease. Jpn Circ J 39: 463-470.

241. Befter WI, Leaman WGJ, Lucchesi PF, Maher IE, Dworin M (1947) The hear in acute anterior poliomyelitis. Am Heart J 33: 228-239.

242. Archard LC, Khan MA, Soteriou BA, Zhang H, Why HJ, et al. (1998) Characterization of Coxsackie B virus RNA in myocardium from patients with dilated cardiomyopathy by nucleotide sequencing of reverse transcription-nested polymerase chain reaction products. Hum Pathol 29: 578-584.

243. Fujioka S, Koide H, Kitaura Y, Deguchi H, Kawamura K, et al. (1996) Molecular detection and differentiation of enteroviruses in endomyocardial biopsies and pericardial effusions from dilated cardiomyopathy and myocarditis. Am Heart J 131: 760-765.

244. Jin O, Sole MJ, Butany JW, Chia WK, McLaughlin PR, et al. (1990) Detection of enterovirus RNA in myocardial biopsies from patients with myocarditis and cardiomyopathy using gene amplification by polymerase chain reaction. Circulation 82: 8-16.

245. Bowles NE, Richardson PJ, Olsen EG, Archard LC (1986) Detection of Coxsackie-B-virus-specific RNA sequences in myocardial biopsy samples from patients with myocarditis and dilated cardiomyopathy. Lancet 1: 1120-1123.

246. Schwaiger A, Umlauft F, Weyrer K, Larcher C, Lyons J, et al. (1993) Detection of enteroviral ribonucleic acid in myocardial biopsies from patients with idiopathic dilated cardiomyopathy by polymerase chain reaction. Am Heart J 126: 406-410.

247. Why HJ, Meany BT, Richardson PJ, Olsen EG, Bowles NE, et al. (1994) Clinical and prognostic significance of detection of enteroviral RNA in the

myocardium of patients with myocarditis or dilated cardiomyopathy. Circulation 89: 2582-2589.

248. Drory Y, Turetz Y, Hiss Y, Lev B, Fisman EZ, et al. (1991) Sudden unexpected death in persons less than 40 years of age. Am J Cardiol 68: 1388-1392.

249. Roivainen M, Alfthan G, Jousilahti P, Kimpimaki M, Hovi T, et al. (1998) Enterovirus infections as a possible risk factor for myocardial infarction. Circulation 98: 2534-2537.

250. Chapman NM, Kim KS, Drescher KM, Oka K, Tracy S (2008) 5' terminal deletions in the genome of a coxsackievirus B2 strain occurred naturally in human heart. Virology 375: 480-491.

251. Kim KS, Chapman NM, Tracy S (2008) Replication of coxsackievirus B3 in primary cell cultures generates novel viral genome deletions. J Virol 82: 2033-2037.

252. Blom N, Hansen J, Blaas D, Brunak S (1996) Cleavage site analysis in picornaviral polyproteins: discovering cellular targets by neural networks. Protein Sci 5: 2203-2216.

253. Badorff C, Berkely N, Mehrotra S, Talhouk JW, Rhoads RE, et al. (2000) Enteroviral protease 2A directly cleaves dystrophin and is inhibited by a dystrophin-based substrate analogue. J Biol Chem 275: 11191-11197.

254. Xiong D, Yajima T, Lim BK, Stenbit A, Dublin A, et al. (2007) Inducible cardiac-restricted expression of enteroviral protease 2A is sufficient to induce dilated cardiomyopathy. Circulation 115: 94-102.

255. Xiong D, Lee GH, Badorff C, Dorner A, Lee S, et al. (2002) Dystrophin deficiency markedly increases enterovirus-induced cardiomyopathy: a genetic predisposition to viral heart disease. Nat Med 8: 872-877.

256. Lamphear BJ, Yan R, Yang F, Waters D, Liebig HD, et al. (1993) Mapping the cleavage site in protein synthesis initiation factor eIF-4 gamma of the 2A proteases from human Coxsackievirus and rhinovirus. J Biol Chem 268: 19200-19203.

257. Joachims M, Van Breugel PC, Lloyd RE (1999) Cleavage of poly(A)-binding protein by enterovirus proteases concurrent with inhibition of translation in vitro. J Virol 73: 718-727.

258. DeWolf C, McCauley P, Sikorski AF, Winlove CP, Bailey AI, et al. (1997) Interaction of dystrophin fragments with model membranes. Biophys J 72: 2599-2604.

259. Helliwell TR, Ellis JM, Mountford RC, Appleton RE, Morris GE (1992) A truncated dystrophin lacking the C-terminal domains is localized at the muscle membrane. Am J Hum Genet 50: 508-514.

260. Rafael JA, Cox GA, Corrado K, Jung D, Campbell KP, et al. (1996) Forced expression of dystrophin deletion constructs reveals structure-function correlations. J Cell Biol 134: 93-102.

261. Dunckley MG, Wells KE, Piper TA, Wells DJ, Dickson G (1994) Independent localization of dystrophin N- and C-terminal regions to the sarcolemma of mdx mouse myofibres in vivo. J Cell Sci 107 (Pt 6): 1469-1475.

262. Barnabei MS, Martindale JM, Townsend D, Metzger JM (2011) Exercise and Muscular Dystrophy: Implications and Analysis of Effects on Musculoskeletal and Cardiovascular Systems. Compr Physiol 1: 1353-1363.

Chapter 2

Influence of genetic background on *ex vivo* and *in vivo* cardiac function in several commonly used inbred mouse strains[1]

Abstract

Inbred mouse strains play a critical role in biomedical research. Genetic homogeneity within inbred strains and their general amenability to genetic manipulation has made them an ideal resource for dissecting the physiological function(s) of individual genes. However, the inbreeding that makes inbred mice so useful also results in genetic divergence between them. This genetic divergence is often unaccounted for, but may be a confounding factor when comparing studies which have utilized distinct inbred strains. Here, we compared the cardiac function of C57BL/6J mice to seven other commonly used inbred mouse strains: FVB/NJ, DBA/2J, C3H/HeJ, BALB/cJ, 129X1/SvJ, C57BL/10SnJ and 129SvImJ. The assays used to compare cardiac function were the *ex vivo* isolated Langendorff heart preparation and *in vivo* real time hemodynamic analysis using conductance micromanometry. We report significant strain–dependent differences in cardiac function between C57BL/6J

[1] This manuscript was previously published in *Physiological Genomics* and is copyrighted by the American Physiological Society (APS). It has been reproduced here in accordance with APS copyright policy (http://www.the-aps.org/publications/authorinfo/copyright.htm).

and other commonly used inbred strains. C57BL/6J maintained better cardiac function than most inbred strains during *ex vivo* ischemia, particularly when compared to 129SvImJ, 129X1/SvJ and C57BL/10SnJ strains. However, during *in vivo* acute hypoxia 129X1/SvJ and 129SvImJ maintained relatively normal cardiac function, whereas C57BL/6J animals showed dramatic cardiac decompensation. Additionally, C3H/HeJ showed rapid and marked cardiac decompensation in response to esmolol infusion compared with other strains. These findings demonstrate the complexity of genetic divergence between inbred strains on cardiac function. These results may help inform analysis of gene ablation or transgenic studies and further demonstrate specific quantitative traits that could be useful in discovery of genetic modifiers relevant to cardiac health and disease.

Introduction

For decades biomedical research has relied heavily on the use of inbred mouse strains. The genetic homogeneity within these strains allows for well-controlled and highly reproducible studies. Over 450 distinct inbred strains have been described in the literature [1], the genomes of numerous commonly used inbred strains have been sequenced [2], and the Jackson Laboratory alone maintains over 180 inbred mouse strains (http://jaxmice.jax.org/list/cat481365.html). The most common strain of inbred mice used in research is the C57BL/6 mouse. This strain is the most commonly

used background of genetically modified mouse strains maintained by the Jackson Laboratory (http://jaxmice.jax.org/manual/strains_cataolog.pdf).

Though not as widely used, other inbred strains have found niches in biomedical research due to ease of genetic manipulation or differing propensities for developing specific pathologies. For instance, FVB/N mice are commonly used in conventional transgenesis [3] and 129 substrains have been used almost exclusively for the isolation of embryonic stem (ES) cells used for gene targeting [4,5]. Alternatively, other inbred strains have found use as disease models due to naturally occurring mutations in genes linked to human disease [6,7,8,9]. Even in the absence of engineered or known naturally occurring mutations, different inbred mouse strains can vary drastically in their susceptibility to clinically relevant diseases. Previous reports have taken advantage of this naturally occurring variation in susceptibility to a particular disease to identify quantitative trait loci (QTL) which modify disease pathogenesis [10,11,12,13,14].

Cardiovascular disease is the single leading cause of death in the United States, affecting approximately 1 in 3 Americans and causing over 800,000 deaths in 2006 [15]. To effectively investigate the pathological processes associated with cardiovascular disease and devise new therapeutic strategies, the cardiovascular field has embraced genetically modified inbred mouse strains as tools to help understand the fundamental physiological processes governing function in the normal and diseased heart. A survey of the Jackson Labs website shows that they maintain over 225 genetically modified mouse lines used for cardiovascular research derived from inbred mouse strains. C57BL/6 is the most

common genetic background (Figure 2-1a). However, mutations are also maintained on other common inbred backgrounds as well. The majority of these mice were created using embryonic stem (ES) cells derived from a substrain of the 129 inbred strain, then often backcrossed and maintained on a C57BL/6 or mixed C57BL/6 x 129 background (Figure 2-1b).

Several studies have reported strain-dependent differences in cardiovascular function between inbred mouse strains by various *in vitro* and *in vivo* methods [16,17,18,19,20,21]. The majority of these strain-dependent differences in cardiac physiology have been carried out on a small subset of inbred strains in the absence of disease-related injury/stress. Previous reports have also demonstrated the potent effects of genetic background on modifying the cardiac phenotype of genetically modified mice [22,23,24]. For instance, two distinct transgenic lines expressing hypertrophic cardiomyopathy-linked mutant tropomyosin E108G showed drastically different phenotypes, one displaying relatively mild diastolic dysfunction [25] and the other developing overt hypertrophic cardiomyopathy and heart failure [26]. Excluding possible differences in animal care and housing, the main difference between these transgenic mice is their genetic background; one mouse was created on the FVB/N background, the other on the C57BL/6 background. Although the precise mechanism underlying this effect is not understood, the phenotypic variation between these two transgenic lines contributes to the impetus for this study.

The purpose of this study was to compare the cardiac function of eight commonly used inbred mouse strains at rest and following physiologically

relevant stress/injury. The rationale for conducting these studies is two-fold. First, the large number of inbred strains used in medical research necessitates a consideration for the physiological differences that arise from genetic divergence between strains. Secondly, the fixed genetic divergence between inbred mouse strains serves as a potential substrate for the identification of reproducible quantitative traits that differ between inbred strains. Eight common inbred strains were used, six of which are listed on Jackson Laboratory's list of the most popular inbred mouse strains (http://jaxmice.jax.org/findmice/popular.html). The techniques used to measure cardiac function for this study are the Langendorff perfused isolated heart preparation and *in vivo* cardiac hemodynamic function as measured by catheter-based conductance micromanometry. The Langendorff preparation is a well established technique for assessing function of a heart performing isovolumic contractions at a controlled end diastolic pressure [27,28]. *In vivo* hemodynamic analysis provides pressure and volume measurements of hearts in the intact animal where physiological loading and autonomic innervation remain intact [29]. Additionally, we studied strain-dependent differences in cardiac function following physiologically relevant stresses. Specifically, isolated hearts were subjected to ischemia and reperfusion (Day, Nature Med, 2005). Mice instrumented for *in vivo* hemodynamic measurements were subjected to β-adrenergic blockade and an acute hypoxic challenge. Strain-dependent differences in cardiac function were found both at baseline and following physiologically relevant stress. Collectively, this study highlights strain-dependent differences between inbred mice which provide insight into marked

physiological divergence reported for cardiac transgenic mice generated on differing backgrounds. The identification here of strain-dependent quantitative hemodynamic traits may form the foundation of future studies aimed at identifying QTL that modify cardiac function.

Materials and Methods

Mouse Strains. All mouse strains analyzed in this study were acquired from Jackson labs. Mouse strains and stock numbers were as follows: C57BL/6J (000664), FVB/NJ (001800), DBA/2J (000671), BALB/cJ (000651), C3H/HeJ (000659), 129X1/SvJ (000691), C57BL/10SnJ (000666), and 129S1/SvImJ (002448). Male mice ages 4-6 months were used in this study. The procedures used in this study are in agreement with the guidelines of the University of Minnesota and approved by the University of Minnesota Committee on the Use and Care of Animals.

Isolated heart model and ischemia/reperfusion. Ex vivo measurements of left ventricular function were carried out as previously described [30]. Mice were injected with 300 units sodium heparin and anesthetized with sodium pentobarbital. The heart and lungs were then removed following thoracotomy and placed immediately in ice cold Hank's Buffered Salt Solution without calcium and magnesium. The lungs and thymus were trimmed away to expose the aorta which was then cannulated. Hearts were then perfused at a constant pressure of 80 mmHg with modified Krebs-Henseleit Buffer (118 mM NaCl, 4.7 mM KCl, 1.2

mM $MgSO_4$, 1.2 mM KH_2PO_4, 10 mM glucose, 25 mM $NaHCO_3$, 2.5 mM $CaCl_2$, 0.5 mM EDTA) warmed to 37 degrees and brought to pH = 7.4 by bubbling with 95% 02, 5% CO_2. Hearts were paced at 7 Hz and changes in left ventricular pressure were monitored by insertion of a water-filled balloon with an in-line pressure transducer into the left ventricle. Within the left ventricle, the balloon was inflated to an end diastolic pressure of 3-8 mmHg. Following 10-15 minutes of stabilization time, hearts were subjected to global no-flow ischemia for 20 minutes. Hearts were not paced during ischemia. Hearts were then reperfused for 60 minutes and pacing was reinitiated at 8 minutes following the end of ischemia. Data was collected at a sampling rate of 400 hz and analyzed using Chart 6 software (ADInstruments).

In Vivo Conductance Micromanometry. Measurements of real time in vivo cardiovascular hemodynamics were obtained using conductance micromanometry as previously [31,32,33,34]. Mice were anesthetized and ventilated via a tracheal cannulation and ventilated via a pressure controlled ventilator with 2% isoflurane at a peak inspiratory pressure of 15 cm H_2O and a respiratory rate of 60 breaths/min. With aid of a dissecting microscope, the heart was exposed via a thoracotomy. A 1.4 French Millar pressure-volume catheter (PVR-1045; Millar Instruments Inc., Houston, Texas, USA) was then placed into the left ventricular chamber via an apical stab. LV pressure and volume measurements were collected at a sampling rate of 1 kHz. Data were analyzed with Ponemah software, P3 Plus (DSI International, St. Paul, MN, USA).

Transient inferior vena cava (IVC) occlusions were performed to obtain the end systolic and end diastolic pressure-volume relationships. IVC occlusions were performed at baseline and at the end of the esmolol (Brevibloc) infusion. After obtaining baseline hemodynamics (ventilated with isoflurane and O_2), mice received a continuous infusion of esmolol (188 ug/kg/min) for five minutes to block all adrenergic responsiveness. After esmolol infusion, mice were infused with dobutamine (42 ug/kg/min) to enable recovery of baseline function (Table 2-1). After dobutamine infusion cardiac function was allowed to return to baseline levels. Mice were then exposed to an acute hypoxic challenge (7% O_2 balanced in nitrogen) and monitored until cardiac pump failure. End-point cardiac decompensation was defined as the point when peak LV systolic pressure dropped below 60 mmHg. At this point mice were recovered using 100% O_2 in order to obtain instrument calibration.

Statistics. All results are expressed as mean ± SEM. Significance was established as $P < 0.05$. All multivariable assays were assessed using a one way analysis of variance (ANOVA) with Dunnets post-hoc test comparing all groups to C57BL/6. Survival after the *in vivo* acute hypoxic challenge was assessed by the Fisher exact test.

Results

Baseline ex vivo cardiac function. To quantify strain-specific differences in *ex vivo* cardiac function, hearts from eight inbred mouse strains were isolated

and perfused retrograde through the aorta. To simplify data analysis, all inbred strains were compared to the C57BL/6J strain. In general, baseline *ex vivo* whole heart function of the inbred strains tested was similar to C57BL/6J (Table 1). One notable exception was FVB/NJ, which showed significantly higher left ventricular developed pressure (LVDP) than C57BL/6J (Table 2-2, $P < 0.05$). Additionally, FVBN/J mice showed significantly higher coronary flow rates than C57BL/6J mice at baseline (Table 2-3, $P < 0.05$). There were no significant differences between C57BL/6J and other inbred strains as measured by the maximum derivative of left ventricular pressure, another measure of systolic function (Table 2-2). There were no significant differences in diastolic function at baseline between C57BL/6J and other inbred strains as measured by the minimum derivative of left ventricular pressure and the rate constant tau (Table 2-2). A previous report showed that BALB/c mice have highly variable contractile function in the isolated working heart preparation associated inter-animal variability in α-skeletal actin expression [35]. However, in our hands the variance of left ventricular developed pressure for BALB/cJ mice was statistically similar to all other strains by Bartlett's analysis of variance (data not shown).

Effects of ischemia and reperfusion on ex vivo cardiac function. To study strain dependent differences in the response to a physiologically relevant stress, isolated hearts were subjected to 20 minutes of global ischemia followed by 60 minutes of reperfusion (Figures 2-2, 2-3). During reperfusion, three strains showed reduced cardiac function compared to C57BL/6J: 129X1/SvJ,

129S1/SvImJ, and C57BL/10SnJ. Each of these strains showed reduced systolic function during early (20 minutes) reperfusion compared to C57BL/6J as shown by reduced LVDP and % recovery of baseline LVDP (Figure 2-2, 2-3a, $P < 0.05$). Additionally, these strains showed reduced diastolic function compared to C57BL/6J as shown by increased LVEDP (Figure 2-2, 2-3a, $P < 0.05$). During late (60 minutes) reperfusion, 129S1/SvImJ showed reduced systolic function compared to C57BL/6J as shown by reduced LVDP and recovery of baseline LVDP (Figure 2-2, 2-3b, $P < 0.05$). 129X1/SvJ showed reduced diastolic function compared to C57BL/6J during late reperfusion as shown by increased LVEDP (Figures 2-2, 2-3b, $P < 0.05$). Additionally, the duration of sustained ventricular tachycardia (VTach) during reperfusion was also recorded as a measure of ischemic injury [36]. C57BL/6J rarely entered into VTach during reperfusion. However, 129X1/SvJ and C57BL/10SnJ entered into VTach for >20 minutes during reperfusion (Figure 2-3c, $P < 0.05$ compared to C57BL/6J). Because VTach generally occurs early in reperfusion, this finding suggests that depressed systolic function of 129X1/SvJ and C57BL/10SnJ during early reperfusion is caused by increased heart rate as described by the Frank-Starling relationship. This is supported by the finding that systolic function of 129X1/SvJ and C57BL/10SnJ were similar to C57BL/6J once VTach had resolved during late reperfusion. 129SvImJ rarely entered into VTach, suggesting that reduced systolic function in these mice was due to reduced contractility following ischemic injury. In addition to 129X1/SvJ, C57BL/10SnJ, and 129S1/SvImJ, several other strains showed more subtle differences in cardiac function compared to

C57BL/6J during *ex vivo* ischemia and reperfusion. These data can be found in Figure 2-4.

Additionally, to demonstrate the stability and reproducibility of these findings, Figure 2-5 shows the results of an initial study carried out with cohorts of FVB/NJ, C3H/HeJ and BALB/cJ mice. As above, isolated hearts from these mice were subjected to *ex vivo* ischemia and reperfusion. The findings of this initial study were comparable with those of the main study, supporting the reproducibility of our findings.

In Vivo Baseline Hemodynamic Function. To study differences in real time *in vivo* hemodynamic function between inbred strains, mice were instrumented with a 1.4 French Millar conductance micromanometry catheter. This methodology allows for precise, real-time assessment of cardiac function by simultaneous measurement of left ventricular pressure and volume [29]. There were significant differences in systolic and diastolic function between C57BL/6J and other strains at baseline, with C57BL/6J generally displaying higher cardiac function than the other strains tested (Figure 2-6, Table 2-4). In measures of systolic function, C57BL/6J mice showed increased left ventricular systolic pressure (LVSP) compared to FVB/NJ, DBA/2J, BALB/cJ and C3H/HeJ mice, as well as increased maximal dP/dt compared to BALB/cJ mice (Figure 2-6, $P < 0.05$). C3H/HeJ mice showed a greater ejection fraction than C57BL/6J. However, this may have been a manifestation of smaller cardiac dimensions in C3H/HeJ mice as they showed reduced heart weight and maximum volume

compared to C57BL/6J mice (Table 2-5, Figure 2-6, $P < 0.05$). C57BL/6J mice also displayed greater diastolic function compared to other inbred strains, as shown by a more negative minimum dP/dt compared to DBA/2J and BALB/cJ (Figure 2-6, $P < 0.05$).

In Vivo Hemodynamic function during β-adrenergic blockade. We next investigated strain-dependent differences in the effects of adrenergic signaling on cardiac function. Here, *in vivo* hemodynamic function was recorded during an acute infusion of the beta-blocker esmolol. This manipulation allows the dissection of the role of adrenergic signaling in maintaining normal cardiovascular performance in different mouse strains. Comparison of the response to esmolol infusion revealed strain dependent variation in cardiac function during β-blockade (Figure 2-7, Table 2-6). In the absence of beta-adrenergic signaling, and similar to baseline *in vivo* functional measurements, C57BL/6J mice maintained higher levels of cardiac function compared to most, but not all, of the inbred strains tested (Figure 2-7b). As described above, there were significant differences in cardiac function between inbred strains at baseline. To account for these differences in baseline function when assessing the effects of beta-adrenergic blockade on cardiac function, the difference between functional parameters at baseline and following 3 minutes of esmolol infusion was determined (Figure 2-7c). Esmolol infusion caused a general depression in cardiac function of all strains tested. However, there were strain-dependent differences in the degree to beta-blockade depressed cardiac

function. In particular, esmolol infusion had a marked effect on the cardiac function of C3H/HeJ mice (Figure 2-7c). All C3H/HeJ mice underwent severe cardiac decompensation within 3 minutes of the start of esmolol infusion as shown by greater reductions in LVSP, EF, and maximum dP/dt compared to C57BL/6J (Figure 2-7c, $P < 0.05$). The effects of beta-blockade were also more severe on 129X1/SvJ compared to C57BL/6J as shown by greater reductions in maximum dP/dt and LVSP (Figure 2-7c, $P < 0.05$). C57BL/10SnJ showed a greater decrease in EF compared to C57BL/6J followed esmolol infusion as well (Figure 2-7c, $P < 0.05$).

In vivo Hemodynamic function during an acute hypoxic challenge. To assess the capacity for inbred mouse strains to respond to an acute cardiac stress, mice instrumented with a pressure-volume catheter were exposed to an acute hypoxic challenge by ventilation with 7% oxygen [30]. Significant differences in cardiac function and survival were observed between C57BL/6J and other inbred strains during this challenge (Figure 2-8). To assess cardiac function during hypoxia, hemodynamic parameters were compared 6 minutes, 40 seconds into the hypoxic challenge at which time C57BL/6J mice underwent cardiac decompensation as defined in the methods section. Unlike our findings at baseline and during esmolol infusion, C57BL/6J mice showed relatively poor cardiac function during an acute hypoxic challenge compared to other inbred strains (Figure 2-8b and Table 2-7). To account for differences in baseline function when determining the strain-dependent differences in the response to

hypoxia, the difference between functional parameters at baseline and following acute hypoxia was determined (Figure 2-8c). Unlike the effects of beta-blockade, acute hypoxia had much more severe effects on the cardiac function of C57BL/6J mice than most other inbred strains tested. 129X1/SvJ, 129SvImJ and FVB/NJ maintained contractility to a greater degree compared to C57BL/6J during acute hypoxia as shown by less negative change in LVSP following hypoxia (Figure 2-8c, $P < 0.05$). Additionally, FVB/NJ, BALB/cJ, 129X1/SvJ and 129S1/SvImJ showed greater maintenance of EF, SV, and maximum dP/dt following hypoxia compared to C57BL/6J (Figure 2-8c, $P < 0.05$). FVB/NJ, DBA/2J, BALB/cJ, C3H/HeJ, 129X1/SvJ and 129S1/SvImJ showed greater maintenance of stroke work following hypoxia compared to C57BL/6J (Figure 2-8c, $P < 0.05$). Analysis of survival during acute hypoxia also emphasizes the functional deficit of C57BL/6J mice compared to other inbred strains. C57BL/6J mice showed significantly shorter survival during hypoxia compared to DBA/2J, FVB/NJ, C3H/HeJ, BALB/cJ, 129X1/SvJ and 129SvImJ (Figure 2-8c, $P < 0.05$). C57BL/10SnJ was the only strain that did not perform significantly better than C57Bl/6J during acute hypoxia.

Discussion

To our knowledge this is the first detailed comparative analysis of *in vivo* and *ex vivo* heart performance between several commonly used inbred strains. In the past decade, there have been tremendous advances in cardiac biology enabled by exquisite cardiac transgenesis and gene targeting studies in mice

[37,38,39,40,41,42,43]. Cardiac transgenic, knockout and other genetically modified mice have been created and backcrossed to a wide array of inbred mouse strains, including those tested in this study. As the number of genetically modified mouse models used in cardiovascular research continues to grow, so to does the need to identify and appreciate the differences in cardiovascular physiology that arise specially from the genetic diversity within these inbred mouse strains.

One main finding of this study is that genetic divergence between commonly used inbred mouse strains significantly affects cardiac function. All inbred strains showed functional divergence from C57BL/6J to some degree. In *ex vivo* preparations, most inbred strains were similar to C57BL/6J which is in general agreement with previously published findings on baseline *ex vivo* cardiac function [17]. However, following ischemic injury 129X1/SvJ, C57BL/10SnJ and 129S1/SvImJ showed significantly reduced cardiac function compared to C57BL/6J. C57BL/10SnJ and 129X1/SvJ showed reduced function that was associated with a higher incidence of sustained VTach during the early periods of reperfusion compared to C57BL/6J. This is in agreement with previously published findings that isolated C57BL/6 hearts are relatively resistant to arrhythmia [44]. This suggests that C57BL/10SnJ and 129S1/SvJ differ from C57BL/6J in their propensity for arrhythmogenicity, and not in contractility, following ischemic injury. Conversely, 129S1/SvImJ showed reduced cardiac function throughout reperfusion in the absence of VTach, suggesting that ischemic injury compromises contractility of these mice without promoting

arrhythmia. *In vivo* hemodynamic analyses also showed strain-dependent differences in cardiac function between C57BL/6J and other inbred strains. The most striking of these was the effect of esmolol on C3H/HeJ mice. As expected, beta-adrenergic blockade reduced cardiac function of all mice to some degree. However, esmolol infusion caused severe cardiac decompensation of C3H/HeJ within 3 minutes, whereas other inbred strains maintained a reduced, but sustainable, level of cardiac function. Additionally, C57BL/6J mice showed greater susceptibility to hypoxia compared to all inbred strains with the exception of the closely related C57BL/10SnJ. This finding under hypoxic challenge is in contrast to the majority of findings in this study, where C57BL/6J performed as well or better than other inbred strains in cardiac performance tests. A recently published study by Shah and colleagues reported a similar finding when comparing the cardiac function of four inbred strains of mice *in vivo* by echocardiography and *in vitro* by recording sarcomere shortening and intracellular calcium handling (CITE SHAH). Compared to other strains tested (BALB/c, C57BL/6 and FVB), 129 mice showed reduced contractility as measured by echo but increased calcium handling and sarcomere shortening *in vitro* [45]. Collectively, these findings suggest that the mechanism by which cardiac performance is modified by genetic divergence between strains are complex and may be governed by specific genetic loci that respond differentially to regulate cardiac function depending on the conditions being used to assess cardiac function.

Although *a priori* we predicted cardiac function to be similar between *in vivo* and *ex vivo* preparations, it is not surprising that differences were observed given the significant differences between these assays [29,46]. Specifically, the absence of physiological loading conditions and autonomic innervation in the *ex vivo* Langendorff preparation are possible reasons for these differences. Additionally, these techniques also differ in their methods of anesthesia. Prior to the extraction and perfusion of the heart for *ex vivo* functional measurements mice are anesthetized with pentobarbital. Pentobarbital is known to depress cardiac function *in vivo* [47,48]. However, once isolated and perfused it is generally believed that the effects of pentobarbital are quickly washed out from the heart [46]. This is supported by the lack of *ex vivo* functional differences between C57BL/6J and DBA/2J hearts, despite previously published findings that DBA mice are highly susceptible to pentobarbital compared to C57BL/6 mice [49]. Conversely, during *in vivo* measurement of cardiac function, mice were constantly anesthetized with isoflurane. Isoflurane has been shown to have strain-dependent cardiodepressive effects *in vivo* [50,51,52,53,54]. Additionally, isoflurane anesthesia has been shown to be cardioprotective from ischemic injury through mechanisms that are not fully understood, but are thought to mimic ischemic preconditioning [55]. Collectively, these previously published findings may provide insights to explain the discrepancies in cardiac function between *ex vivo* and *in vivo* preparations. Specifically, the cardiodepressive effects of isoflurane may differentially affect each inbred strain, confounding our comparison of their intrinsic cardiac function. Additionally, given that isoflurane

has been shown to be cardioprotective during ischemia, it stands to reason that isoflurane may have a similar effect during hypoxia. If so, and if the magnitude of this effect is strain-dependent, then this may be another mechanism to explain the differences between our *ex vivo* and *in vivo* findings.

Our findings of significant differences in cardiac function between inbred mouse strains are telling of the impact of genetic divergence between strains on cardiovascular physiology. Although strain-dependent differences in physiological function can be challenging when comparing findings of studies in which multiple inbred strains have been used, they can also be taken advantage of to expand our understanding of complex disease processes. Similar to humans, selected cohorts of mice show distinct susceptibility to specific disease processes and these characteristics can be used to inform experimental design. For example, when creating a transgenic mouse which expresses a gene thought to confer resistance to cardiac ischemic injury, it may be beneficial to create or cross this transgenic line to a strain which shows particular susceptibility to cardiac ischemic injury such as 129S1/SvImJ as shown here. Carefully selecting the genetic background of novel genetically engineered mice in this way may maximize the differences between treated and untreated groups when attempting to test a particular therapeutic strategy. Additionally, because disease therapies are designed to treat patients that presumably show increased susceptibility to the disease of interest, it makes sense that research studies be designed in a similar fashion.

Another useful outcome of this study is the identification of quantitative traits that arose from the phenotypic diversity between inbred mouse strains. Future studies could center on tracking and identification of quantitative trait loci (QTL) that modify particular cardiac disease-related physiological processes. Previous studies have demonstrated the feasibility of using the genetic homogeneity of inbred mouse strains to isolate and identify physiologically significant QTL [10,11,12,13,14,22,23]. In this study, we observed significant functional differences between inbred strains that were evident when subjected to the stresses of ischemia/reperfusion, beta-blockade, and acute hypoxia. Because these challenges have direct clinical correlates, we anticipate that future studies focused on identifying the QTL to mechanistically explain observed functional differences between these strains will be of value. For example, a QTL analysis could be designed with C3H/HeJ and C57BL/6J mice to indentify loci that cause the marked loss of function in C3H/HeJ mice following esmolol infusion. Such a study may provide new mechanistic and clinically relevant insight into the regulation of cardiac function by β-adrenergic signaling by elucidating alterations in this pathway between these strains. This may be valuable in identifying factors that alter adrenergic signaling in the normal and diseased heart [56,57]. Finally, the finding that under baseline hemodynamic testing C57BL/6J mice had improved heart performance compared to other strains, including FVB/N, may help explain earlier reports of marked differences in mutant transgene outcomes between these inbred strains [25,26].

Collectively, the results of this study emphasize the importance of genetic divergence between inbred mouse strains and the complex manner in which this influences cardiac function. Additionally, we found that differences in cardiac function between inbred strains are modified by both genetic background and the physiological test setting (ex vivo/ in vivo) used to assess cardiac function. Finally, in this study we have identified numerous quantitative traits that may serve as the substrate for future studies on genetic modifiers of cardiac function. The demonstration here of reproducible and robust physiological traits, provoked under baseline or pathophysiological challenges, should aid future works attempting to identify new genetic modifiers of heart performance.

Tables

	C57BL/6J	FVB/NJ	DBA/2J	BALB/cJ	C3H/HeJ	129X1/SvJ	C57BL/10SnJ	129S1/SvImJ
ESp (mmHg)	96.1 ± 5.6	75.8 ± 2.0 *	88.9 ± 4.5	73.3 ± 2.9	85.3 ± 8.2	88.4 ± 5.9 *	107.5 ± 3.3	98.7 ± 4.3
EDp (mmHg)	7.2 ± 0.8	6.9 ± 1.5	11.3 ± 1.9 *	10.9 ± 0.9 *	6.9 ± 1.0	6.9 ± 1.4	6.0 ± 1.1	5.1 ± 0.9
HR (bpm)	605.3 ± 4.7	569.9 ± 12.7	527.2 ± 12.5	523.0 ± 14.5	572.5 ± 14.0	551.5 ± 4.8	597.9 ± 8.2	603.2 ± 9.9 *
+ dP/dt (mmHg/sec)	12451 ± 1085	9011 ± 543.5 *	8492 ± 249.4	5683 ± 646.7 *	9691 ± 1333	8702 ± 927.9 *	13190 ± 544.6	11129 ± 883.9
- dP/dt (mmHg/sec)	11557 ± 1354	8347 ± 448.4 *	8086 ± 288.5	5909 ± 702.6	7657 ± 522.1 *	9593 ± 1079	11701 ± 388.8	11242 ± 1240
Tau (msec)	5.7 ± 0.6	6.1 ± 1.2	8.0 ± 1.3 *	10.8 ± 1.0 *	6.2 ± 1.1	5.4 ± 0.9	4.2 ± 0.8	4.3 ± 0.7
Vmax (µL)	41.0 ± 5.8	35.5 ± 3.4	39.7 ± 3.0	25.44 ± 2.5 *	32.9 ± 4.8	36.8 ± 2.7	37.5 ± 3.0	36.5 ± 5.3
SV (µL)	25.4 ± 2.4	21.8 ± 1.3	21.9 ± 1.3	10.1 ± 1.8	20.2 ± 2.1	21.4 ± 1.7	24.9 ± 2.0	22.6 ± 2.8
EF (percent)	64.4 ± 3.8 *	63.5 ± 5.4	57.0 ± 5.2	38.7 ± 5.4	65.2 ± 8.2	58.7 ± 4.4	68.38 ± 6.0	63.6 ± 5.1
SW (mmHg*µL)	2045 ± 272.5	1333 ± 97.6	1486 ± 152.0	543.4 ± 146.6	1366 ± 230.6	1543 ± 203.7	2150 ± 182.3	1904 ± 296.6

Table 2-1. Parameters derived just before hypoxia for each strain. Parameters analyzed include end systolic pressure (ESp) LV end diastolic pressure (EDp), heart rate (HR), the positive derivative of pressure development (+ dP/dt), the negative derivative of pressure development (- dP/dt), tau, maximum LV volume (Vmax), stroke volume (SV), ejection fraction (EF), and stroke work (SW). * $P < 0.05$ vs. baseline values (from Figure 2-6 and Table 2-4) for the same strain by t-test.

	C57BL/6J	FVB/NJ	DBA/2J	BALB/cJ	C3H/HeJ	129X1/SvJ	C57BL/10SnJ	129S1/SvImJ
LVEDP (mmHg)	3.6 ± 0.4	3.1 ± 0.5	4.3 ± 0.5	5.5 ± 1.3	4.7 ± 1.2	4.5 ± 0.2	3.7 ± 0.3	3.9 ± 0.3
LVESP (mmHg)	126.3 ± 3.3	147.7 ± 5.9*	130.6 ± 7.0	132.4 ± 3.8	125.6 ± 2.7	121.7 ± 3.7	125.9 ± 1.8	124.1 ± 3.4
LVDP (mmHg)	122.8 ± 3.6	144.6 ± 5.9*	126.3 ± 7.2	126.9 ± 4.5	120.9 ± 2.3	117.2 ± 3.7	122.2 ± 1.8	120.2 ± 3.5
-dP/dt (mmHg*s-1)	-3456 ± 185	-4137 ± 148	-3618 ± 310	-3929 ± 216	-3681 ± 223	-3386 ± 267	-3781 ± 157	-3184 ± 157
+dP/dt (mmHg*s-1)	4614 ± 396	4697 ± 200	4429 ± 445	4708 ± 284	4338 ± 291	4263 ± 345	4321 ± 147	3654 ± 162
Tau (ms)	22.0 ± 2.0	24.1 ± 0.7	24.4 ± 1.1	21.9 ± 1.6	22.5 ± 2.0	24.2 ± 1.5	22.6 ± 0.5	25.9 ± 0.6

Table **2-2. Baseline functional data for isolated hearts of inbred mouse strains**. Systolic function indicated by left ventricular end systolic pressure (LVESP), left ventricular developed pressure (LVDP) and the maximum derivative of left ventricular pressure (+dP/dt). Diastolic function indicated by left ventricular end diastolic pressure (LVEDP), minimum derivative of left ventricular pressure (-dP/dt), and the rate constant tau. All values expressed as mean ± SEM. * = P < 0.05 compared to C57BL/6J mice. n = 5-8 for each group.

	C57BL/6J	FVB/NJ	DBA/2J	BALB/cJ	C3H/HeJ	129X1/SvJ	C57BL/10SnJ	129S1/SvlmJ
Baseline flow rate (mL/min)	2.1 ± 0.2	3.3 ± 0.5***	2.9 ± 0.5**	2.9 ± 0.2*	2.2 ±0.1	2.4 ± 0.1	2.6 ± 0.1	2.3 ± 0.1
Flow rate @ 60 min. reperfusion (mL/min)	1.5 ± 0.1	1.8 ± 0.1	2.1 ± 0.1 *	1.8 ± 0.3	1.5 ± 0.1	1.5 ± 0.1	2.1 ± 0.2*	1.2 ± 0.1
% decrease in flow rate	29.2 ± 3.2	44.3 ± 6.3	30.0 ± 3.7	38.6 ± 4.9	32.4 ± 3.1	36.9 ± 3.8	24.0 ± 3.4	44.3 ± 4.6*
Normalized flow rate (ml/min*g)	12.2 ± 0.8	18.8 ± 2.8***	13.3 ± 0.7	16.3 ± 1.5*	12.1 ± 0.4	13.7 ± 0.8	13.2 ± 0.3	15.0 ± 0.6
Normalized flow rate @ 60 min. reperfusion	8.6 ± 0.6	10.1 ± 0.8	9.5 ± 0.7	10.1 ± 1.7	8.2 ± 0.6	8.6 ± 0.6	10.6 ± 0.6	8.1 ± 0.6

Table 2-3. Baseline coronary flow rates and coronary flow rates at 60 minutes reperfusion for inbred strains tested. Flow rates were also normalized to average heart weight for each strain. All values expressed as mean ± SEM. Normalized body weight = flow rate divided by heart weight. *, **, *** = $P < 0.05$, 0.01, 0.001 compared to C57BL/6J mice, respectively. n = 5-7 for each group.

	C57BL/6J	FVB/NJ	DBA/2J	BALB/cJ	C3H/HeJ	129X1/SvJ	C57BL/10SnJ	129S1/SvImJ
LVEDP (mmHg)	7.0 ± 0.6	6.7 ± 1.0	7.3 ± 0.8	6.6 ± 0.6	4.9 ± 0.7	4.6 ± 0.6	5.9 ± 1.0	4.7 ± 0.3
PRSW	94.93 ± 8.2	64.33 ± 4.3	73.90 ± 7.0	79.35 ± 6.3	84.1 ± 10.4	109.7 ± 23.4	125.3 ± 25.2	90.1 ± 8.4
SV (µL)	21.5 ± 2.6	20.5 ± 1.2	23.5 ± 1.4	14.7 ± 1.8 *	19.7 ± 1.2	22.1 ± 1.0	22.8 ± 1.0	20.6 ± 1.4
SW (mmHg * µL)	1878 ± 227.4	1377 ± 49.2	1666 ± 165.1	1030 ± 174.0 *	1557 ± 104.8	1936 ± 117.2	2005 ± 166.2	1699 ± 200.0

Table 2-4. Hemodynamic performance at baseline. Parameters include LV end diastolic pressure (LVEDP), preload recruitable stroke work (PRSW), stroke volume (SV), and stroke work (SW). All data are mean ± sem. Statistics were performed using a 1 way ANOVA with Dunnett's post hoc analysis comparing each strain to C57BL/6J, * $P < 0.05$.

	C57BL/6J	FVB/NJ	DBA/2J	BALB/cJ	C3H/HeJ	129X1/SvJ	C57BL/10SnJ	129S1/SvlmJ
Body weight (BW, g)	30.3 ± 0.9	26.8 ± 0.5	30.3 ± 1.2	30.0 ± 0.9	29.0 ± 1.1	29.0 ± 0.6	28.6 ± 1.3	24.0 ± 0.5***
Tibia length (TL, mm)	17.3 ± 0.1	18.5 ± 0.4*	17.9 ± 0.4	17.2 ± 0.3	17.3 ± 0.2	17.6 ± 0.2	17.2 ± 0.2	17.7 ± 0.1
Heart weight (HW, mg)	137 ± 3.7	125.5 ± 3.5	173 ± 8.5***	143 ± 4.7	117.8 ± 4.1*	143.3 ± 4.2	144 ± 6.0	105.5 ± 4.2***
HW/BW (mg/g)	4.5 ± 0.1	4.8 ± 0.1	5.9 ± 0.3***	4.8 ± 0.3	4.1 ± 0.2	4.9 ± 0.1	5.1 ± 0.3	4.3 ± 0.2
BW/TL (mm/g)	1.8 ± 0.1	1.5 ± 0.03**	1.7 ± 0.1	1.7 ± 0.1	1.7 ± 0.1	1.7 ± 0.03	1.7 ± 0.1	1.4 ± 0.03***
HW/TL (mg/mm)	7.9 ± 0.2	6.8 ± 0.2	9.7 ± 0.5***	8.3 ± 0.3	6.8 ± 0.2*	8.1 ± 0.2	8.4 ± 0.4	6.0 ± 0.2***

Table 2-5. Body weight, tibia length, heart weight and morphometric parameters for inbred strains tested. All values expressed as mean ± SEM. *, **, *** = P < 0.05, 0.01, 0.001 compared to C57BL/6J mice, respectively. n = 5-9 for each group.

	C57BL/6J	FVB/NJ	DBA/2J	BALB/cJ	C3H/HeJ	129X1/SvJ	C57BL/10SnJ	129S1/SvImJ
LVEDP (mmHg)	9.3 ± 1.0	10.0 ± 1.2	11.4 ± 1.4	11.2 ± 0.7	8.9 ± 0.7	7.5 ± 0.7	8.7 ± 1.4	6.4 ± 1.1
HR (bpm)	503.6 ± 6.6	445.7 ± 16.9 *	446.2 ± 7.3	437.2 ± 17.6*	465.9 ± 20.3	495.7 ± 2.4	497.5 ± 5.2	507.6 ± 13.0
Vmax (µL)	49.3 ± 5.0	44.5 ± 3.5	43.5 ± 2.3	39.0 ± 4.9	30.5 ± 1.5 *	42.5 ± 3.4	43.0 ± 2.4	42.2 ± 4.6
Tau (sec)	8.3 ± 0.8	9.0 ± 0.8	9.7 ± 1.0	11.7 ± 0.4	32.4 ± 5.6 *	10.0 ± 1.0	7.6 ± 0.6	5.9 ± 0.7
SW (mmHg * µL)	678.4 ± 105.7	437.3 ± 66.0	696.2 ± 68.3	237.8 ± 25.0*	58.6 ± 22.5*	380.4 ± 78.6	771.5 ± 101.9	1162 ± 197.2*

Table 2-6. Hemodynamic performance during esmolol infusion. Mean data are shown for cardiac performance at 3 minutes into the esmolol infusion. Parameters analyzed include LV end diastolic pressure (LVEDP), heart rate (HR), maximum LV volume (Vmax), the time constant for isovolumic relaxation (Tau), and stroke work (SW). All data are mean ± SEM. Statistics were performed using a 1 way ANOVA with Dunnett's post hoc analysis comparing each strain to C57BL/6J, * $P < 0.05$.

	C57BL/6J	FVB/NJ	DBA/2J	BALB/cJ	C3H/HeJ	129X1/SvJ	C57BL/10SnJ	129S1/SvImJ
LVEDP (mmHg)	6.7 ± 1.0	9.2 ± 1.1	11.3 ± 1.4	11.9 ± 0.8*	6.8 ± 1.4	7.3 ± 1.6	6.0 ± 1.5	6.4 ± 1.1
HR (bpm)	576.4 ± 14.5	586.2 ± 17.8	519.9 ± 18.9	541.7 ± 12.3	595.3 ± 12.6	583.1 ± 9.3	575.4 ± 10.3	586.2 ± 37.3
Vmax (μL)	33.9 ± 4.6	35.3 ± 2.8	43.0 ± 3.4	25.6 ± 1.6	31.9 ± 2.6	38.3 ± 2.4	36.4 ± 5.3	39.1 ± 4.8
Δ LVEDP (mmHg)	-0.2 ± 0.3	1.0 ± 1.3	-0.006 ± 0.7	1.0 ± 0.4	-0.3 ± 1.4	0.4 ± 0.4	-0.5 ± 0.5	1.3 ± 0.4
Δ HR (bpm)	-26.8 ± 14.7	20.4 ± 18.2	-7.4 ± 10.0	18.7 ± 14.8	22.8 ± 12.9	31.6 ± 10.1	-22.5 ± 9.0	-12.5 ± 30.8
Δ –dP/dt (mmHg/sec)	-4693 ± 790.3	-713.5 ± 456.8*	-2140 ± 764.0	-340.0 ± 746.3*	-1072 ± 392.2*	526.2 ± 929.4*	-5358 ± 702.9	197.7 ± 1425*
Δ Vmax (μL)	-1.8 ± 1.7	-0.1 ± 3.4	3.3 ± 1.1	-2.1 ± 1.3	-1.5 ± 4.6	1.5 ± 1.4	-2.5 ± 3.0	2.6 ± 0.9

Table 2-7. Hemodynamic performance during hypoxia. Mean data are shown for cardiac performance at 6:40 into the hypoxic challenge and the delta change from the start of hypoxia (see Table 2-1). Parameters analyzed include LV end diastolic pressure (LVEDP), heart rate (HR), the negative derivative of pressure development (-dP/dt), and the maximum LV volume (Vmax). All data are mean ± sem. Statistics were performed using a 1 way ANOVA with Dunnett's post hoc analysis comparing each strain to C57BL/6J, * $P < 0.05$.

Figures

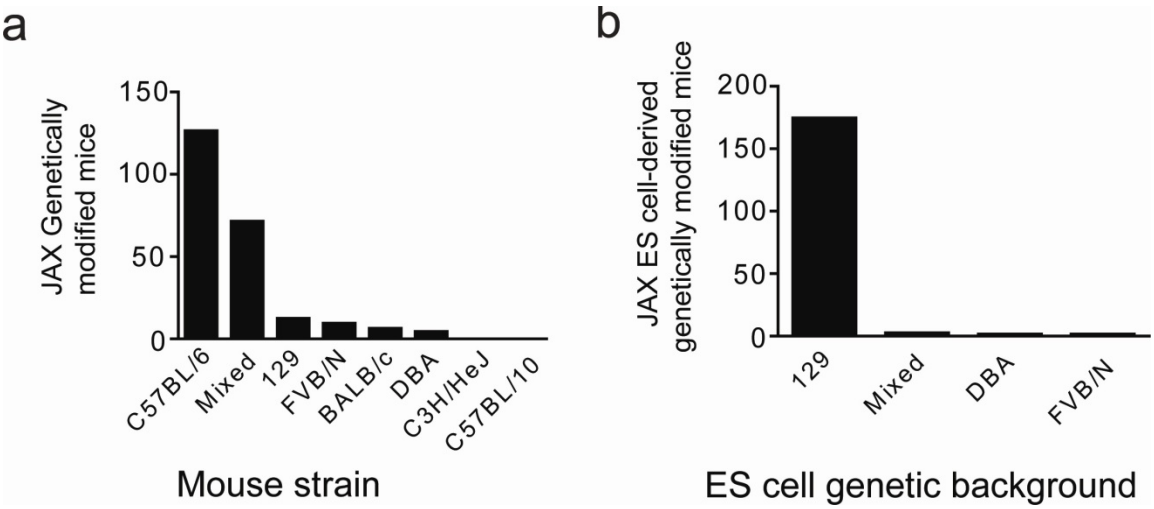

Figure 2-1. Summary of strain background of genetically modified mice and ES cells. a) Genetic background of genetically modified mouse strains designed for cardiovascular research maintained at Jackson Labs. b) Genetic background of embryonic stem cells used to create genetically modified mouse strains maintained at Jackson Labs.

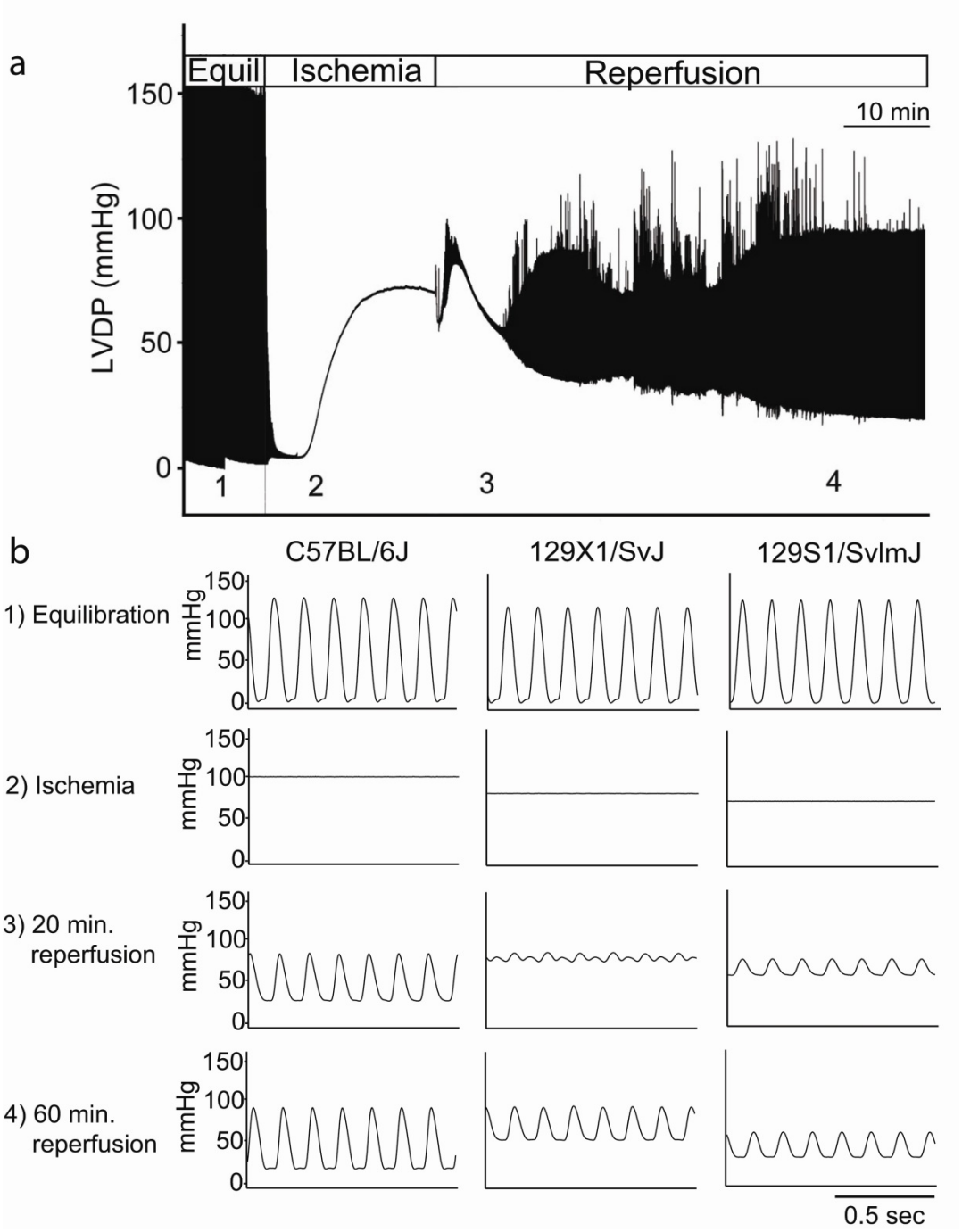

Figure 2-2. Effects of ischemia and reperfusion on isolated hearts of inbred mouse strains. a) Representative compressed pressure tracing from an experiment in which an isolated heart was subjected to global ischemia and reperfusion. b) Representative traces from C57BL/6J, 129X1/SvJ, 129S1/SvImJ hearts during (1) baseline equilibration, (2) ischemic contracture (at 20 minutes of ischemia, just before reperfusion), (3) 20 minutes following initiation of reperfusion, (4) 60 minutes following initiation of reperfusion.

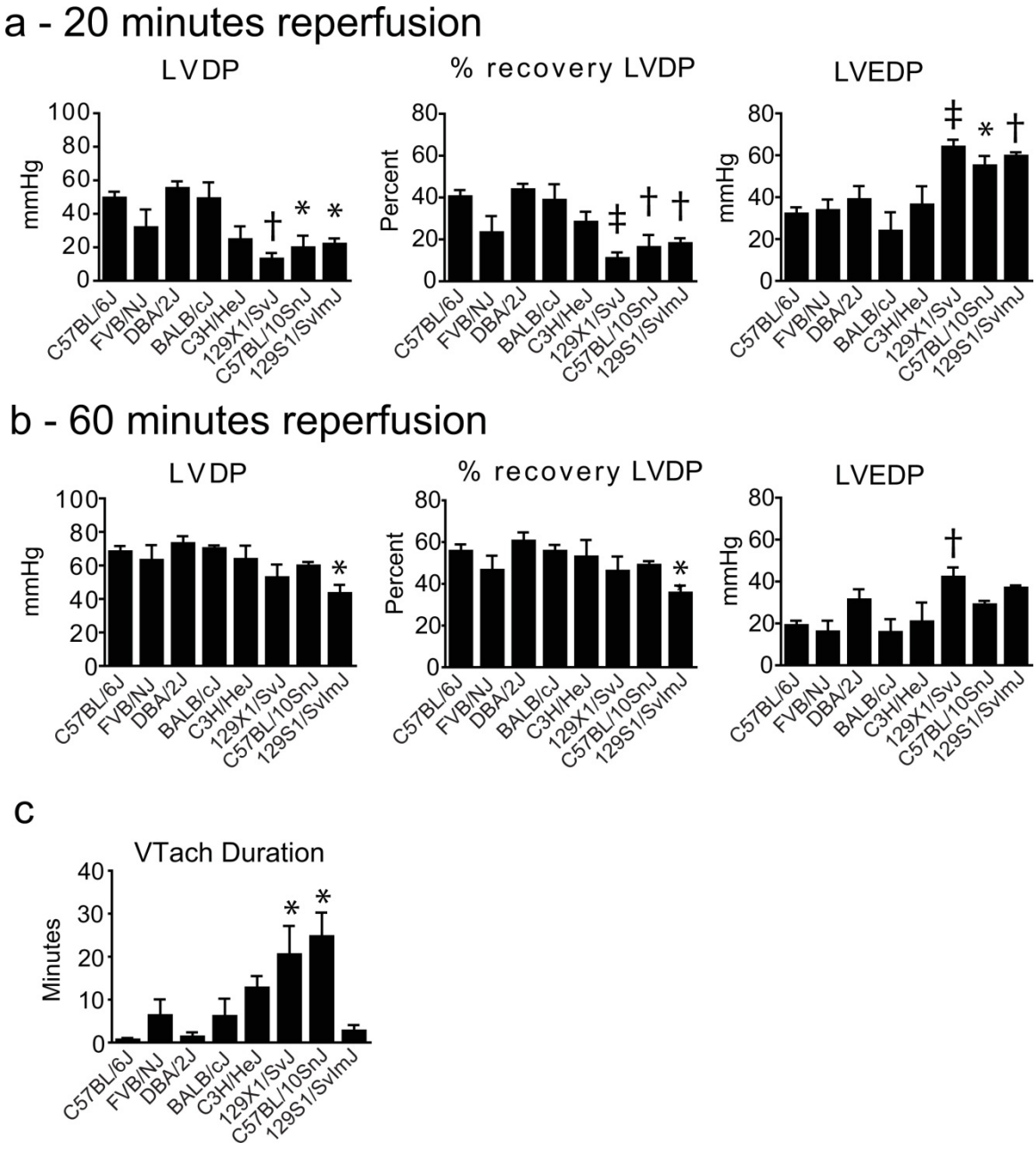

Figure 2-3. ***Ex vivo*** **cardiac function of isolated hearts measured during reperfusion**. a) Left ventricular developed pressure (LVDP), percent recovery of baseline LVDP and left ventricle end diastolic pressure (LVEDP) of isolated hearts during early (20 minutes) reperfusion. b) Left ventricular developed pressure (LVDP), percent recovery of baseline LVDP and left ventricle end diastolic pressure (LVEDP) of isolated hearts during late (60 minutes) reperfusion. c) Duration of sustained ventricular tachycardia (VTach) during reperfusion. Values are expressed as mean ± SEM. n = 5-8 for each group. * - $P < 0.05$, † - $P < 0.01$, ‡ - $P < 0.01$ compared to C57BL/6J.

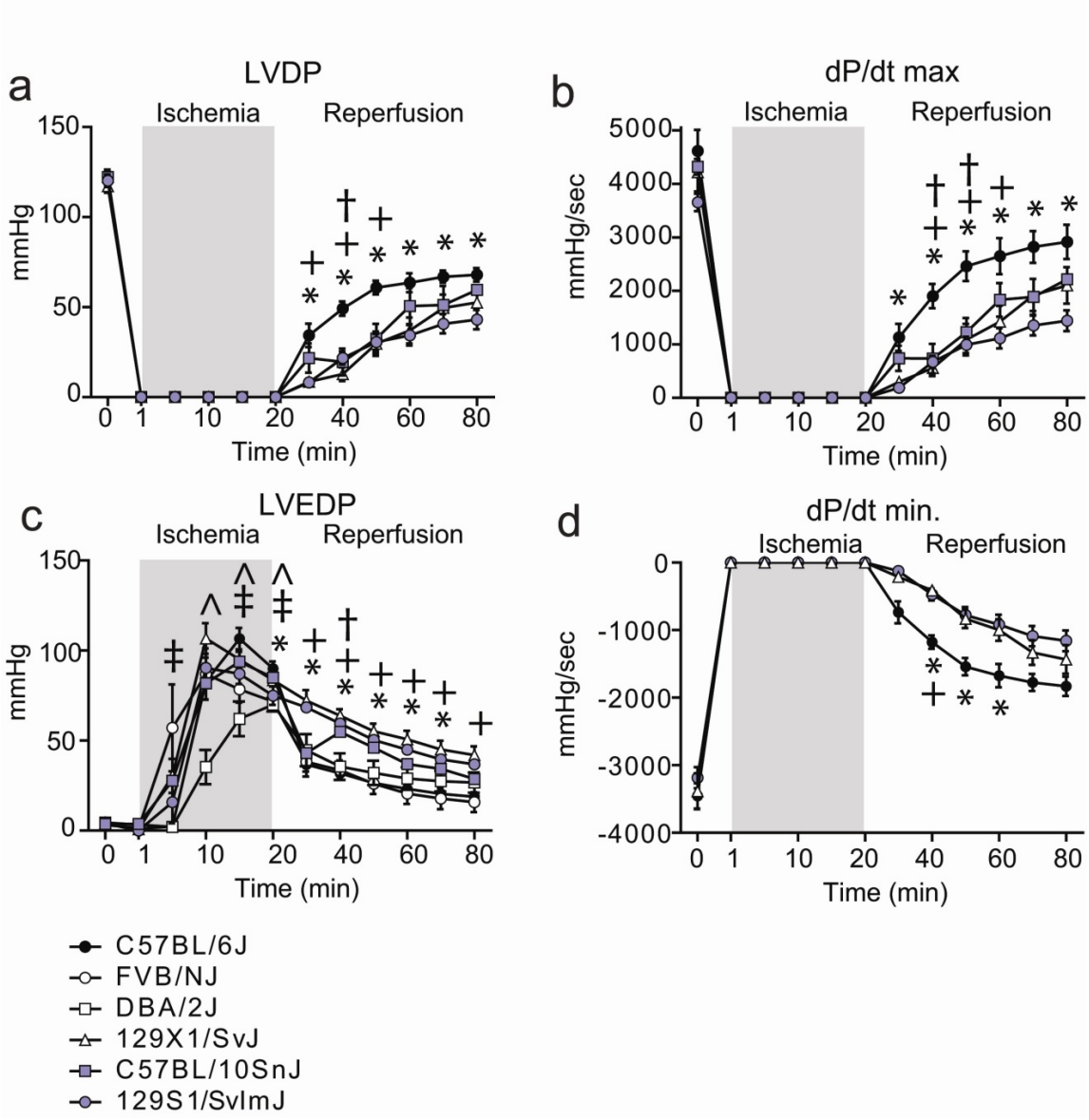

Figure 2-4. Cardiac performance of isolated hearts measured during global ischemia and reperfusion. For clarity, inbred strains which showed no significant differences from C57BL/6J during ischemia and reperfusion are not included in these Figures but were included in statistical analysis. a, b - Systolic function quantified by left ventricular developed pressure (LVDP) and the maximum derivative of left ventricular pressure (max. dP/dt), respectively. c, d - Diastolic function quantified by the minimum derivative of left ventricular pressure (min. dP/dt) and tau, respectively. Differences from C57BL/6J detected by one-way ANOVA. Values are expressed as mean ± SEM. n = 5-8 for each group. a-d - significant differences from C57BL/6J indicated by the following symbols. ‡, ^, +, †, * - FVB/NJ, DBA/2J, 129X1/SvJ, C57BL/10SnJ, 129SvImJ, respectively.

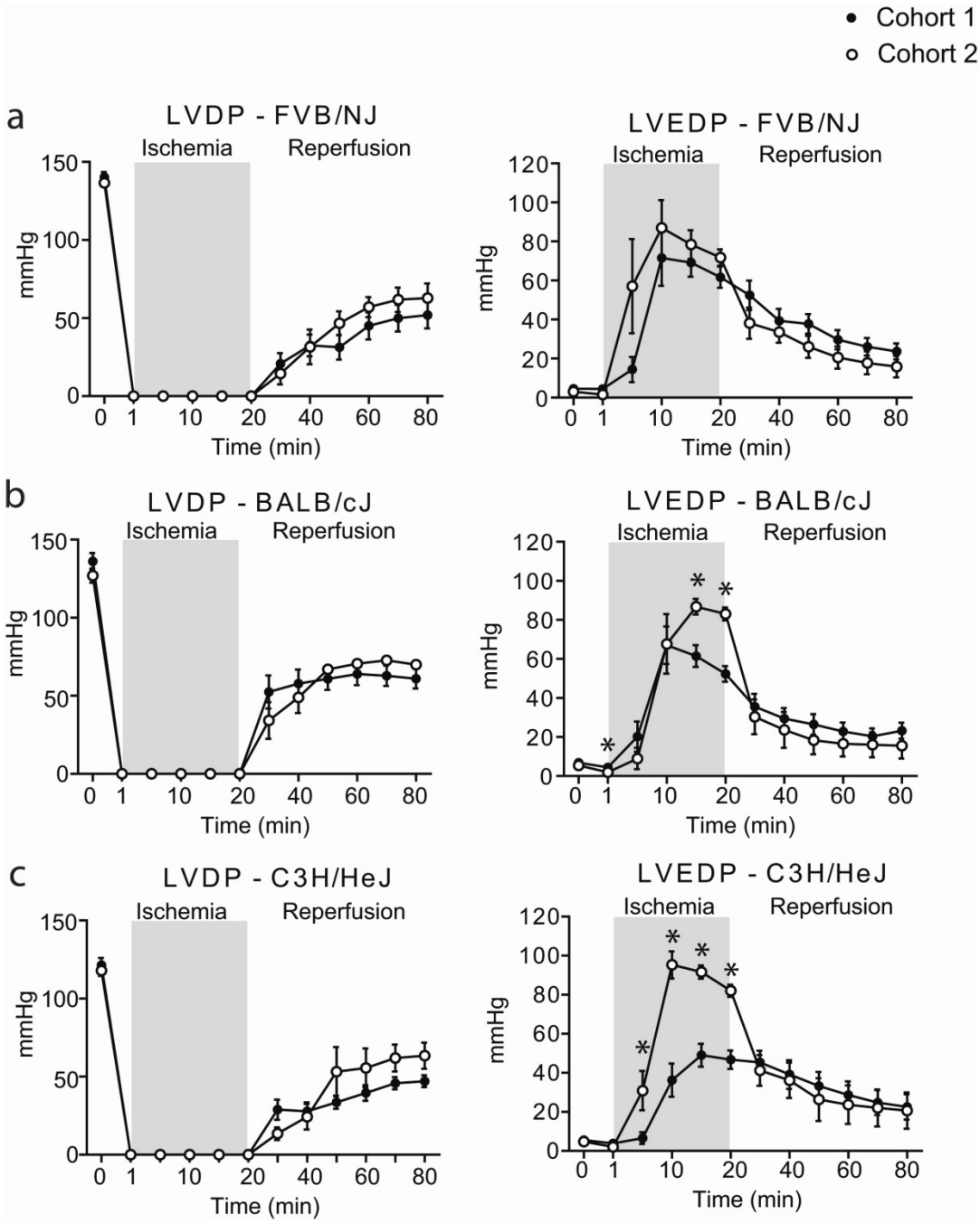

Figure 2-5. The reproducibility of *ex vivo* function measurements. Comparison of *ex vivo* functional data generated from two distinct cohorts of FVB/NJ, C3H/HeJ and BALB/cJ isolated hearts carried out several months apart. Cohort 1 was a pilot study carried out prior to the larger scale Cohort 2, from which all other data presented was generated. Isolated hearts were subjected to global ischemia and reperfusion. n = 5-7. * $P < 0.05$ compared to Cohort 1 by t-test.

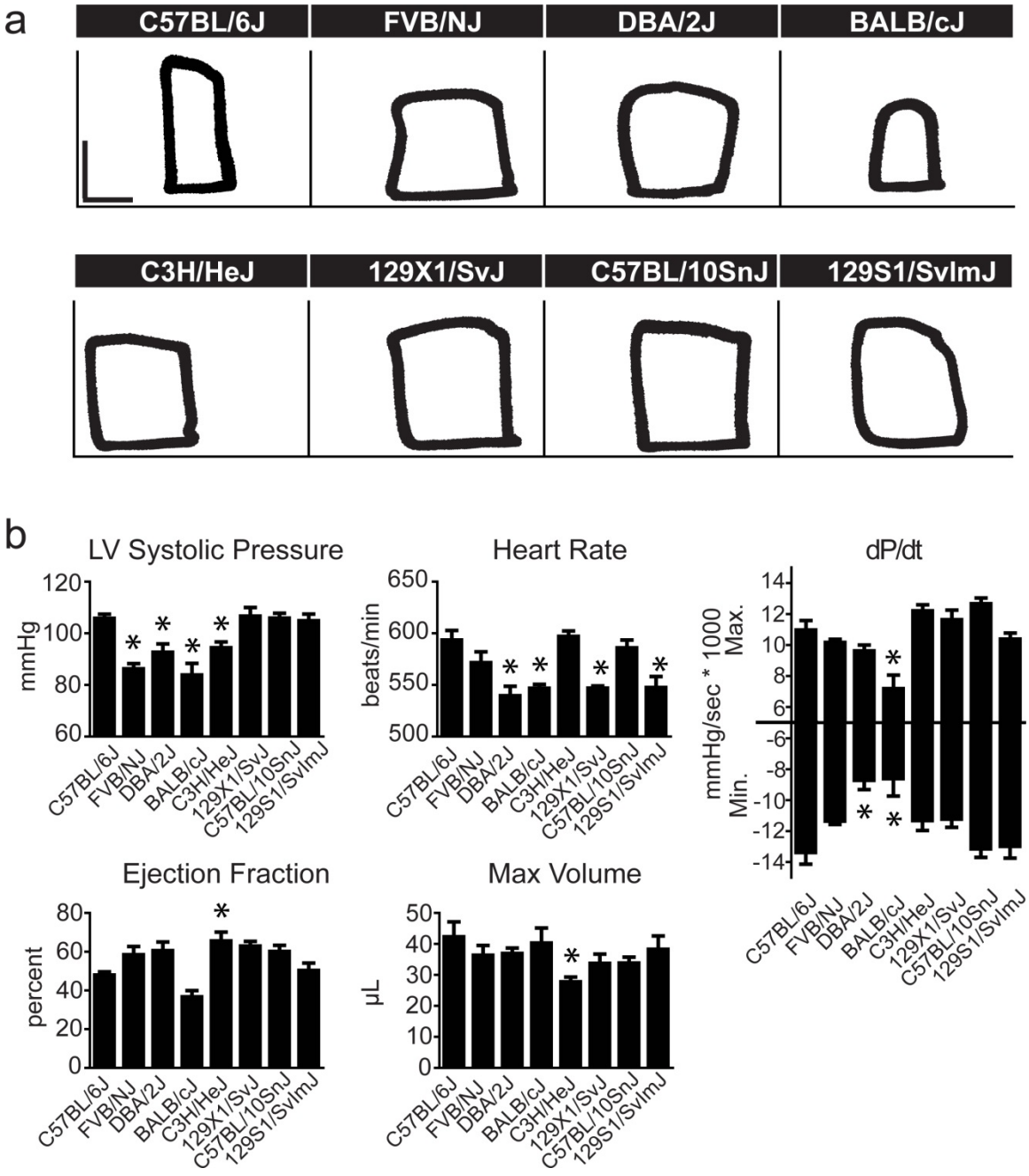

Figure 2-6. Baseline *in vivo* hemodynamic function of inbred mouse strains. a) Representative raw pressure-volume loops for each strain acquired by conductance micromanometry at baseline (PV loops: vertical scale bar: 50 mmHg; horizontal scale bar: 10 uL). b) Mean data for each strain for various cardiac hemodynamic parameters derived from real-time PV analysis. For all groups n = 7-9. Values are expressed as mean ± SEM. * $P < 0.05$ compared to C57BL/6J.

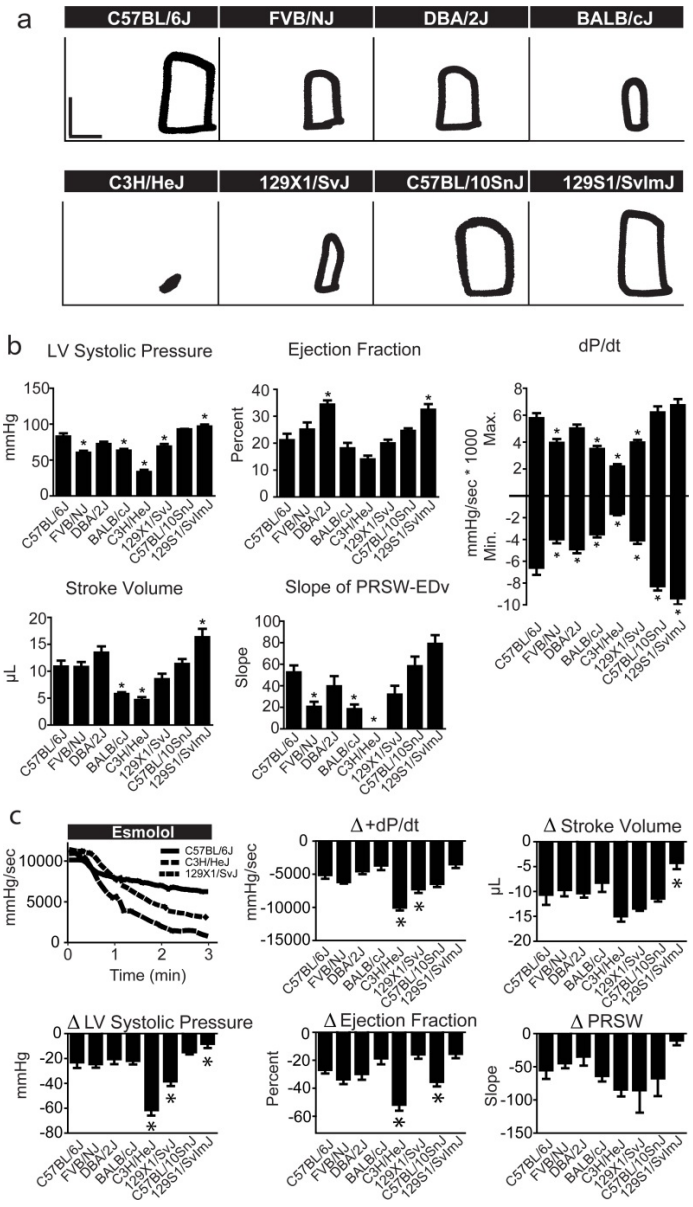

Figure 2-7. ***In vivo*** **hemodynamic function of inbred mouse strains during beta-blockade**. a) Representative raw pressure-volume loops for each strain acquired by conductance micromanometry after 3 minutes of esmolol infusion (PV loops: vertical scale bar: 50 mmHg; horizontal scale bar: 10 uL). b) Absolute values for cardiac function during esmolol infusion. Mean data for each strain for various cardiac hemodynamic parameters derived from real-time PV loop analysis at 3 minutes following the start of esmolol infusion. c) Representative changes in the positive pressure derivative (+dP/dt) during the time course of esmolol infusion showing marked differences in adrenergic tone between strains (top left). Mean data for each strain for various cardiac hemodynamic parameters derived from real-time PV analysis. For all groups n = 7-9. Values are expressed as mean ± SEM. * $P < 0.05$ compared to C57BL/6J.

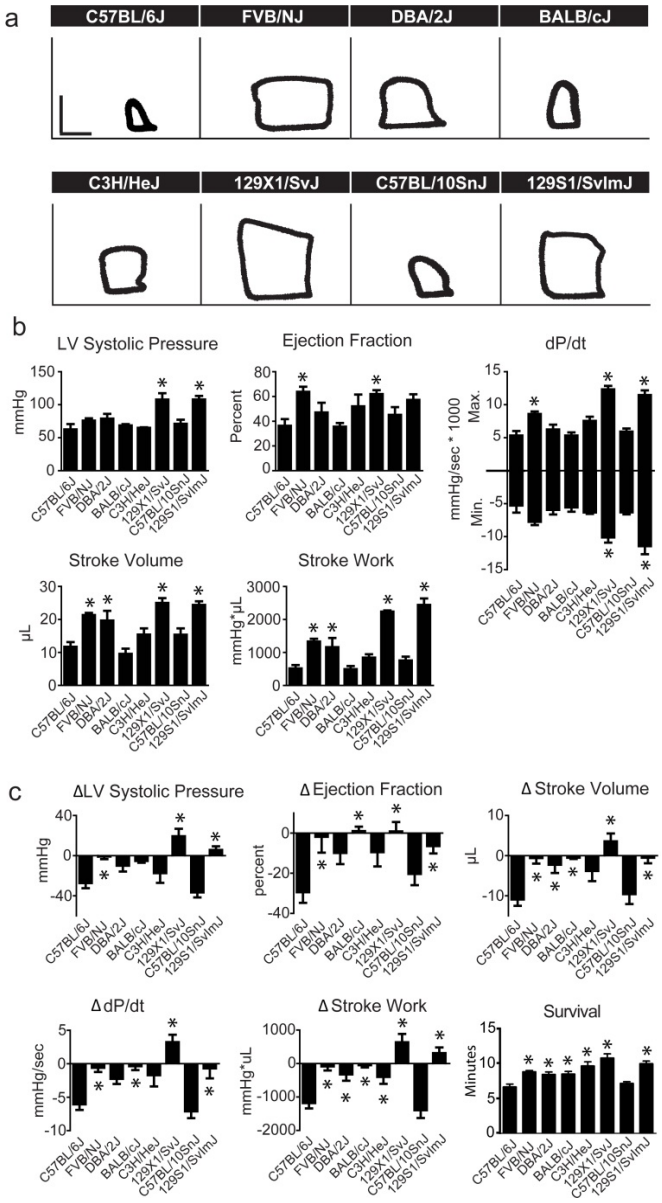

Figure 2-8. ***In vivo*** **hemodynamic function of inbred mouse strains during acute hypoxia**. a) Representative raw pressure-volume loops for each strain acquired by conductance micromanometry at 6:40 into the hypoxia challenge (PV loops: vertical scale bar: 50 mmHg; horizontal scale bar: 10 uL). b) Absolute values for cardiac function during acute hypoxia. Mean data for each strain for various cardiac hemodynamic parameters derived from real-time PV analysis at 6 minutes, 40 seconds following the start of esmolol infusion. c) The mean change in cardiac function from the start of hypoxia to 6:40 into the hypoxic challenge indicating the delta values for given hemodynamic parameters during hypoxia compared to baseline. Mean survival values for each strain during the acute hypoxic challenge showing significant differences between groups compared to C57BL/6J (bottom right). For all groups n = 7-9. Values are expressed as mean ± SEM. * $P < 0.05$ compared to C57BL/6J.

Literature cited

1. Beck JA, Lloyd S, Hafezparast M, Lennon-Pierce M, Eppig JT, et al. (2000) Genealogies of mouse inbred strains. Nat Genet 24: 23-25.

2. Keane TM, Goodstadt L, Danecek P, White MA, Wong K, et al. Mouse genomic variation and its effect on phenotypes and gene regulation. Nature 477: 289-294.

3. Taketo M, Schroeder AC, Mobraaten LE, Gunning KB, Hanten G, et al. (1991) FVB/N: an inbred mouse strain preferable for transgenic analyses. Proc Natl Acad Sci U S A 88: 2065-2069.

4. Seong E, Saunders TL, Stewart CL, Burmeister M (2004) To knockout in 129 or in C57BL/6: that is the question. Trends Genet 20: 59-62.

5. Ware CB, Siverts LA, Nelson AM, Morton JF, Ladiges WC (2003) Utility of a C57BL/6 ES line versus 129 ES lines for targeted mutations in mice. Transgenic Res 12: 743-746.

6. Bittner RE, Anderson LV, Burkhardt E, Bashir R, Vafiadaki E, et al. (1999) Dysferlin deletion in SJL mice (SJL-Dysf) defines a natural model for limb girdle muscular dystrophy 2B. Nat Genet 23: 141-142.

7. Ho M, Post CM, Donahue LR, Lidov HG, Bronson RT, et al. (2004) Disruption of muscle membrane and phenotype divergence in two novel mouse models of dysferlin deficiency. Hum Mol Genet 13: 1999-2010.

8. Sicinski P, Geng Y, Ryder-Cook AS, Barnard EA, Darlison MG, et al. (1989) The molecular basis of muscular dystrophy in the mdx mouse: a point mutation. Science 244: 1578-1580.

9. Ryder-Cook AS, Sicinski P, Thomas K, Davies KE, Worton RG, et al. (1988) Localization of the mdx mutation within the mouse dystrophin gene. Embo J 7: 3017-3021.

10. Bauman LE, Sinsheimer JS, Sobel EM, Lange K (2008) Mixed effects models for quantitative trait loci mapping with inbred strains. Genetics 180: 1743-1761.

11. Blizard DA, Lionikas A, Vandenbergh DJ, Vasilopoulos T, Gerhard GS, et al. (2009) Blood pressure and heart rate QTL in mice of the B6/D2 lineage: sex differences and environmental influences. Physiol Genomics 36: 158-166.

12. Doorenbos C, Tsaih SW, Sheehan S, Ishimori N, Navis G, et al. (2008) Quantitative trait loci for urinary albumin in crosses between C57BL/6J and A/J inbred mice in the presence and absence of Apoe. Genetics 179: 693-699.

13. Stylianou IM, Langley SR, Walsh K, Chen Y, Revenu C, et al. (2008) Differences in DBA/1J and DBA/2J reveal lipid QTL genes. J Lipid Res 49: 2402-2413.

14. Sugiyama F, Churchill GA, Li R, Libby LJ, Carver T, et al. (2002) QTL associated with blood pressure, heart rate, and heart weight in CBA/CaJ and BALB/cJ mice. Physiol Genomics 10: 5-12.

15. Lloyd-Jones D, Adams RJ, Brown TM, Carnethon M, Dai S, et al. (2009) Heart Disease and Stroke Statistics--2010 Update. A Report From the American Heart Association. Circulation.

16. Bendall JK, Heymes C, Wright TJ, Wheatcroft S, Grieve DJ, et al. (2002) Strain-dependent variation in vascular responses to nitric oxide in the isolated murine heart. J Mol Cell Cardiol 34: 1325-1333.

17. Reichelt ME, Willems L, Hack BA, Peart JN, Headrick JP (2009) Cardiac and coronary function in the Langendorff-perfused mouse heart model. Exp Physiol 94: 54-70.

18. Stull LB, Hiranandani N, Kelley MA, Leppo MK, Marban E, et al. (2006) Murine strain differences in contractile function are temperature- and frequency-dependent. Pflugers Arch 452: 140-145.

19. Schlager G (1966) Systolic blood pressure in eight inbred strains of mice. Nature 212: 519-520.

20. Hoit BD, Kiatchoosakun S, Restivo J, Kirkpatrick D, Olszens K, et al. (2002) Naturally occurring variation in cardiovascular traits among inbred mouse strains. Genomics 79: 679-685.

21. Blizard DA, Welty R (1971) Cardiac activity in the mouse: strain differences. J Comp Physiol Psychol 77: 337-344.

22. Heydemann A, Huber JM, Demonbreun A, Hadhazy M, McNally EM (2005) Genetic background influences muscular dystrophy. Neuromuscul Disord 15: 601-609.

23. Heydemann A, Ceco E, Lim JE, Hadhazy M, Ryder P, et al. (2009) Latent TGF-beta-binding protein 4 modifies muscular dystrophy in mice. J Clin Invest 119: 3703-3712.

24. Suzuki M, Carlson KM, Marchuk DA, Rockman HA (2002) Genetic modifier loci affecting survival and cardiac function in murine dilated cardiomyopathy. Circulation 105: 1824-1829.

25. Michele DE, Gomez CA, Hong KE, Westfall MV, Metzger JM (2002) Cardiac dysfunction in hypertrophic cardiomyopathy mutant tropomyosin mice is

transgene-dependent, hypertrophy-independent, and improved by beta-blockade. Circ Res 91: 255-262.

26. Prabhakar R, Boivin GP, Grupp IL, Hoit B, Arteaga G, et al. (2001) A familial hypertrophic cardiomyopathy alpha-tropomyosin mutation causes severe cardiac hypertrophy and death in mice. J Mol Cell Cardiol 33: 1815-1828.

27. Langendorff (1898) Untersuchungen am überlebenden Säugetierherzen. Pflügers Archiv 61: 291–332.

28. Skrzypiec-Spring M, Grotthus B, Szelag A, Schulz R (2007) Isolated heart perfusion according to Langendorff---still viable in the new millennium. J Pharmacol Toxicol Methods 55: 113-126.

29. Pacher P, Nagayama T, Mukhopadhyay P, Batkai S, Kass DA (2008) Measurement of cardiac function using pressure-volume conductance catheter technique in mice and rats. Nat Protoc 3: 1422-1434.

30. Day SM, Westfall MV, Fomicheva EV, Hoyer K, Yasuda S, et al. (2006) Histidine button engineered into cardiac troponin I protects the ischemic and failing heart. Nat Med 12: 181-189.

31. Townsend D, Yasuda S, Li S, Chamberlain JS, Metzger JM (2008) Emergent dilated cardiomyopathy caused by targeted repair of dystrophic skeletal muscle. Mol Ther 16: 832-835.

32. Townsend D, Blankinship MJ, Allen JM, Gregorevic P, Chamberlain JS, et al. (2007) Systemic administration of micro-dystrophin restores cardiac geometry and prevents dobutamine-induced cardiac pump failure. Mol Ther 15: 1086-1092.

33. Palpant NJ, Szatkowski ML, Wang W, Townsend D, Bedada FB, et al. (2009) Artificial selection for whole animal low intrinsic aerobic capacity co-segregates with hypoxia-induced cardiac pump failure. PLoS One 4: e6117.

34. Palpant NJ, D'Alecy LG, Metzger JM (2009) Single histidine button in cardiac troponin I sustains heart performance in response to severe hypercapnic respiratory acidosis in vivo. Faseb J 23: 1529-1540.

35. Hewett TE, Grupp IL, Grupp G, Robbins J (1994) Alpha-skeletal actin is associated with increased contractility in the mouse heart. Circ Res 74: 740-746.

36. Ferrier GR, Guyette CM (1991) Ventricular tachycardia in an isolated guinea pig ventricular free wall model of ischemia and reperfusion. J Cardiovasc Pharmacol 17: 228-238.

37. Nilles KM, London B (2007) Knockin animal models of inherited arrhythmogenic diseases: what have we learned from them? J Cardiovasc Electrophysiol 18: 1117-1125.

38. Tamargo J, Caballero R, Nunez L, Gomez R, Vaquero M, et al. (2007) Genetically engineered mice as a model for studying cardiac arrhythmias. Front Biosci 12: 22-38.

39. Barbosa ME, Alenina N, Bader M (2005) Induction and analysis of cardiac hypertrophy in transgenic animal models. Methods Mol Med 112: 339-352.

40. Du XJ (2004) Gender modulates cardiac phenotype development in genetically modified mice. Cardiovasc Res 63: 510-519.

41. Gros D, Dupays L, Alcolea S, Meysen S, Miquerol L, et al. (2004) Genetically modified mice: tools to decode the functions of connexins in the heart-new models for cardiovascular research. Cardiovasc Res 62: 299-308.

42. Eckhart AD, Koch WJ (2001) Transgenic studies of cardiac adrenergic receptor regulation. J Pharmacol Exp Ther 299: 1-5.

43. Dillmann WH (1999) Calcium regulatory proteins and their alteration by transgenic approaches. Am J Cardiol 83: 89H-91H.

44. Waldeyer C, Fabritz L, Fortmueller L, Gerss J, Damke D, et al. (2009) Regional, age-dependent, and genotype-dependent differences in ventricular action potential duration and activation time in 410 Langendorff-perfused mouse hearts. Basic Res Cardiol 104: 523-533.

45. Shah AP, Siedlecka U, Gandhi A, Navaratnarajah M, Al-Saud SA, et al. (2010) Genetic Background Affects Function and Intracellular Calcium Regulation of Mouse Hearts. Cardiovasc Res.

46. Dhein S, Mohr FW, Delmar M (2005) Practical Methods in Cardiovascular Research Springer. 1010 p.

47. Skolleborg KC, Gronbech JE, Grong K, Abyholm FE, Lekven J (1990) Distribution of cardiac output during pentobarbital versus midazolam/fentanyl/fluanisone anaesthesia in the rat. Lab Anim 24: 221-227.

48. Saha DC, Saha AC, Malik G, Astiz ME, Rackow EC (2007) Comparison of cardiovascular effects of tiletamine-zolazepam, pentobarbital, and ketamine-xylazine in male rats. J Am Assoc Lab Anim Sci 46: 74-80.

49. Nabeshima T, Ho IK (1981) Pharmacological responses to pentobarbital in different strains of mice. J Pharmacol Exp Ther 216: 198-204.

50. Mogil JS, Smith SB, O'Reilly MK, Plourde G (2005) Influence of nociception and stress-induced antinociception on genetic variation in isoflurane anesthetic potency among mouse strains. Anesthesiology 103: 751-758.

51. Boban M, Stowe DF, Buljubasic N, Kampine JP, Bosnjak ZJ (1992) Direct comparative effects of isoflurane and desflurane in isolated guinea pig hearts. Anesthesiology 76: 775-780.

52. Merin RG, Bernard JM, Doursout MF, Cohen M, Chelly JE (1991) Comparison of the effects of isoflurane and desflurane on cardiovascular dynamics and regional blood flow in the chronically instrumented dog. Anesthesiology 74: 568-574.

53. Dalal PG, Corner A, Chin C, Wood C, Razavi R (2008) Comparison of the cardiovascular effects of isoflurane and sevoflurane as measured by magnetic resonance imaging in children with congenital heart disease. J Clin Anesth 20: 40-44.

54. Sonner JM, Gong D, Eger EI, 2nd (2000) Naturally occurring variability in anesthetic potency among inbred mouse strains. Anesth Analg 91: 720-726.

55. Landoni G, Bignami E, Oliviero F, Zangrillo A (2009) Halogenated anaesthetics and cardiac protection in cardiac and non-cardiac anaesthesia. Ann Card Anaesth 12: 4-9.

56. Engelhardt S (2005) Beta-adrenergic receptors in heart failure. Heart Fail Clin 1: 183-191.

57. Insel PA, Hammond HK (1993) Beta-adrenergic receptors in heart failure. J Clin Invest 92: 2564.

Chapter 3

Ex vivo stretch reveals altered mechanical properties of isolated dystrophin-deficient hearts

Abstract

Duchenne muscular dystrophy (DMD) is a progressive and fatal disease of muscle wasting caused by loss of the cytoskeletal protein dystrophin. In the heart, DMD results in progressive cardiomyopathy and dilation of the left ventricle through mechanisms that are not fully understood. Previous reports have shown that loss of dystrophin causes sarcolemmal instability and reduced mechanical compliance of isolated cardiac myocytes. To expand upon these findings, here we have subjected the left ventricles of dystrophin-deficient mdx hearts to whole-organ stretch. Unexpectedly, isolated mdx hearts showed increased left ventricular (LV) compliance compared to controls during stretch as LV volume was increased above normal end diastolic volume. During LV chamber distention, sarcomere lengths increased similarly in mdx and WT hearts despite greater excursions in volume of mdx hearts. This suggests that the mechanical properties of the intact heart cannot be modeled as a simple extrapolation of findings in single cardiac myocytes. To explain these findings, a model is

proposed in which disruption of the dystrophin-glycoprotein complex perturbs cell-extracellular

matrix contacts and promotes the apparent slippage of myocytes past each other during LV distension. In comparison, similar increases in LV compliance were obtained in isolated hearts from β-sarcoglycan-null and laminin-α_2 mutant mice but not in dysferlin-null mice, suggesting that increased whole-organ compliance in mdx mice is a specific effect of disrupted cell-extracellular matrix contacts and not a general consequence of cardiomyopathy via membrane defect processes. Collectively, these findings suggest a novel and cell-death independent mechanism for the progressive pathological LV dilation that occurs in DMD.

Introduction

Duchenne muscular dystrophy (DMD) is an inherited disease of progressive muscle wasting and is the most common form of muscular dystrophy, affecting 1 in 3500 males [1]. The DMD gene resides on the short arm of the X chromosome and encodes the protein dystrophin [2,3,4]. Dystrophin is a 427 kDa cytoskeletal protein and is a member of the dystrophin-glycoprotein complex (DGC) in striated muscles [2,5,6]. The DGC is a multimeric protein assembly that spans the sarcolemma, tethering the extracellular matrix to the cytoskeletal architecture of the cell [7]. Dystrophin is a cytoplasmic component of the DGC and plays a crucial role in this trans-sarcolemma linkage, binding cytoplasmic γ-actin at its N-terminus and the membrane glycoprotein β-dystroglycan at its C-terminus [8,9,10]. The DGC protein α-dystroglycan interacts with the

extracellular matrix by binding laminin in a glycosylation dependent manner [7,11]. In the absence of dystrophin, the mechanical rigors of muscle contraction are damaging to the sarcolemma. This mechanical instability has been observed in dystrophin-deficient skeletal muscle, which is highly susceptible to lengthening contraction-induced sarcolemmal damage and necrotic cell death [12,13]. Previously, we and have demonstrated similar mechanical instability in isolated single cardiac myocytes, by showing that loss of dystrophin causes the formation of “micro-tears” in the sarcolemma during passive mechanical distension of myocyte [14,15,16]. These sarcolemmal disruptions resulted in increased single-cell stiffness with eventual hypercontracture and cell death during physiological stretch due to unregulated influx of extracellular calcium [15,16].

Clinically, DMD is characterized by skeletal muscle weakness and wasting. DMD presents early in life and is rapidly progressive, resulting in loss of ambulation at approximately 10 years of age and premature death in the early twenties [17,18,19,20,21]. Progressive cardiac dysfunction is a significant component of DMD which has been observed since the very first descriptions of the disease [20,22]. Subclinical cardiac involvement is present in the majority of DMD patients in the first decade, the severity of which may be masked by significant skeletal muscle dysfunction [20,23,24].In the later stages of DMD, nearly all patients show clinically significant cardiac muscle disease [25,26]. Structurally, the cardiomyopathy of DMD is characterized by fibrosis and progressive dilation of the left ventricle (LV), leading to dilated cardiomyopathy

(DCM) [26,27]. This frequently progresses to heart failure, which is the primary cause of death in at least 20% of DMD patients [20,25].

There are significant gaps in knowledge regarding the progression of cardiac involvement in DMD. Increased myocyte passive stiffness secondary to membrane damage in dystrophic myocytes may cause remodeling of LV dimensions early in DMD [15]. At present, how dystrophin deficiency causes LV dilation as the disease progresses is unclear. Previous findings regarding the progression of DCM in the non-dystrophic heart suggest that progressive LV dilation may involve myocyte loss, fibrosis, hypertrophy, and myocyte slippage [28,29,30,31,32,33,34]. The degree to which these processes contribute to cardiac dysfunction and dilation in DMD is currently unknown.

In order to build on previous findings in single cardiac myocytes and to gain new mechanistic understanding of the effects of mechanical stress on the dystrophic heart, we tested the hypothesis that isolated dystrophin-deficient hearts have reduced organ level compliance and increased susceptibility to mechanical damage. Using a modified *ex vivo* isolated heart preparation, results show, unexpectedly, that isolated mdx hearts have increased whole-organ compliance compared to normal hearts and tolerate considerable LV chamber distension without showing evidence of myocyte damage. To provide further mechanistic insight, we tested other genetic models of dystrophy in which either the DGC or native membrane repair apparatus were disrupted. We found that defective organ level compliance was evident only when the DGC or its

extracellular binding partner laminin were disrupted but not in hearts lacking the membrane repair protein dysferlin.

Collectively, these results provide evidence that disruption of the DGC predispose the LV to dilation via apparent myocyte slippage, a novel and cell death-independent mechanism for the progressive LV dilation observed in DMD.

Materials and Methods

*Mice.*C57BL/10SnJ (000666), C57BL/10ScSnJ-DMD^{mdx}/J (001801),129-*Dysf*^{tm1Kcam}/J (006830), 129S1/SvImJ (002448), B6.WK-*Lama2*$^{dy\text{-}2J}$/J (000524), B6.129-*Sgcb*^{tm1Kcam}/1J (006832) were purchased from the Jackson Labs (Bar Harbor, Maine). Mdx carrier females were created by breeding C57BL/10SnJ and C57BL/10ScSnJ-DMD^{mdx}/J mice. Dystrophin-utrophin double knockout (DKO) mice were a kind gift from Dr. Dawn Lowe at the University of Minnesota [35]. Mice were used at 8-10 weeks of age, with the exception of DKO mice, which were used at 4 weeks due to their severely shortened lifespan.

Isolated heart preparation. Mice were anaesthetized with sodium pentobarbital and hearts removed via thoracotomy. Hearts were then immediately placed in ice cold modified Krebs-Henseleit buffer (118 mM NaCl, 4.7 mM KCl, 1.2 mM $MgSO_4$, 1.2 mM KH_2PO_4, 10 mM glucose, 25 mM $NaHCO_3$, 2.5 mM $CaCl_2$, 0.5 mM EDTA, 2 mM sodium pyruvate) while the aorta was isolated and cannulated. Hearts were then retrograde-perfused through with warm buffer bubbled with 95% O_2 and 5% CO_2 to maintain a pH of 7.4. For

experiments in non-contracting hearts, isolated hearts were perfused with a similar buffer lacking calcium and including the contractile inhibitor 10 mM 2,3–butanedione monoxime (BDM).The left atrium was then removed and a plastic balloon was inserted into the LV. An in-line pressure transducer allowed for the recording of pressures within the LV. To assess the mechanical compliance of isolated hearts, balloons were inflated to a physiological left ventricular end diastolic pressure (LVEDP) of 8 mmHg. Volume required to bring LVEDP to this normal range was recorded as V_{init}.

Ex vivo stretch protocol. To mechanically stretch isolated hearts, volume was added in 1 µL increments. For contracting hearts, 15 µL was added above V_{init}. For non-contracting hearts, 30 µL was added above V_{init}. In both contracting and non-contracting hearts, the *ex vivo* stretch protocol was performed twice: once to condition the heart and a second time to record functional data. All data reported in this study was taken from the second run through the stretch protocol. Additionally, for this study it was necessary to create balloons with significantly larger volumes than the murine LV to ensure that pressure developed in the balloon was due to pressure against the LV wall and not against the balloon itself.

Determination of sarcomere length. To determine sarcomere length at given LV pressures, balloons were inflated and clamped to hold LVP at 8, 80 or 160 mmHg in non-contracting hearts, which were then perfused with 10% zinc-

formallin and fixed overnight at 4 degrees Celsius. The following day, the LV free wall was dissected, cut transversely at the mid-wall and embedded in paraffin. Serial 5 μm sections were then cut and mounted on histological slides. Immunofluorescence for the Z-disk intermediate filament desmin was then performed to visualize sarcomere length. In brief, sections were dewaxed and rehydrated and blocked with 20% normal goat serum for 1 hour at room temperature. Rabbit anti-desmin primary antibody (Novus Biologicals, NB120-15200) was applied at a 1:300 dilution for 1 hour at room temperature. After washing, goat anti-rabbit IgG-AlexaFluor 594 (Molecular Probes, A-11037) was applied for 1 hour at room temperature. Sections were then washed and mounted with Vectashield for visualization. Slides were visualized using a Zeiss LSM510 META confocal microscope (Carl Zeiss).

Lactate dehydrogenase activity assay. Perfusates were collected from isolated hearts immediately before or after the *ex vivo* stretch protocol and immediately frozen in liquid nitrogen. 5 μL of perfusate was then added to 200 μL of solution containing 0.12 mM NADH, 2.3 mM pyruvate, and 0.035% BSA in 100 mM sodium phosphate pH = 7.5. Absorbance at 340 nm was then measured in a plate reader (FLUOstar Omega, BMG Labtech) at 1 minute intervals for 15 minutes at a constant temperature of 37 degrees Celsius.

Statistics. Comparisons between more than 2 groups were made by one-way analysis of variance with a Tukey post-test. When more than one

independent variable was tested, two-way analysis of variance with a Bonferroni post-test was used to compare groups. All statistical analysis was carried out using Prism (GraphPad Software).

Results

Previously, we have shown that the sarcolemma of single, membrane intact, mdx cardiac myocytes is highly susceptible to passive stretch-induced injury leading to increased stiffness, membrane permeability, aberrant extracellular calcium influx, and myocyte death [15]. To expand upon these findings and determine how single-cell mechanics manifest at the whole-organ level, the effects of mechanical stretch on the left ventricular chamber of WT and mdx hearts were determined (Figure 3-1).

Mechanical compliance of intact, beating mdx hearts. To determine whole-organ cardiac compliance wild-type (WT, C57BL/10SnJ) and mdx hearts were isolated, perfused, and subjected to mechanical stretch using a water filled plastic balloon placed within the LV chamber. WT and mdx mice used in this study were of similar age (65 ± 0.9 vs. 67 ± 1.8 days, n = 14-16, P> 0.05), had similar body weights (27.1 ± 0.4 vs. 27.4 ± 0.9 grams, n = 14-16, P> 0.05) and heart weights (176.4 mg ± 5.4 vs. 158.8 ± 10.3 milligrams, n = 5, P> 0.05). Miniature plastic balloons were first inflated and set at standard physiological LV end diastolic pressure (LVEDP) of 6-8 mmHg [15,36]. Baseline LV hemodynamic performance of mdx and WT hearts was similar (Table 3-1). In order to estimate the LV volume of isolated hearts at standard LVEDP, the

volume required to reach LVEDP of 8 mmHg was recorded (V_{init}, Figure 3-1c). In agreement with previously published findings, we found that mdx hearts have reduced LV volumes at normal LVEDP [15]. To assess whole-organ compliance in isolated hearts, 15 µL was added to the balloon in the LV chamber in 1 µL increments while simultaneously recording LV pressure. Unexpectedly, as volume was added above V_{init} mdx hearts showed a blunted increase in LVEDP indicating an increase in whole-organ compliance compared to WT hearts (representative tracings shown in Figure 3-1a,b). This blunted increase in LVEDP as LV volume increased above V_{init} is quantified in Figure 3-1d by two-way ANOVA, showing significant main effects of strain, volume and an interaction of the two. To account for differences in V_{init} between WT and mdx, changes in LVEDP during stretch were also plotted against $\%V_{init}$. Similar results were observed when plotting the results this way despite the smaller V_{init} of mdx hearts, further accentuating the enhanced whole-organ compliance of mdx hearts (Figure 3-1e). To visualize the true LV EDP-volume relationship, LVEDP was plotted against LV volume (V_{init} + volume added during stretch protocol, Figure 3-1f). Here, mdx hearts initially showed a left-shifted LVEDP-volume curve compared to WT at lower volumes. As LV volume was increased, the blunted slope of the LVEDP-LV volume relationship in mdx hearts approached that of WT mice (Figure 3-1f). Collectively, these results demonstrate the increased compliance of isolated mdx hearts compared to WT.

Because we have previously shown that LV dimensions are normalized in mdx mice upon application of membrane sealant poloxamer 188 *in vivo*[15], we

conducted parallel studies in isolated hearts perfused with buffer containing P188. Inclusion of P188 did not affect the increase in LVEDP as volume was added above V_{init} in isolated mdx hearts, suggesting that the alteration in mechanical properties we observe are not related to mechanical instability of the sarcolemma (Figure 3-2a, b).

To determine if the observed differences in whole-organ compliance were due to mechanical injury of the heart or to ischemia caused by high LV pressures, we recorded the flow rate of perfusate through the coronary vasculature. Throughout the *ex vivo* stretch protocol there was no difference in coronary flow between mdx and WT hearts (Figure 3-2c). Additionally, to determine if the observed differences in whole-organ compliance were due to mechanical injury of mdx hearts during the stretch protocol, we assessed lactate dehydrogenase (LDH) activity in perfusates from isolated hearts before and after stretch. WT and mdx hearts showed similar initial perfusate LDH activity and showed no increase in perfusate LDH activity following stretch (Figure 3-2d). All values for LDH activity recorded for hearts used in the stretch protocol were less than those recorded following ischemia/reperfusion injury, suggesting that minimal cell injury or death occurred during the stretch protocol. Additionally, isolated hearts recovered cardiac performance to pre-stretch levels following the *ex vivo* stretch protocol (Figure 3-1a, b and Figure 3-2e). Collectively, these findings are evidence that the stretch protocol used in this study causes minimal injury to isolated hearts and had negligible effects on cardiac function.

To further characterize the effects of altered dystrophin expression on the mechanical properties of the myocardium, isolated hearts of mdx carrier females were subjected to the LV chamber stretch protocol. In these mice, 50% of cardiac myocytes lack dystrophin due to random X inactivation [37]. Isolated hearts of mdx carrier females showed whole-organ compliance similar to WT hearts (Figure 3-1d, g). We also assessed the whole-organ compliance of hearts from the dystrophin/utrophin double knockout (DKO) mouse. Utrophin is a homolog of dystrophin which is upregulated in mdx mice, compensating for dystrophin loss and contributing to a relatively mild phenotype compared to DMD patients [35,38,39]. DKO mice have a severe dystrophic phenotype which is similar to DMD patients [35,38,39]. DKO mice showed increased compliance compared to both WT and mdx mice (Figure 3-1d, h). DKO mice were used at 4 weeks of age in this study due to their severe dystrophic phenotype and had smaller LV volumes (Figure 3-1c). Because similar volumes were introduced to all hearts regardless of V_{init}, smaller hearts would be predicted to show greater increases in LVEDP as LV volume is increased V_{init} if compliance were equivalent. Whole-heart compliance was reduced in DKO mice compared to controls despite this smaller initial volume. Additionally, the sarcomeric protein titin is a central determinant of passive compliance in cardiac muscle [40,41]. Alternative splicing of titin early in life and may contribute to altered cardiac compliance as the heart develops [42]. However, in the mouse, the adult isoforms of titin are predominant after day 5 [42].

Effects of altering perfusate calcium on mechanical properties of isolated dystrophic and WT hearts. To determine the effects of altering extracellular calcium concentrations on the mechanical properties of the myocardium, isolated hearts were perfused with a modified Kreb's buffer containing high (3 mM) calcium or low (1.75 mM) calcium (all solutions contained 0.5 mM EDTA). Similar to our findings under standard conditions (2.5 mM calcium + 0.5 mM EDTA) isolated mdx hearts perfused with high and low calcium showed a similar blunted increase in LVEDP as volume was increased above V_{init} as compared to controls (Figure 3-3a, b). To further characterize the effects of altering extracellular calcium on myocardial compliance, hearts were perfused with buffer lacking calcium and containing 10 mM 2, 3-butanedione monoxime to inhibit excitation-contraction coupling. Perfusion with this solution halted all contractile activity of isolated hearts. Non-contracting hearts were then subjected to mechanical stretch by adding 30 µL to the heart in 1 µL increments as above. Similar to our findings in beating hearts, non-contracting mdx hearts showed increased whole-organ compliance compared to WT, as shown by a blunted increase in LVEDP as LV volume increased (Figure 3-3c). This is alternatively quantified in Figure 3-3d as the volume required to raise LVEDP to a given value. Statistical analysis by two-way ANOVA shows significant main effects for strain, volume, and an interaction of the two, indicating that mdx hearts require significantly greater volume to raise LVEDP to 60, 80, 100, and 120 mmHg (Figure 3-3d). The congruence of our findings in contracting and non-contracting hearts suggests that, in contrast to individual myocytes, the altered whole-organ

compliance of mdx hearts is not due to calcium-dependent processes such as sarcomeric contraction or trans-sarcolemmal influx of extracellular calcium[15].

The use of non-contracting hearts also allowed for quantitative assessment of diastolic sarcomere lengths at a set LVEDP. This analysis is confounded in contracting hearts due to obligatory contraction-induced changes in sarcomere length. Accordingly, we measured sarcomere length at a range of set LV pressures to determine the single-cell manifestations of whole-organ stretch in non-contracting WT and mdx hearts. Non-contracting hearts were perfusion-fixed at LVEDP pressures of 8, 80, or 160 mmHg. Immunofluorescent staining for desmin was then used to visualize and measure average sarcomere lengths of the mid-LV free wall (Figure 3-4a). At each LV pressure tested, mdx and WT hearts had similar sarcomere lengths (Figure 3-4b). Given that mdx hearts require significantly larger volumes to increase LVP from 8 mmHg to 60, 80, 100, and 120 mmHg (Figure 3-3d), this suggests altered stretch at the level of individual myocytes did not contribute to increased whole-organ compliance in mdx hearts.

Whole-organ heart compliance in other genetic models of muscular dystrophy. Based on the findings above, we hypothesized that increased whole-organ compliance observed in mdx hearts is due to disruption of DGC-mediated connectivity between the extracellular matrix and the intracellular architecture of the cell. To test this hypothesis, we determined the whole-organ compliance of other mouse models of muscular dystrophy in which the DGC or its binding

partners are disrupted: β-sarcoglycan-null mice and dy^{2j} mice. β-sarcoglycan is a DGC protein normally expressed in the heart, the lack of which causes Limb-Girdle Muscular Dystrophy Type 2E [43,44]. Dy^{2j} mice carry a mutation in the LAMA2 gene which causes abnormal splicing of the laminin-α_2 transcript and expression of a truncated protein [45]. The α_2 heavy chain subunit of the extracellular matrix protein laminin is bound by α-dystroglycan, facilitating the interaction of the DGC with the extracellular matrix. [46]. Mutations in LAMA2 cause merosin-deficient muscular dystrophy [47].Similar to mdx mice, the hearts of both β-sarcoglycan null and dy^{2j} hearts showed smaller LV volumes at normal LVEDP and increased whole-organ compliance compared to WT hearts (Figure 3-5a, b, e). Here, similar to mdx mice, we observed increased compliance despite smaller V_{init} for β-sarcoglycan null and dy^{2j} hearts (Figure 3-5). To determine if the observed effects on compliance in mdx, dy^{2j}, and β-sarcoglycan-null hearts are due to specific effects on the DGC or other effects of membrane dysfunction in muscular dystrophy, we also performed the stretch protocol on dysferlin-null hearts. Dysferlin is a membrane repair protein which is not associated with the DGC, the lack of which causes Limb Girdle Muscular Dystrophy Type 2B [48]. These mice have no defect in expression of DGC proteins [49]. Results showed no differences in LV volumes or whole-organ compliance of dysferlin-null and WT hearts (Figure 3-5c, d, e). Collectively, the findings of altered whole-organ compliance in β-sarcoglycan null and dy^{2J}hearts, but not in dysferlin-null hearts, support the hypothesis that specific disruption of

the cytoskeleton-DGC-extracellular matrix alters the mechanical properties of the myocardium and increases whole-organ compliance.

Discussion

The main new finding of this study is that whole-organ compliance is increased in mdx mice and in other genetic models of muscular dystrophy involving DGC disruption, but not in a model of dystrophy caused by membrane repair dysfunction. These results suggest that the DGC is a central determinant of organ-level mechanical compliance of the heart. This, in conjunction with our findings of similar changes in sarcomere length despite significantly greater excursions in LV volume lead us to speculate that side-to-side translation of myoyctes past each other (myocyte slippage) accounts for the increased compliance observed in mdx, dy^{2J} and β-sarcoglycan-null hearts.

Numerous studies have shown that loss of dystrophin alters the response of striated muscle to mechanical stress. In skeletal muscle, loss of dystrophin alters passive mechanical properties and increases susceptibility to mechanical injury [50,51,52]. In cardiac tissue, we and others have previously shown that dystrophin deficient cardiac myocytes are highly susceptible to mechanical injury and show increased passive stiffness [14,15,16]. Here we have subjected isolated hearts to mechanical distension to determine the effects of dystrophin loss on whole-organ compliance and susceptibility to mechanical damage. In contrast to individual cardiac myocytes, isolated mdx hearts show increased compliance compared to normal tissue as LV chamber volume is increased. This

defect is exacerbated in dystrophin/utrophin double knockout hearts and fully prevented in mdx carrier females expressing dystrophin in only 50% of cardiac myocytes. During the distension protocol mdx hearts underwent significant expansion of the LV with no significant effects on cardiac function, membrane damage or cell death. Given the stiffness and mechanical fragility of individual mdx cardiac myocytes during passive stretch [14,15], this suggested that factors other than mechanical instability of the membrane contribute to the increased whole-organ compliance of mdx isolated hearts. This is further supported by the finding that the altered compliance of mdx hearts was not corrected by P188. In a previous report Wilding and colleagues performed *ex vivo* stretch and showed no difference between isolated mdx and WT hearts in LV volumes as LVEDP was increased up to 30 mmHg [53].Our findings are in agreement with this study since we show no significant difference in LVEDP between mdx and WT as volume is increased within this range (Figure 3-1d). However, here we have conducted a more exhaustive analysis of the pressure-volume relationship to reveal significant differences compared to WT.

To determine possible mechanisms for the observed changes in the mechanical properties of isolated hearts, perfusate calcium concentrations were altered. Increasing, decreasing, or removing calcium altogether did not alter the enhanced compliance mdx hearts. This is evidence that neither trans-sarcolemmal calcium entry through membrane “micro-tears” nor sarcomeric contraction contributes to the increased compliance of mdx hearts. Additionally, since α-dystroglycan binding to laminin is dependent on calcium [7], the

persistence of increased compliance in mdx hearts in the absence of calcium suggests that secondary alterations in non-DGC proteins may contribute to apparent myocyte slippage in DMD. Although it was not investigated in the current study, caveolin-3, which is upregulated in mdx mice[54], interacts with the DGC and numerous cell signaling molecules[55,56], and participates in buffering mechanical membrane stress [57], may contribute to the altered mechanical properties of the mdx myocardium.

To determine the effects of whole-organ stretch on individual myocytes in WT and mdx hearts, we determined sarcomere length at a given LV pressure in non-contracting hearts. Sarcomere lengths were similar at all LV pressures tested despite the considerably larger volumes required to alter LV volume in mdx hearts, suggesting that enhanced stretch of the myocytes does not account for increased compliance in isolated mdx hearts. Since alterations in LV volume expansion are not strictly tracked by proportional changes in sarcomere length, this indicates the mechanical properties of the dystrophic myocardium are not a simple extrapolation of findings from isolated cells. To explain these findings, we propose a model for the accelerated pathological dilation of the ventricle in DMD where disruption of the DGC promotes side-to-side myocyte slippage during whole-organ stretch (Figure 3-6). Specifically, we propose that as isolated mdx hearts are stretched, loss of dystrophin and disruption of the DGC causes myocytes to translate past each other to a greater degree than occurs in normal hearts. Therefore, in this model, enhanced compliance in mdx isolated hearts is primarily due to disruptions in the cytoskeleton-DGC-extracellular matrix axis.

Additional experiments in β-sarcoglycan-null, dy^{2J}, and dysferlin-null mice are consistent with our hypothesis that disruption of the DGC-mediated linkage of cells with the extracellular matrix promotes enhanced whole-organ cardiac compliance. Collectively, these findings suggest a mechanism for the increased whole-organ compliance of mdx isolated hearts which is independent of sarcolemma instability and single myocyte compliance. In the broader context of pathophysiological processes associated in DMD cardiomyopathy, the findings presented here suggest a novel mechanism for the pathological ventricular dilation that occurs in DMD and highlight the complex physiological interactions that should be considered when studying diseases at the whole-organ level.

When formulating the working model for the increase compliance of dystrophic hearts observed here, we have also considered other possible explanations for our findings. Specifically, previous reports have shown that chronic ventricular dilation is associated with alterations in the collagen I/collagen III content, promoting a more compliant ventricular wall [58,59,60]. However, the tight-skin mouse which expresses a ~20% excess of collagen in the heart shows no abnormalities in passive ventricular compliance [61]and mdx mice typically show no significant deposition of collagen within the myocardium at the ages tested in this study [62]. Additionally, the sarcomeric protein titin has previously been shown to be truncated in skeletal muscle of DMD patients [41,63,64]. However, our lab has previously shown that permeabilized cardiac myocytes from the golden retriever muscular dystrophy dog show no difference in passive compliance over a wide range of sarcomere lengths, suggesting that loss of

dystrophin does not alter the compliance of the contractile machinery within cardiac myocytes [14]. Previous reports have highlighted the complex arrangement of myocytes in the LV, the anisotropic mechanical properties of the myocardium, and how layers of cardiac myocytes may shear past one another during stretch [65,66,67]. Although our model is consistent with the data reported, we cannot exclude that the observed increase in compliance of dystrophic hearts is due to cardiac myocyte rearrangement, perhaps through shear along myocardial cleavage planes, or altered myocyte orientation within the LV. Additionally, we as shown in Figures 3-1 and 3-5, the initial LV volumes varied between strains, with some dystrophic strains showing significantly smaller LV volumes compared to controls. In this study we have assumed that the observed differences in LV geometry will not significantly affect our measurement of compliance.

Although LV dilation is associated with numerous disease states of the heart, the basis for this pathological change in organ structure is not well understood. Previous studies suggest that myocyte slippage contributes to LV dilation in numerous disease states including aortic stenosis, acute and chronic myocardial infarction, and end-stage dilated cardiomyopathy [31,68,69,70,71,72]. Specifically, these studies have shown that pathological dilation of the LV is associated with LV free wall thinning and reductions in transmural cell number which are not accounted for by hypertrophy, myocyte lengthening or fibrosis [31,68,69,70,72]. Ultrastructural analysis of the chronically dilated LV has shown that pathological LV dilation is associated with disruption of normal sarcolemmal

registry in a dog model of DCM, suggesting myocyte slippage [71]. These findings, along with other reports of disrupted DGC expression in cardiomyopathy brought on by enteroviral infection [73,74], ischemia [75,76], acute isoproterenol toxicity [77], or in idiopathic dilated cardiomyopathy [75,76] lead us to speculate that DGC-mediated changes in whole-heart compliance may be a common pathway to pathological LV dilation in numerous forms of cardiac disease. Additionally, the mice used in this study were at an early stage in the progressive cardiomyopathy of mdx mice and typically show minimal evidence of histopathology [62]. Therefore, it is possible that the observed changes in whole-organ compliance in mdx hearts are an initiating event in the remodeling of the dystrophin deficient myocardium. Future studies aimed at determining the age-related changes in cardiac compliance of mdx mice may be useful for understanding the progression of cardiomyopathy in DMD.

With regard to the relevance of the findings presented here to the pathogenesis of heart disease in DMD, there are limitations of this study that need to be considered. The retrograde perfused isolated heart preparation used in this study is a well-established and widely used technique for assessing whole-organ cardiac function as measured during isovolumic contraction and relaxation[78,79]. However, this technique does not faithfully recapitulate the mechanical rigors of contraction and relaxation due to lack of physiological loading conditions [79]. Previous reports have shown that cardiac function of the dystrophin deficient heart suffers greatly under conditions of physiological loading [80,81]. Although this is certainly a limitation of this study, the absence of

physiological loading allowed us to isolate and study mechanical properties of the intact dystrophin deficient heart independent of myocardial damage caused by physiological loading conditions. We assert that, in addition to the effects of myocyte damage and loss due to mechanical instability of the membrane, the dystrophin deficient heart exhibits a heightened propensity to undergo myocyte slippage which contributes to the progressive pathological dilation of the ventricle in DMD. In addition to this limitation, when using our *ex vivo* stretch protocol we observed differences in whole-organ compliance between WT and mdx hearts at LVEDP well above the normal physiological range. We speculate that the processes resulting in increased compliance in isolated hearts at high LVEDP may also occur under normal conditions *in vivo*, but at a much slower rate. This is in line with the slowly progressive dilation that occurs over the course of years in DMD [25,26]. Additionally, our model of myocyte slippage at high LVEDP is in agreement with previous findings showing that while the sarcomeric filament and disregulgated calcium handling influences the mechanical properties of the myocardium at lower sarcomere lengths, extracellular matrix proteins contribute significantly at higher sarcomere lengths [15,82,83]. Increased compliance in dystrophic hearts was only seen at increased sarcomere lengths, suggesting that these defects were cause by altered extracellular matrix interactions.

In addition to our findings in mdx hearts, we also found similar disturbances in the whole-organ mechanical properties of β-sarcoglycan-null and dy^{2J} hearts. Mutations in β-sarcoglycan and laminin-α_2 cause muscular dystrophy and, importantly, dilated cardiomyopathy[45,84,85,86,87]. However,

there is evidence from previous studies in skeletal muscle to suggest divergence in the mechanisms by which these mutations cause disease when compared to mdx mice. β-sarcoglycan-null mice show muscle wasting and increased membrane permeability [84]. It is not known if β-sarcoglycan-null mice show enhanced susceptibility to contraction-induced injury, but previous studies have shown significant divergence in susceptibility to contraction-induced injury in genetic models of sarcoglycan deficiency [88,89,90]. Dy^{2J} mice show muscle wasting but no evidence of membrane permeability or susceptibility to contraction-induced injury [91,92]. Expression of the anti-apoptotic protein BCL2 corrects muscle defects in laminin deficient mice but not mdx mice, suggesting that aberrant apoptosis plays a role in the pathology of these mice [93]. Despite these differences in the mechanisms of muscle wasting in mdx, dy^{2J}, and β-sarcoglycan-null mice, each of these models shows enhanced whole-heart compliance. We speculate that these mouse models share the phenotype of increased whole-heart compliance due to disruptions of cell-extracellular matrix interactions. Genetic ablation of β-sarcoglycan weakens the interaction of α-dystroglycan with the DGC [87] and the mutant laminin-α_2 heavy chain expressed by dy^{2J} mice is defective in its ability to form stable polymers[94], suggesting mechanisms for the disruption of the contacts between myocytes and the basement membrane. Collectively, the finding of altered mechanical properties in the hearts of mdx, β-sarcoglycan-null and dy^{2J} mice suggests that altering cell-extracellular matrix contacts may be a common mechanism for pathological dilation of the heart in diseases which alter cell-extracellular matrix interactions

by a variety of different mechanisms. The lack of mechanical defects in the hearts of dysferlin-null mice further supports this hypothesis. Mutations in dysferlin cause muscular dystrophy, but development of dilated cardiomyopathy is rare[95,96]. Since dysferlin is not known to directly participate in cell-cell or cell-matrix contacts, the finding of normal compliance in dysferlin-null hearts supports the hypothesis that changes in whole-organ mechanical compliance are specifically caused by disruptions in the cell-extracellular matrix axis of connectivity. The findings presented in this study may therefore have relevance for other disease processes which involve pathological cardiac dilation.

Tables

	LVDP	LVEDP	dP/dt max.	dP/dt min.
C57BL/10SnJ	134.2 ± 2.9	6.9 ± 0.1	4936 ± 162	-3708 ± 137
mdx	133.7 ± 2.7	7.1 ± 0.3	4929 ± 123	-3339 ± 140

Table 3-1. Baseline *ex vivo* functional data for isolated WT and mdx hearts. Contractile function as shown by LV developed pressure (LVDP) and the maximum derivatives of LV pressure (dP/dt max.) were similar between groups. Lusitropic function as measured by LV end diastolic pressure (LVEDP) and the minimum derivative of LV pressure (dP/dt min.) were also similar between the groups by student's t-test. n = 12-15.

Figures

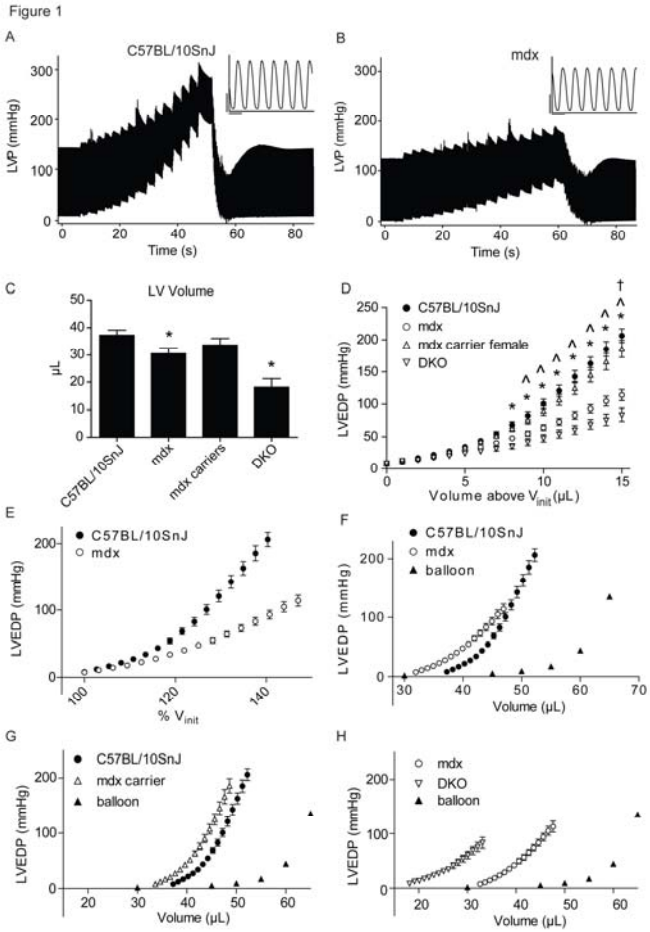

Figure 3-1. Response of isolated, contracting dystrophic isolated hearts to *ex vivo* stretch. A, B) Compressed representative pressure tracings from WT(A) and mdx (B) hearts during *ex vivo* stretch protocol. Inset: uncompressed pressure tracings from mdx and WT hearts prior to stretch, vertical scale bar = 50 mmHg, horizontal scale bar = 1/7 sec. C) Volume required to reach 8 mmHg EDP within the LV (V_{init}). D) Altered whole-organ compliance of mdx and DKO hearts as shown by plotting LVEDP against volume added above V_{init} during *ex vivo* stretch. Mdx carrier females show normal whole-organ compliance. E) Differences in compliance of mdx and WT hearts are further exaggerated when plotting the $\%V_{init}$ versus LVEDP. F) Estimation of the true LV volume-EDP relationship based on data from 1C and 1D. Balloon only controls are shown to prove that recorded changes in pressure were not due to overfilled balloon. G) Whole-organ compliance of isolated WT and mdx carrier female hearts shown as the LV volume versus LVEDP. H) Whole-organ compliance of isolated mdx and DKO hearts shown as LV volume versus LVEDP. n = 5-14. For C, * - $P < 0.05$ by t-test. For D, * - $p < 0.05$ for C57BL/10SnJ vs. DKO, ^ - $P < 0.05$ for C57BL/10SnJ vs. mdx, † - $p < 0.05$ for mdx versus DKO by two-way ANOVA with main effects for strain, volume, and an interaction of the two.

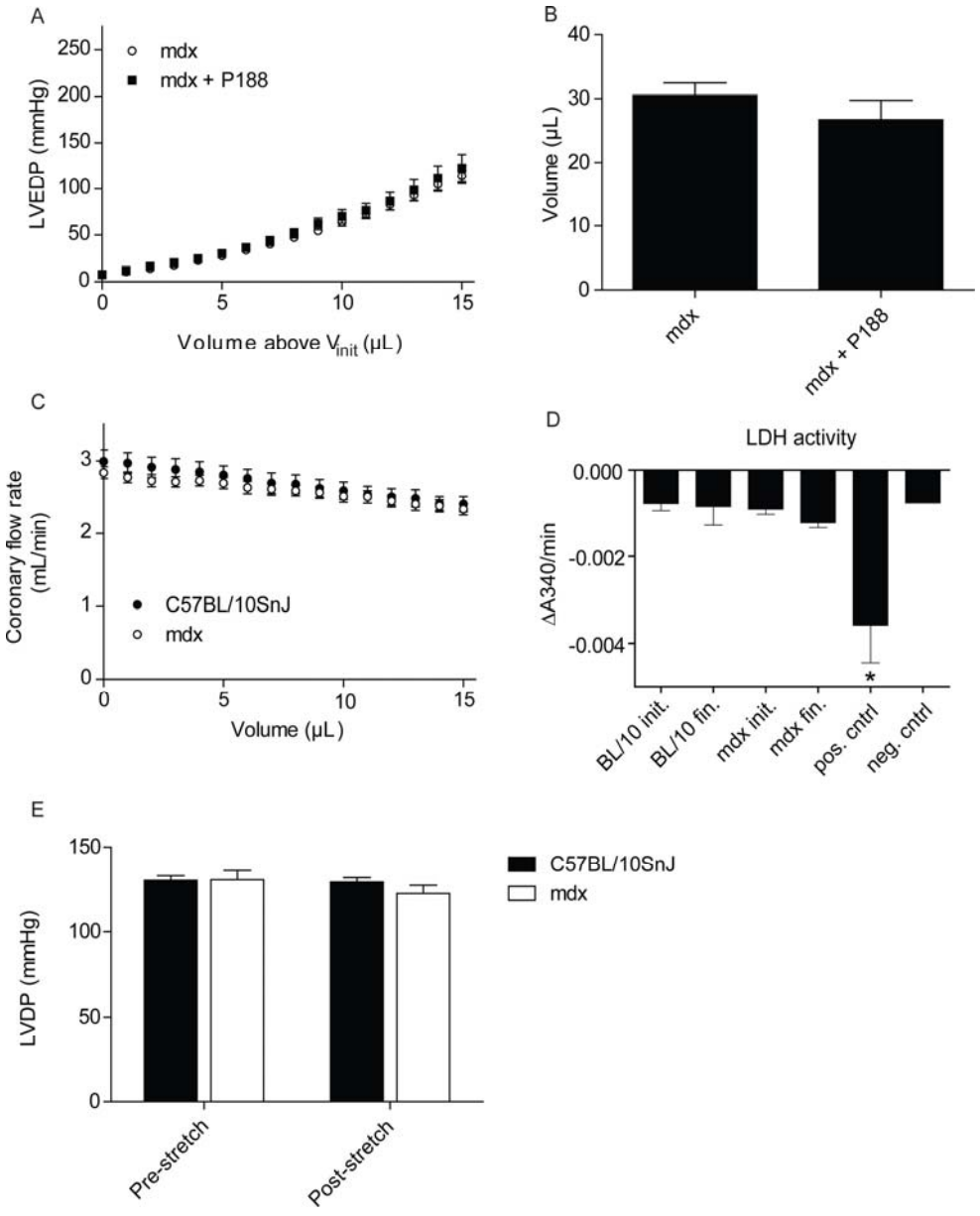

Figure 3-2. P188 does not affect whole-organ compliance and e*x vivo* stretch does not cause ischemia or impair cardiac function. A) Whole-organ compliance of isolated mdx hearts with and without poloxamer 188 in the perfusate (mdx data is same data used in figure 1). B) V_{init} of mdx perfused with and without poloxamer 188 perfusate (mdx data is same data used in figure 1). C) Rate of perfusate flow through the coronary vasculature in mdx and WT hearts during *ex vivo* stretch protocol. D) LDH activity in perfusates from WT and mdx hearts taken before and after *ex vivo* stretch protocol. E) Comparison of LVDP before and after *ex vivo* stretch protocol. No significant differences between observed between WT and mdx mice by two-way ANOVA. For A, B, n = 7-14. For C, n = 11-14. For D, n = 5-9. For E, n =8-12.* - $p < 0.05$ vs. all other groups by one-way ANOVA.

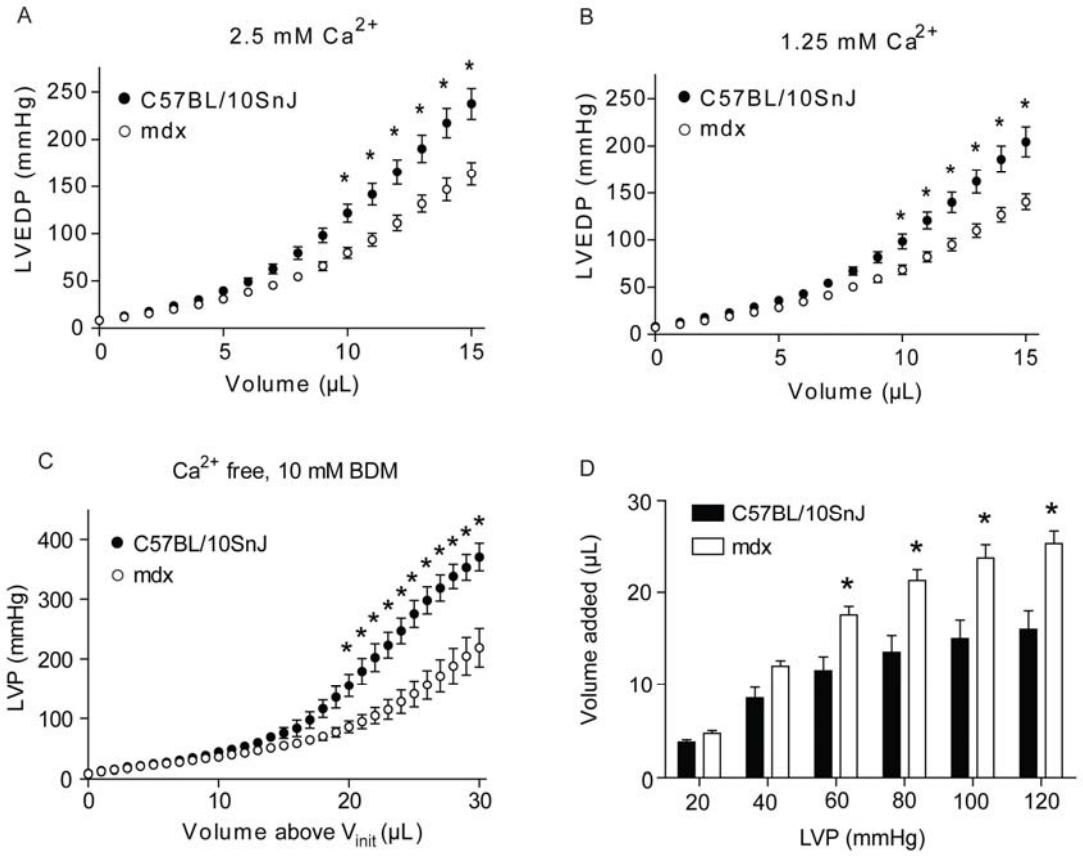

Figure 3-3. Response of non-contracting WT and mdx hearts to altered perfusate calcium. A, B) Altered compliance in mdx hearts as shown by plotting LVEDP against volume added above V_{init} during *ex vivo* stretch when perfused with 2.5 (A) or 1.25 mM (B) Ca^{2+}. C) Increased compliance in non-contracting hearts perfused with BDM and without calcium during stretch as shown by plotting LVEDP against volume added above V_{init}. D) Quantification of altered compliance in mdx hearts, plotted as volume required to raise LVP from 8 mmHg (V_{init}) to 20, 40, 60, 80, 100, or 120 mmHg. E) Volume required to reach 8 mmHg EDP within the LV (V_{init}). n = 5-10. * - $p < 0.05$ by two-way ANOVA with main effects for strain, volume, and an interaction of the two.

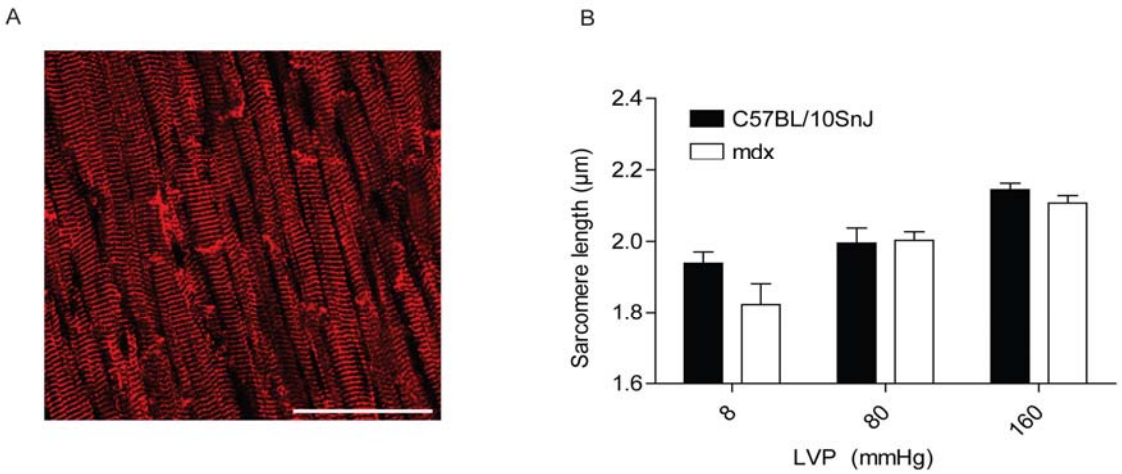

Figure 3-4. Quantification of changes in sarcomere length during whole-organ stretch in non-contracting hearts. A) Representative image of desmin stained section of fixed heart tissue. Average sarcomere length of circumferentially oriented myocytes from the mid LV free wall was determined. Scale bar = 50 μm. B) Quantitation of average sarcomere length at a range of fixed LV pressures. n = 5-10. No significant differences were detected by two-way ANOVA.

Figure 4

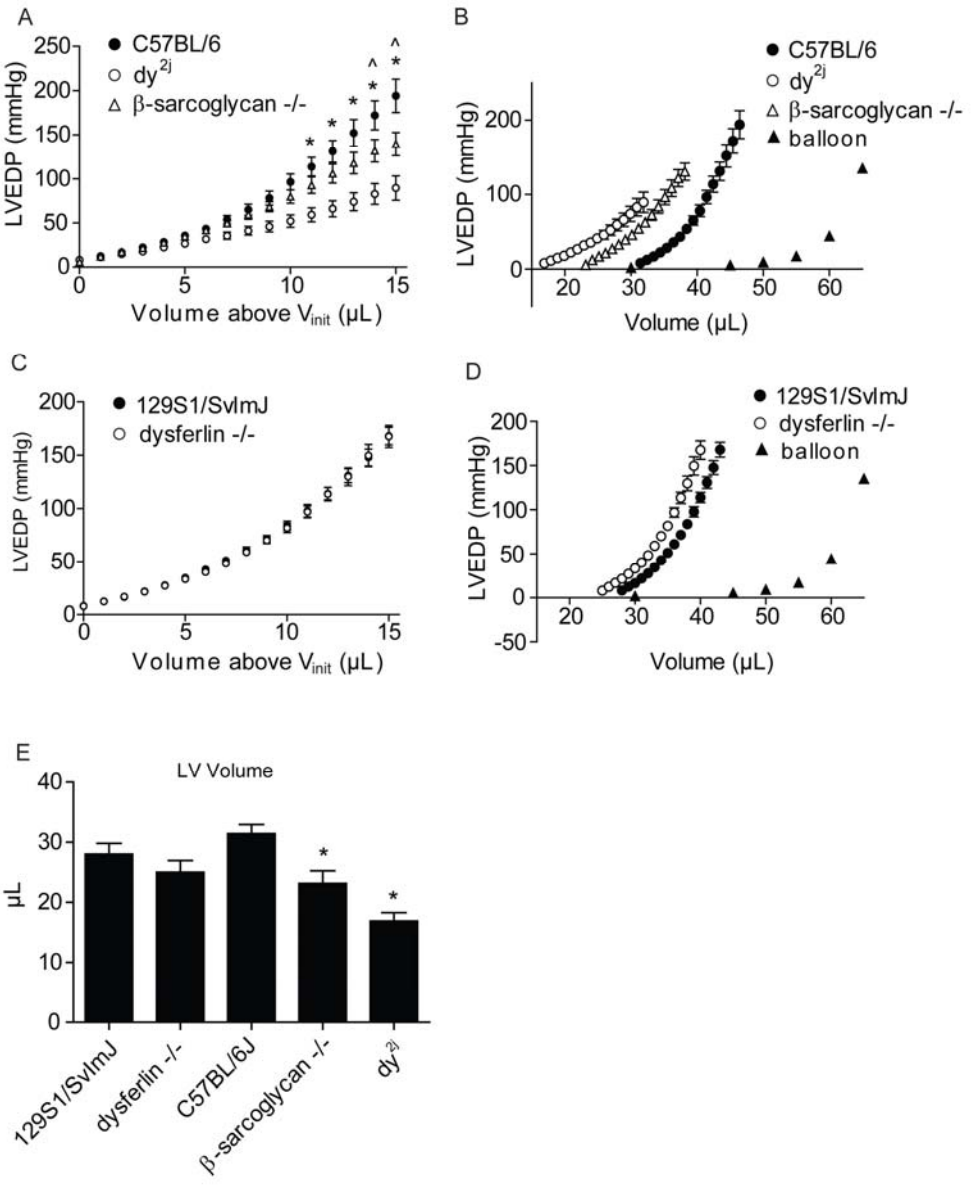

Figure 3-5. **Whole-organ passive compliance of isolated hearts of other models of muscular dystrophy**. A) Left, altered compliance of β-sarcoglycan-null and dy^{2J} hearts as shown by plotting LVEDP against volume added above V_{init} during *ex vivo* stretch. Right, estimation of the true LV volume-EDP relationship, plotted as in figure 1F. B) Left, normal compliance of dysferlin-null hearts as shown by plotting LVEDP against volume added above V_{init} during *ex vivo* stretch. Right, estimation of the true LV volume-EDP relationship. n = 5-7. * - $p < 0.05$ for dy^{2J} versus C57BL/6, ^ - $p < 0.05$ for β-sarcoglycan-null versus C57BL/6. Statistical comparisons made by two-way ANOVA with main effects for strain, volume, and an interaction of the two.

Figure 5

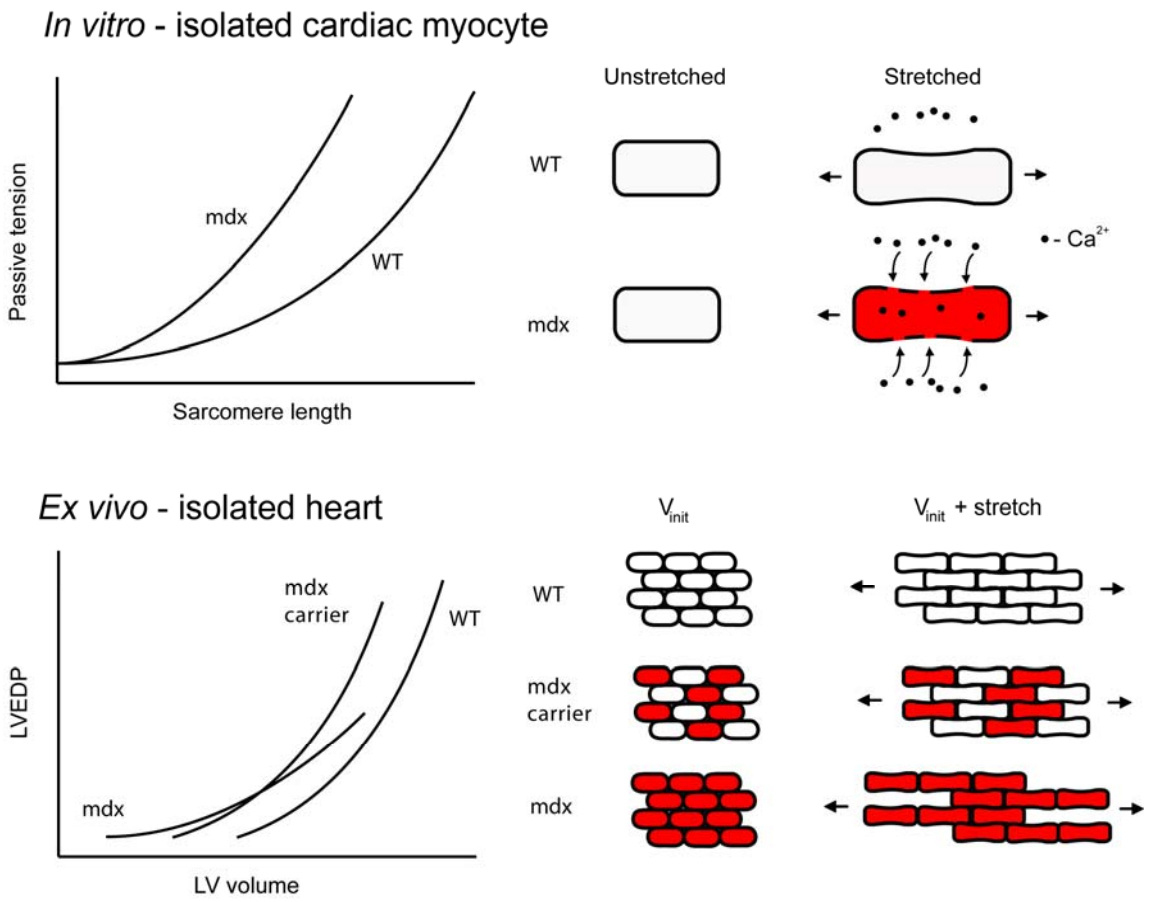

Figure 3-6. Proposed model for the mechanical properties of the dystrophic myocardium. Top, model for the increased stiffness of mdx myocytes. Stretch causes membrane permeability and influx of extracellular calcium, leading to unregulated contraction (indicated in red). Bottom, model for the effects of dystrophin expression on myocardial compliance. In mdx hearts, membrane permeability may initially cause contraction of LV volume at normal LVEDP, resulting in a left shift in the LV volume-EDP curve. As volume is increased, loss of dystrophin leads to increased slippage of myocytes past one another, leading to increased compliance. This is corrected by expression of dystrophin in 50% of myocytes in mdx carrier females.

Literature cited

1. Emery AE (1991) Population frequencies of inherited neuromuscular diseases--a world survey. Neuromuscul Disord 1: 19-29.

2. Hoffman EP, Brown RH, Jr., Kunkel LM (1987) Dystrophin: the protein product of the Duchenne muscular dystrophy locus. Cell 51: 919-928.

3. Davies KE, Pearson PL, Harper PS, Murray JM, O'Brien T, et al. (1983) Linkage analysis of two cloned DNA sequences flanking the Duchenne muscular dystrophy locus on the short arm of the human X chromosome. Nucleic Acids Res 11: 2303-2312.

4. Koenig M, Hoffman EP, Bertelson CJ, Monaco AP, Feener C, et al. (1987) Complete cloning of the Duchenne muscular dystrophy (DMD) cDNA and preliminary genomic organization of the DMD gene in normal and affected individuals. Cell 50: 509-517.

5. Yoshida M, Ozawa E (1990) Glycoprotein complex anchoring dystrophin to sarcolemma. J Biochem 108: 748-752.

6. Ervasti JM, Ohlendieck K, Kahl SD, Gaver MG, Campbell KP (1990) Deficiency of a glycoprotein component of the dystrophin complex in dystrophic muscle. Nature 345: 315-319.

7. Ervasti JM, Campbell KP (1993) A role for the dystrophin-glycoprotein complex as a transmembrane linker between laminin and actin. J Cell Biol 122: 809-823.

8. Suzuki A, Yoshida M, Yamamoto H, Ozawa E (1992) Glycoprotein-binding site of dystrophin is confined to the cysteine-rich domain and the first half of the carboxy-terminal domain. FEBS Lett 308: 154-160.

9. Hemmings L, Kuhlman PA, Critchley DR (1992) Analysis of the actin-binding domain of alpha-actinin by mutagenesis and demonstration that dystrophin contains a functionally homologous domain. J Cell Biol 116: 1369-1380.

10. Way M, Pope B, Cross RA, Kendrick-Jones J, Weeds AG (1992) Expression of the N-terminal domain of dystrophin in E. coli and demonstration of binding to F-actin. FEBS Lett 301: 243-245.

11. Michele DE, Barresi R, Kanagawa M, Saito F, Cohn RD, et al. (2002) Post-translational disruption of dystroglycan-ligand interactions in congenital muscular dystrophies. Nature 418: 417-422.

12. Vilquin JT, Brussee V, Asselin I, Kinoshita I, Gingras M, et al. (1998) Evidence of mdx mouse skeletal muscle fragility in vivo by eccentric running exercise. Muscle Nerve 21: 567-576.

13. Weller B, Karpati G, Carpenter S (1990) Dystrophin-deficient mdx muscle fibers are preferentially vulnerable to necrosis induced by experimental lengthening contractions. J Neurol Sci 100: 9-13.

14. Townsend D, Turner I, Yasuda S, Martindale J, Davis J, et al. Chronic administration of membrane sealant prevents severe cardiac injury and ventricular dilatation in dystrophic dogs. J Clin Invest 120: 1140-1150.

15. Yasuda S, Townsend D, Michele DE, Favre EG, Day SM, et al. (2005) Dystrophic heart failure blocked by membrane sealant poloxamer. Nature 436: 1025-1029.

16. Fanchaouy M, Polakova E, Jung C, Ogrodnik J, Shirokova N, et al. (2009) Pathways of abnormal stress-induced Ca2+ influx into dystrophic mdx cardiomyocytes. Cell Calcium 46: 114-121.

17. Kohler M, Clarenbach CF, Bahler C, Brack T, Russi EW, et al. (2009) Disability and survival in Duchenne muscular dystrophy. J Neurol Neurosurg Psychiatry 80: 320-325.

18. Eagle M, Baudouin SV, Chandler C, Giddings DR, Bullock R, et al. (2002) Survival in Duchenne muscular dystrophy: improvements in life expectancy since 1967 and the impact of home nocturnal ventilation. Neuromuscul Disord 12: 926-929.

19. Finsterer J, Stollberger C (2003) The heart in human dystrophinopathies. Cardiology 99: 1-19.

20. Gulati S, Saxena A, Kumar V, Kalra V (2005) Duchenne muscular dystrophy: prevalence and patterns of cardiac involvement. Indian J Pediatr 72: 389-393.

21. Eagle M, Bourke J, Bullock R, Gibson M, Mehta J, et al. (2007) Managing Duchenne muscular dystrophy--the additive effect of spinal surgery and home nocturnal ventilation in improving survival. Neuromuscul Disord 17: 470-475.

22. Conte G, Gioia L (1836) Scrofola del sistema muscolare. Annali Clinici dell'Ospedale degli Incurabili 66.

23. Spurney CF Cardiomyopathy of Duchenne muscular dystrophy: current understanding and future directions. Muscle Nerve 44: 8-19.

24. McNally EM (2007) New approaches in the therapy of cardiomyopathy in muscular dystrophy. Annu Rev Med 58: 75-88.

25. Cox GF, Kunkel LM (1997) Dystrophies and heart disease. Curr Opin Cardiol 12: 329-343.

26. Nigro G, Comi LI, Politano L, Bain RJ (1990) The incidence and evolution of cardiomyopathy in Duchenne muscular dystrophy. Int J Cardiol 26: 271-277.

27. Quinlan JG, Hahn HS, Wong BL, Lorenz JN, Wenisch AS, et al. (2004) Evolution of the mdx mouse cardiomyopathy: physiological and morphological findings. Neuromuscul Disord 14: 491-496.

28. Anversa P, Olivetti G, Capasso JM (1991) Cellular basis of ventricular remodeling after myocardial infarction. Am J Cardiol 68: 7D-16D.

29. White HD (1992) Remodelling of the heart after myocardial infarction. Aust N Z J Med 22: 601-606.

30. Francis GS, Chu C (1995) Post-infarction myocardial remodelling: why does it happen? Eur Heart J 16 Suppl N: 31-36.

31. Beltrami CA, Finato N, Rocco M, Feruglio GA, Puricelli C, et al. (1995) The cellular basis of dilated cardiomyopathy in humans. J Mol Cell Cardiol 27: 291-305.

32. Olivetti G, Melissari M, Capasso JM, Anversa P (1991) Cardiomyopathy of the aging human heart. Myocyte loss and reactive cellular hypertrophy. Circ Res 68: 1560-1568.

33. Kajstura J, Zhang X, Liu Y, Szoke E, Cheng W, et al. (1995) The cellular basis of pacing-induced dilated cardiomyopathy. Myocyte cell loss and myocyte cellular reactive hypertrophy. Circulation 92: 2306-2317.

34. Schmitt JP, Kamisago M, Asahi M, Li GH, Ahmad F, et al. (2003) Dilated cardiomyopathy and heart failure caused by a mutation in phospholamban. Science 299: 1410-1413.

35. Deconinck AE, Rafael JA, Skinner JA, Brown SC, Potter AC, et al. (1997) Utrophin-dystrophin-deficient mice as a model for Duchenne muscular dystrophy. Cell 90: 717-727.

36. Day SM, Westfall MV, Fomicheva EV, Hoyer K, Yasuda S, et al. (2006) Histidine button engineered into cardiac troponin I protects the ischemic and failing heart. Nat Med 12: 181-189.

37. Bostick B, Yue Y, Long C, Duan D (2008) Prevention of dystrophin-deficient cardiomyopathy in twenty-one-month-old carrier mice by mosaic dystrophin expression or complementary dystrophin/utrophin expression. Circ Res 102: 121-130.

38. Janssen PM, Hiranandani N, Mays TA, Rafael-Fortney JA (2005) Utrophin deficiency worsens cardiac contractile dysfunction present in dystrophin-deficient mdx mice. Am J Physiol Heart Circ Physiol 289: H2373-2378.

39. Grady RM, Teng H, Nichol MC, Cunningham JC, Wilkinson RS, et al. (1997) Skeletal and cardiac myopathies in mice lacking utrophin and dystrophin: a model for Duchenne muscular dystrophy. Cell 90: 729-738.

40. LeWinter MM, Wu Y, Labeit S, Granzier H (2007) Cardiac titin: structure, functions and role in disease. Clin Chim Acta 375: 1-9.

41. Fukuda N, Terui T, Ishiwata S, Kurihara S Titin-based regulations of diastolic and systolic functions of mammalian cardiac muscle. J Mol Cell Cardiol 48: 876-881.

42. Lahmers S, Wu Y, Call DR, Labeit S, Granzier H (2004) Developmental control of titin isoform expression and passive stiffness in fetal and neonatal myocardium. Circ Res 94: 505-513.

43. Lim LE, Duclos F, Broux O, Bourg N, Sunada Y, et al. (1995) Beta-sarcoglycan: characterization and role in limb-girdle muscular dystrophy linked to 4q12. Nat Genet 11: 257-265.

44. Bonnemann CG, Modi R, Noguchi S, Mizuno Y, Yoshida M, et al. (1995) Beta-sarcoglycan (A3b) mutations cause autosomal recessive muscular dystrophy with loss of the sarcoglycan complex. Nat Genet 11: 266-273.

45. Xu H, Wu XR, Wewer UM, Engvall E (1994) Murine muscular dystrophy caused by a mutation in the laminin alpha 2 (Lama2) gene. Nat Genet 8: 297-302.

46. Hohenester E, Tisi D, Talts JF, Timpl R (1999) The crystal structure of a laminin G-like module reveals the molecular basis of alpha-dystroglycan binding to laminins, perlecan, and agrin. Mol Cell 4: 783-792.

47. Helbling-Leclerc A, Zhang X, Topaloglu H, Cruaud C, Tesson F, et al. (1995) Mutations in the laminin alpha 2-chain gene (LAMA2) cause merosin-deficient congenital muscular dystrophy. Nat Genet 11: 216-218.

48. Liu J, Aoki M, Illa I, Wu C, Fardeau M, et al. (1998) Dysferlin, a novel skeletal muscle gene, is mutated in Miyoshi myopathy and limb girdle muscular dystrophy. Nat Genet 20: 31-36.

49. Bansal D, Miyake K, Vogel SS, Groh S, Chen CC, et al. (2003) Defective membrane repair in dysferlin-deficient muscular dystrophy. Nature 423: 168-172.

50. Brooks SV (1998) Rapid recovery following contraction-induced injury to in situ skeletal muscles in mdx mice. J Muscle Res Cell Motil 19: 179-187.

51. Petrof BJ, Shrager JB, Stedman HH, Kelly AM, Sweeney HL (1993) Dystrophin protects the sarcolemma from stresses developed during muscle contraction. Proc Natl Acad Sci U S A 90: 3710-3714.

52. Menke A, Jockusch H (1991) Decreased osmotic stability of dystrophin-less muscle cells from the mdx mouse. Nature 349: 69-71.

53. Wilding JR, Schneider JE, Sang AE, Davies KE, Neubauer S, et al. (2005) Dystrophin- and MLP-deficient mouse hearts: marked differences in morphology and function, but similar accumulation of cytoskeletal proteins. FASEB J 19: 79-81.

54. Vaghy PL, Fang J, Wu W, Vaghy LP (1998) Increased caveolin-3 levels in mdx mouse muscles. FEBS Lett 431: 125-127.

55. Garcia-Cardena G, Martasek P, Masters BS, Skidd PM, Couet J, et al. (1997) Dissecting the interaction between nitric oxide synthase (NOS) and caveolin. Functional significance of the nos caveolin binding domain in vivo. J Biol Chem 272: 25437-25440.

56. Song KS, Scherer PE, Tang Z, Okamoto T, Li S, et al. (1996) Expression of caveolin-3 in skeletal, cardiac, and smooth muscle cells. Caveolin-3 is a component of the sarcolemma and co-fractionates with dystrophin and dystrophin-associated glycoproteins. J Biol Chem 271: 15160-15165.

57. Sinha B, Koster D, Ruez R, Gonnord P, Bastiani M, et al. Cells respond to mechanical stress by rapid disassembly of caveolae. Cell 144: 402-413.

58. Liang H, Muller J, Weng YG, Wallukat G, Fu P, et al. (2004) Changes in myocardial collagen content before and after left ventricular assist device application in dilated cardiomyopathy. Chin Med J (Engl) 117: 401-407.

59. Marijianowski MM, Teeling P, Mann J, Becker AE (1995) Dilated cardiomyopathy is associated with an increase in the type I/type III collagen ratio: a quantitative assessment. J Am Coll Cardiol 25: 1263-1272.

60. Yoshikane H, Honda M, Goto Y, Morioka S, Ooshima A, et al. (1992) Collagen in dilated cardiomyopathy--scanning electron microscopic and immunohistochemical observations. Jpn Circ J 56: 899-910.

61. Omens JH, Rockman HA, Covell JW (1994) Passive ventricular mechanics in tight-skin mice. Am J Physiol 266: H1169-1176.

62. Van Erp C, Loch D, Laws N, Trebbin A, Hoey AJ Timeline of cardiac dystrophy in 3-18-month-old MDX mice. Muscle Nerve 42: 504-513.

63. Wu Y, Bell SP, Trombitas K, Witt CC, Labeit S, et al. (2002) Changes in titin isoform expression in pacing-induced cardiac failure give rise to increased passive muscle stiffness. Circulation 106: 1384-1389.

64. Matsumura K, Shimizu T, Nonaka I, Mannen T (1989) Immunochemical study of connectin (titin) in neuromuscular diseases using a monoclonal antibody: connectin is degraded extensively in Duchenne muscular dystrophy. J Neurol Sci 93: 147-156.

65. LeGrice IJ, Takayama Y, Covell JW (1995) Transverse shear along myocardial cleavage planes provides a mechanism for normal systolic wall thickening. Circ Res 77: 182-193.

66. McCulloch AD, Smaill BH, Hunter PJ (1989) Regional left ventricular epicardial deformation in the passive dog heart. Circ Res 64: 721-733.

67. Nielsen PM, Le Grice IJ, Smaill BH, Hunter PJ (1991) Mathematical model of geometry and fibrous structure of the heart. Am J Physiol 260: H1365-1378.

68. Olivetti G, Capasso JM, Sonnenblick EH, Anversa P (1990) Side-to-side slippage of myocytes participates in ventricular wall remodeling acutely after myocardial infarction in rats. Circ Res 67: 23-34.

69. Olivetti G, Capasso JM, Meggs LG, Sonnenblick EH, Anversa P (1991) Cellular basis of chronic ventricular remodeling after myocardial infarction in rats. Circ Res 68: 856-869.

70. Weisman HF, Bush DE, Mannisi JA, Weisfeldt ML, Healy B (1988) Cellular mechanisms of myocardial infarct expansion. Circulation 78: 186-201.

71. Ross J, Jr., Sonnenblick EH, Taylor RR, Spotnitz HM, Covell JW (1971) Diastolic geometry and sarcomere lengths in the chronically dilated canine left ventricle. Circ Res 28: 49-61.

72. Vitali-Mazza L, Anversa P, Tedeschi F, Mastandrea R, Mavilla V, et al. (1972) Ultrastructural basis of acute left ventricular failure from severe acute aortic stenosis in the rabbit. J Mol Cell Cardiol 4: 661-671.

73. Lee GH, Badorff C, Knowlton KU (2000) Dissociation of sarcoglycans and the dystrophin carboxyl terminus from the sarcolemma in enteroviral cardiomyopathy. Circ Res 87: 489-495.

74. Badorff C, Lee GH, Lamphear BJ, Martone ME, Campbell KP, et al. (1999) Enteroviral protease 2A cleaves dystrophin: evidence of cytoskeletal disruption in an acquired cardiomyopathy. Nat Med 5: 320-326.

75. Vatta M, Stetson SJ, Jimenez S, Entman ML, Noon GP, et al. (2004) Molecular normalization of dystrophin in the failing left and right ventricle of patients treated with either pulsatile or continuous flow-type ventricular assist devices. J Am Coll Cardiol 43: 811-817.

76. Vatta M, Stetson SJ, Perez-Verdia A, Entman ML, Noon GP, et al. (2002) Molecular remodelling of dystrophin in patients with end-stage cardiomyopathies and reversal in patients on assistance-device therapy. Lancet 359: 936-941.

77. Toyo-Oka T, Kawada T, Nakata J, Xie H, Urabe M, et al. (2004) Translocation and cleavage of myocardial dystrophin as a common pathway to advanced heart failure: a scheme for the progression of cardiac dysfunction. Proc Natl Acad Sci U S A 101: 7381-7385.

78. Langendorff (1895) Untersuchungen am überlebenden Säugetierherzen. Pflügers Archiv 61: 291–332.

79. Dhein S, Mohr FW, Delmar M (2005) Practical Methods in Cardiovascular Research Springer. 1010 p.

80. Townsend D, Blankinship MJ, Allen JM, Gregorevic P, Chamberlain JS, et al. (2007) Systemic administration of micro-dystrophin restores cardiac geometry and prevents dobutamine-induced cardiac pump failure. Mol Ther 15: 1086-1092.

81. Danialou G, Comtois AS, Dudley R, Karpati G, Vincent G, et al. (2001) Dystrophin-deficient cardiomyocytes are abnormally vulnerable to mechanical stress-induced contractile failure and injury. Faseb J 15: 1655-1657.

82. Wu Y, Cazorla O, Labeit D, Labeit S, Granzier H (2000) Changes in titin and collagen underlie diastolic stiffness diversity of cardiac muscle. J Mol Cell Cardiol 32: 2151-2162.

83. Granzier HL, Labeit S (2004) The giant protein titin: a major player in myocardial mechanics, signaling, and disease. Circ Res 94: 284-295.

84. Araishi K, Sasaoka T, Imamura M, Noguchi S, Hama H, et al. (1999) Loss of the sarcoglycan complex and sarcospan leads to muscular dystrophy in beta-sarcoglycan-deficient mice. Hum Mol Genet 8: 1589-1598.

85. Barresi R, Di Blasi C, Negri T, Brugnoni R, Vitali A, et al. (2000) Disruption of heart sarcoglycan complex and severe cardiomyopathy caused by beta sarcoglycan mutations. J Med Genet 37: 102-107.

86. Spyrou N, Philpot J, Foale R, Camici PG, Muntoni F (1998) Evidence of left ventricular dysfunction in children with merosin-deficient congenital muscular dystrophy. Am Heart J 136: 474-476.

87. Durbeej M, Cohn RD, Hrstka RF, Moore SA, Allamand V, et al. (2000) Disruption of the beta-sarcoglycan gene reveals pathogenetic complexity of limb-girdle muscular dystrophy type 2E. Mol Cell 5: 141-151.

88. Hack AA, Lam MY, Cordier L, Shoturma DI, Ly CT, et al. (2000) Differential requirement for individual sarcoglycans and dystrophin in the assembly and function of the dystrophin-glycoprotein complex. J Cell Sci 113 (Pt 14): 2535-2544.

89. Hack AA, Cordier L, Shoturma DI, Lam MY, Sweeney HL, et al. (1999) Muscle degeneration without mechanical injury in sarcoglycan deficiency. Proc Natl Acad Sci U S A 96: 10723-10728.

90. Blaauw B, Agatea L, Toniolo L, Canato M, Quarta M, et al. Eccentric contractions lead to myofibrillar dysfunction in muscular dystrophy. J Appl Physiol 108: 105-111.

91. Straub V, Rafael JA, Chamberlain JS, Campbell KP (1997) Animal models for muscular dystrophy show different patterns of sarcolemmal disruption. J Cell Biol 139: 375-385.

92. Head SI, Bakker AJ, Liangas G (2004) EDL and soleus muscles of the C57BL6J/dy2j laminin-alpha 2-deficient dystrophic mouse are not vulnerable to eccentric contractions. Exp Physiol 89: 531-539.

93. Dominov JA, Kravetz AJ, Ardelt M, Kostek CA, Beermann ML, et al. (2005) Muscle-specific BCL2 expression ameliorates muscle disease in laminin {alpha}2-deficient, but not in dystrophin-deficient, mice. Hum Mol Genet 14: 1029-1040.

94. Colognato H, Yurchenco PD (1999) The laminin alpha2 expressed by dystrophic dy(2J) mice is defective in its ability to form polymers. Curr Biol 9: 1327-1330.

95. Kuru S, Yasuma F, Wakayama T, Kimura S, Konagaya M, et al. (2004) [A patient with limb girdle muscular dystrophy type 2B (LGMD2B) manifesting cardiomyopathy]. Rinsho Shinkeigaku 44: 375-378.

96. Wenzel K, Geier C, Qadri F, Hubner N, Schulz H, et al. (2007) Dysfunction of dysferlin-deficient hearts. J Mol Med 85: 1203-1214.

Chapter 4

The C-terminal fragment of dystrophin cleavage by enteroviral protease 2A causes dystrophic cardiomyopathy

Abstract

Cardiac enterovirus (EV) infection is a clinically relevant disease state which causes cardiomyopathy and heightened susceptibility to ischemic injury. Previously, it has been shown that dystrophin is targeted for cleavage by the 2A protease ($2A^{pro}$) expressed by enteroviruses. This has led to the hypothesis that dystrophin cleavage contributes to the cardiomyopathy of EV infection. However, because $2A^{pro}$ cleaves numerous substrates, it is unclear if dystrophin contributes to cardiomyopathy during EV infection or is a byproduct of other pathological processes. To address this question, transgenic mice were created expressing the N- and C-terminal products of $2A^{pro}$-mediated dystrophin cleavage (NtermDys and CtermDys, respectively). CtermDys transgenic mice show a dystrophic cardiomyopathy as shown by enhanced Evans blue dye (EBD) uptake during isoproterenol stress, enhanced myocardial fibrosis, and increased susceptibility to ischemic injury. CtermDys transgenic mice also show ~70% reduction in expression of dystrophin along with a ~5-10 fold increase in other DGC proteins.

Conversely, NtermDys transgenic mice show no dystrophic cardiomyopathy as indicated by normal EBD uptake during isoproterenol stress and express normal levels of dystrophin and other DGC proteins. To more accurately simulate EV infection, double transgenic mice were generated which also show a dystrophic cardiomyopathy as shown by EBD uptake during isoproterenol stress that is similar to CtermDys mice. Collectively, these results show that expression of CtermDys is sufficient to cause a dystrophic cardiomyopathy with the NtermDys protein having no detrimental effects. These findings provide evidence that CtermDys acts as a dominant negative to DGC function and, therefore, could contribute significantly to the cardiomyopathy of EV infection.

Introduction

Cardiotropic enterovirus (EV) infection is a clinically relevant disease process associated with numerous forms of cardiac dysfunction. Cardiac EV infection varies greatly in its clinical presentation. Interestingly, 5-10% of healthy, asymptomatic individuals show evidence of EV infection in the heart [1,2]. However, EV infection is also the most common cause of acute myocarditis [3] which can manifest as mild cardiomyopathy as well as in sudden and catastrophic loss of heart pump function [4]. EV infection has been detected in 20-40% of patients who die suddenly following acute myocardial infarction and 40% of patients with apparently idiopathic dilated cardiomyopathy [1,5,6,7,8,9]. Collectively, these findings suggest that EV infection increases the susceptibility

of the heart to injury and dysfunction. However, the mechanisms by which EV compromises cardiac function are not totally clear.

Dystrophin is a cytoskeletal protein encoded by the Duchenne muscular dystrophy (DMD) gene. Genetic mutations leading to loss of dystrophin cause DMD. Dystrophin exists as a cytoplasmic constituent of the dystrophin-glycoprotein complex (DGC) [10,11]. The DGC is a multimeric, sarcolemma-spanning protein complex which provides a mechanical linkage between the cytoskeleton and the extracellular matrix [12]. Dystrophin participates in this linkage by binding cortical actin at its N-terminus and the DGC protein β-dystroglycan at its C-terminus [13,14,15,16]. Loss of dystrophin causes mechanical fragility of the sarcolemma, leading to muscle necrosis and wasting in skeletal and cardiac muscle [17,18,19,20,21,22]. Previously, it has been shown that the 2A protease ($2A^{pro}$) expressed by the coxsackieviruses cleaves dystrophin within its hinge 3 domain *in vitro* [23,24]. Additional studies have shown that EV infection causes truncation of dystrophin into fragments consistent with $2A^{pro}$ cleavage *in vivo*, and that transgenic expression of $2A^{pro}$ causes cardiomyopathy [23,25]. This has led to the hypothesis that cleavage of dystrophin is a causal mechanism for the pathogenesis of cardiac EV infection. However, in addition to dystrophin, $2A^{pro}$ also cleaves numerous other substrates including poly-A binding protein, eIF-4G and serum response factor [26,27,28]. Therefore, the *specific* contribution of $2A^{pro}$-mediated dystrophin cleavage to the cardiomyopathy of EV infection is unclear.

In addition to loss of full-length dystrophin, the presence of cleaved fragments of dystrophin following EV infection suggests an alternative mechanism for the cardiomyopathy of EV infection. Previously, it has been shown that expression of truncated non-muscle isoforms of dystrophin in skeletal muscle cause dystrophic myopathy by acting in a dominant negative manner to dystrophin [29,30,31,32,33,34]. These isoforms, derived from alternative promoters within the DMD gene, retain dystrophin's C-terminal β-dystroglycan binding domain but lack some or all of dystrophin's actin binding domains (Figure 4-1). The putative products of dystrophin cleavage by $2A^{pro}$ are an N-terminal fragment containing dystrophin's actin binding domains and a C-terminal fragment containing dystrophin's β-dystroglycan binding domain (Figure 4-1). Because this C-terminal dystrophin fragment is very similar to the previously described dominant negative isoforms of dystrophin, we hypothesize that the presence of this fragment is sufficient to cause dystrophic cardiomyopathy in the heart. Additionally, because enterovirus infection has been associated with increased risk of death following acute myocardial infarction [1], we also hypothesized that expression of the C-terminal fragment of dystrophin cleavage by $2A^{pro}$ promotes susceptibility to ischemic injury. To test these hypotheses, we transgenically expressed the N-terminal and C-terminal products of dystrophin cleavage by $2A^{pro}$ in independent lines. The C-terminal dystrophin fragment localizes to the sarcolemma and causes a significant reduction in expression of full-length dystrophin. Transgenic expression of the C-terminal dystrophin fragment also causes membrane instability, myocardial fibrosis, and reduced

recovery of heart pump function following ischemic injury. The N-terminal fragment of dystrophin cleavage by $2A^{pro}$ was found at the sarcolemma and, surprisingly, in the nucleus of cardiac myocytes. Expression of this fragment neither affected levels of endogenous dystrophin nor caused disruption of membrane stability. Collectively, these results show that expression of the C-terminal product of dystrophin cleavage by $2A^{pro}$ is sufficient to cause dystrophic cardiomyopathy and increase susceptibility to ischemic injury by exerting a dominant negative effect of DGC function.

Materials and Methods

Generation of transgenic mice. The NtermDys and CtermDys transgenic constructs were PCR cloned from the murine dystrophin cDNA containing an N-terminal flag tag (a kind gift from Dr. James Ervasti). For the NtermDys transgene, the forward primer 5'-tttttttttgcggccgctacggcaaggtgctgtgcacggatctgccc-3' and reverse primer 5'-tttttttttgcggccgccctgaccgtgcccctggactgagcactact-3' were used to generate a 7.3 kbp product with flanking NotI restriction sites. For the CtermDys transgene, the forward primer 5'-tttttttttgcggccgcgagcagaacgtgatctcggaggaggacctgggagcctctgccagtcagactgttactcta-3' and reverse primer 5'-tttttttttgcggccgcactgaaactaaggactccatcgctctgccc were used to generate a 3.9 kbp product with flanking NotI restriction sites. PCR mutagenesis was also used to add an N-terminal myc tag to the CtermDys transgene. These transgenic constructs were then inserted into a transgenic vector with expression dictated by the cardiac specific α-myosin heavy chain

promoter [35]. These constructs were then injected into (C57BL/6 X SJL)F2 mouse eggs and potential founders were screened for the transgene by PCR.

Animals. Transgenic mice were backcrossed onto the C57BL/10SnJ genetic background for 2-3 generations (Jackson Labs, 000666). Care was taken to monitor the hypomorphic dysferlin allele inherited from SJL mice, which was bred out of mice used in this study. Mice of 2-3 months of age were analyzed, with the exception of mice used for histological analyses which were aged to 6 months. To generate transgenic (mdx) mice, male transgenic mice were bred with mdx females (Jackson Labs, #001801). Transgenic male pups from these crosses were then used for experiments.

Total protein extraction. Total cellular protein was extracted using a protocol modified from Bunnell and colleagues [36]. Briefly, hearts were frozen in liquid then pulverized and resuspended in 1% SDS, 5 mM EGTA, and protease inhibitors. Samples were boiled for 2 minutes then centrifuged at 14,000 g for 2 minutes and the supernatant was collected. Protein concentration was determined using a BCA protein assay kit (Thermo Scientific).

*Membrane protein isolation***.** Hearts were prepared as described previously [37]. Briefly, hearts were similarly frozen in liquid nitrogen, pulverized and resuspended in a buffer solution lacking detergent, and centrifuged at 14,000 g for 25 minutes. The supernatant was collected and centrifuged at 100,000 g

for 40 minutes. The pellet resulting from this spin was then resuspended in buffer containing 0.6 M KCl and washed for 1 hour at 4 degrees Celsius. Samples were then centrifuged at 150,000 g for 40 minutes and the resultant pellet was resuspended in a Tris-Sucrose buffer. Protein concentration was determined using a BCA protein assay kit (Thermo Scientific).

*Western blotting***.** 50 µg of protein was loaded per sample in 4-20% Tris-HCl gels for SDS-PAGE (Bio-Rad). Protein was then transferred to nitrocellulose or PVDF membranes. Membranes were blocked in 5% nonfat dry milk in TBS-T and primary antibodies were applied for 1 hour at room temperature: Primary antibodies: rabbit anti-dystrophin (C-terminal, Abcam, ab15277, 1:1000); mouse anti-dystrophin (mid-rod, millipore, mab1692, 1:200), mouse anti-α-dystroglycan (Millipore, 05-593, 1:1000), rabbit anti-desmin (Novus Biologicals, NB120-15200, 1:1000), mouse anti-myc (Cell Signaling Technology, 2276, 1:1000), mouse anti-flag (Sigma, F1804, 1:500), mouse anti-α-sarcoglycan (Vector Labs, VP-A105, 1:100), mouse anti-γ-sarcoglycan (Vector Labs, VP-G803, 1:100), mouse anti-β-dystroglycan (Vector Labs, VP-B205, 1:100),. Secondary antibodies were then applied for 1 hour at room temperature and blots were imaged using an Odyssey Infrared Scanner (LiCor)

Immunofluorescence. Hearts of transgenic mice were embedded in OCT and sectioned. Heart sections were fixed in 3% formaldehyde for 15 minutes at room temperature, then washed in PBS and blocked in 5% normal goat serum +

0.3% Triton X-100 in PBS for 1 hour at room temperature. Sections were then incubated with primary antibodies in 1% BSA + 0.3% Triton X-100 in PBS overnight at 4 degrees Celsius. Primary antibodies: Rabbit anti-Laminin (Sigma, L9393. 1:500), mouse anti-myc (Cell Signaling Technology, 2276, 1:500), mouse anti-dystrophin (Millipore, mab1692, 1:50). Sections were then washed and incubated with secondary antibodies in 1% BSA + 0.3% Triton X-100 in PBS for 1 hour at room temperature. Sections were washed in PBS and mounted using Vectashield mounting media with DAPI (Vector Laboratories). Slides were visualized using Zeiss LSM510 META confocal microscope (Carl Zeiss).

Evans blue dye uptake. Membrane permeability was assessed using a technique adapted from Bostick and colleagues [38]. Mice were given intraperitoneal injections of Evans Blue Dye in PBS at a dose of 200 µg/g body weight. 18 hours later, mice were given 3 injections of isoproterenol at a dose of 500 ng/g body weight at 18, 20, and 22 hours post-Evans blue dye injection. Mice were then euthanized at 24 hours post-Evans blue dye injection. Hearts were then cut into 3 sections across their short axis and frozen in OCT. Percent Evans blue positive area from thin sections of these samples was quantified using ImageJ (National Institutes of Health). For each heart, the Evans blue positive area reported is an average of 3 cross sections. Sections were imaged on a Zeiss Axio Observer Z1 inverted microscope. Mosaic images were created with AxioVision 4.7 (Carl Zeiss).

*Histological Analysis***.** Hearts of 6 month old mice were taken and embedded in OCT or fixed in 10% formalin overnight and embedded in paraffin. Hearts were then sectioned and stained with Sirius Red and Fast Green to detect collagen deposition within the myocardium. Sections were imaged on a Zeiss Axio Observer Z1 inverted microscope. Mosaic images were created with AxioVision 4.7 (Carl Zeiss).

*Isolated heart preparation***.** Mice were injected with 300 units sodium heparin and anesthetized with sodium pentobarbital. The heart and lungs were then removed following thoracotomy and placed immediately in ice-cold Krebs-Henseleit buffer (118 mM NaCl, 4.7 mM KCl, 1.2 mM $MgSO_4$, 1.2 mM KH_2PO_4, 10 mM glucose, 25 mM $NaHCO_3$, 2.5 mM $CaCl_2$, 0.5 mM EDTA). The lungs and thymus were trimmed away to expose the aorta, which was then cannulated. Hearts were then perfused at a constant pressure of 80 mmHg with Krebs-Henseleit buffer warmed to 37°C and brought to pH = 7.4 by bubbling with 95% 0_2, 5% CO_2. Hearts were paced at 7 Hz, and changes in left ventricular pressure were monitored by insertion of a water-filled balloon with an in-line pressure transducer into the left ventricle. Within the left ventricle, the balloon was inflated to an end diastolic pressure of 3-8 mmHg. Following 10–15 min of stabilization time, hearts were subjected to global no-flow ischemia for 20 min. Hearts were not paced during ischemia. Hearts were then reperfused for 60 min, and pacing was reinitiated at 8 min following the end of ischemia. Data were collected at a

sampling rate of 400 Hz and analyzed using Chart 6 software (ADInstruments) [39].

Statistics. Comparisons between 2 groups were made using students t-test. When more than 2 groups were being compared, one-way analysis of variance was used with a Tukey post-test. All statistical analysis was carried out using Prism (GraphPad Software).

Results

Characterizing transgene expression. Transgenic mice were created expressing either the N-terminal or C-terminal product of dystrophin cleavage by $2A^{pro}$ specifically in the heart.

The N-terminal transgene encoded protein (NtermDys) has a predicted molecular weight of 283 kDa and consists of an N-terminal flag epitope tag and the first 2426 amino acids of dystrophin. This includes the N-terminal domain of dystrophin and the N-terminal portion of the central rod domain (including spectrin-like repeats 1 through 19 and hinges 1, 2, and part of hinge 3, see Figure 4-1a). Thus, this fragment retains both the N-terminal and rod domain actin binding regions of dystrophin [40,41]. Previous reports have shown that inclusion of an N-terminal flag epitope tag does not impair dystrophin's actin binding function [42,43,44]. Western blot of total protein extracts from several lines of transgenic mice were performed to assess transgene expression. The NtermDys transgene was detected using an anti-flag antibody as well as an anti-

dystrophin antibody (recognizing amino acids 1181-1388 of dystrophin, present in both dystrophin and the NtermDys transgene). Four transgenic lines were chosen for further study (lines 368, 367, 10, 13) which exhibited a range of transgene expression (Figure 4-1b).

The C-terminal transgene (CtermDys) has a predicted molecular weight of 145 kDa and consists of an N-terminal myc tag and the last 1251 amino acids of dystrophin. This includes dystrophin's cysteine-rich domain, C-terminal domain, and C-terminal portion of the rod domain (containing part of hinge 3, hinge 4, and spectrin-like repeats 20-24, see Figure 4-1). Thus, this transgene retains dystrophin's dystroglycan binding and C-terminal scaffolding regions. For this transgene, only two lines of transgenic mice were obtained that bred successfully. Western blot of total protein extracts were carried out to assess transgene expression. The CtermDys protein was detected using an anti-myc antibody as well as an anti-dystrophin antibody (recognizing amino acids 3661-3677 of dystrophin, present in both dystrophin and the CtermDys transgene). No significant difference was detected in expression of the CtermDys transgene between transgenic lines 1 and 4 (Figure 4-1c). Line 4 was chosen for further study due to ease of breeding.

Expression of DGC proteins in transgenic mice. In total protein extracts, it was noted that expression of dystrophin was normal in NtermDys transgenic mice, but reduced in CtermDys transgenic mice (Figure 4-1c). To determine if expression of DGC proteins at the membrane is altered in transgenic mice,

Western blots for DGC proteins were performed on KCl-washed microsomes. Quantitatively, expression of dystrophin, α-dystroglycan, α-sarcoglycan, β-dystroglycan, and γ-sarcoglycan in NtermDys transgenic mice was similar to non-transgenic mice by Western blot (Figure 4-2a-e,).

Similar to findings in total protein extracts, dystrophin expression at the membrane was significantly reduced in CtermDys transgenic mice to approximately 30% of normal levels (Figure 4-2a). Expression of α-dystroglycan, α-sarcoglycan, β-dystroglycan, and γ-sarcoglycan was significantly increased (~5-10 fold) in CtermDys transgenic mice by Western blot (Figure 4-2b-e).

Subcellular localization of the NtermDys transgene. The subcellular localization of the NtermDys transgene was assessed by immunofluorescence on heart sections of NtermDys transgenic mice. NtermDys transgenic mice (line 368) were crossed onto the dystrophin-deficient mdx genetic background. An anti-dystrophin (mid-rod) antibody was used to show subcellular localization of the NtermDys transgene while also using an anti-laminin antibody to simultaneously show the sarcolemma. The NtermDys transgene localized to the sarcolemma, similar to dystrophin, but was also found more diffusely throughout cardiac myocytes in a striated pattern (Figure 4-3b, d, f). Surprisingly, the NtermDys transgene also appeared to be present in the nucleus of cardiac myocytes as illustrated by colocalization with DAPI (Figure 4-4). The NtermDys transgene appears only in the nuclei of cardiac myocytes, and not in the nuclei of other cells within the heart (Figure 4-4h). Immunoflourescence was also used to

show normal expression of the DGC protein β-dystroglycan was normal in NtermDys(mdx) hearts (Figure 4-3g, h).

Subcellular localization of the CtermDys transgene. Subcellular localization of the CtermDys transgene was determined by immunofluorescence on heart sections from CtermDys transgenic mice. Localization of the CtermDys transgene was determined using an anti-myc antibody while using an anti-laminin antibody to visualize the sarcolemma. The CtermDys transgene localized at or near the sarcolemma, similar to dystrophin (Figure 4-5b, d, f). In agreement with our quantitative assessment of DGC protein expression, CtermDys mice also showed increased expression of β-dystroglycan at the membrane (Figure 4-5g, h).

Sarcolemmal stability in transgenic mice. Previous reports have shown that transgenic expression of non-muscle isoforms of dystrophin that bind dystroglycan but not actin cause dystrophic myopathy in skeletal muscle by acting as a dominant negative to dystrophin [29,33,34]. The non-muscle isoforms that show a dominant negative effect are structurally similar to the CtermDys protein. Thus, to determine if expression of the NtermDys or CtermDys transgenes causes dystrophic cardiomyopathy as shown by mechanical instability of the sarcolemma, Evans blue dye (EBD) uptake was measured with isoproterenol stress (see Materials and Methods). Non-transgenic mice show EBD uptake in only a few scattered cardiac myocytes

during this stress (Figure 4-6b). The four NtermDys transgenic lines showed similar EBD uptake to non-transgenic mice during isoproterenol stress (Figure 4-6). In contrast, CtermDys transgenic mice showed significantly enhanced EBD uptake compared to non-transgenic mice which appeared as focal areas of membrane instability (Figure 4-6a, g). EBD uptake in CtermDys mice was similar to the dystrophin-deficient mdx mouse, which showed significantly enhanced EBD uptake compared to non-transgenic mice (Figure 4-6a, i).

Since cleavage of dystrophin by $2A^{pro}$ results in both N- and C-terminal cleavage products, CtermDys (line 4) mice were crossed to NtermDys (line 368) mice to create double transgenic (DTg) mice. DTg mice show EBD uptake during isoproterenol stress that is significantly greater than non-transgenic mice but similar to mdx and CtermDys transgenic mice (Figure 4-6a, h). Collectively, these results show that expression of CtermDys, but not NtermDys, is sufficient to cause sarcolemmal instability and dystrophic cardiomyopathy.

Previous reports have shown that, in addition to causing dystrophic myopathy in normal skeletal muscle, some non-muscle isoforms of dystrophin which lack all actin binding functionality also exacerbate the already dystrophic phenotype of the mdx mouse and is thought to contribute to their mild phenotype compared to DMD patients [32,33,34]. This occurs through competition with utrophin, which is upregulated in mdx mice [32,45]. To determine if the CtermDys transgene can similarly compete with utrophin for binding to β-dystroglycan in mdx mice, the CtermDys transgene was bred onto the mdx genetic background and membrane stability was assessed by EBD uptake during

isoproterenol stress. CtermDys(mdx) mice showed no signficant difference in EBD uptake in CtermDys (mdx) mice compared with mdx mice (Figure 4-6a, k)[1]. The NtermDys (line 368) transgene was also crossed onto the mdx genetic background and sarcolemmal stability was similarly tested. EBD uptake in NtermDys(mdx) was elevated compared to non-transgenic mice, but similar to mdx mice (Figure 4-6a, j). Collectively, these results show that the NtermDys transgene does not further impair sarcolemma stability in mdx mice. Additionally, these results show a non-significant trend towards sarcolemmal instability in CtermDys(mdx) mice compared to mdx mice which warrants further study.

Histological evidence of cardiomyopathy in transgenic mice. Mdx mice show progressive histopathology within the myocardium as seen by inflammation and fibrosis [18]. To determine if similar processes occur in our transgenic mice, heart sections from NtermDys, CtermDys, non-transgenic littermates, and mdx mice were stained with Sirius Red to visualize collagen deposition in the myocardium. At 6 months of age, non-transgenic and NtermDys mice show very little evidence of fibrosis in the myocardium (Figure 4-7a-d). Conversely, aged mdx and CtermDys mice show large focal regions of fibrosis within the myocardium which may result from remodeling due to focal cardiac myocyte damage observed by EBD uptake (Figure 4-7e-h). These results suggest that CtermDys transgenic mice show histological pathology comparable to that observed in dystrophic cardiomyopathy.

[1] This is a nascent data set with n = 4 for Cterm(mdx) mice. Currently, we observe a non-significant trend towards greater EBD uptake in Cterm(mdx) mice. Further studies are in progress to determine if this is a physiologically significant difference.

Enhanced susceptibility to ischemic injury in CtermDys transgenic mice. A previous study has shown that EV infection predisposes human patients to death following acute myocardial infarction [1]. The mechanism by which EV infection increases susceptibility to ischemic injury is not fully understood but given that CtermDys mice show dystrophic cardiomyopathy, we hypothesized that presence of the CtermDys transgene would increase susceptibility to ischemic injury. To test this hypothesis, hearts of CtermDys and non-transgenic littermate controls were isolated, perfused, and subjected to 20 minutes of ischemia and 60 minutes of reperfusion. Prior to ischemia, non-transgenic and CtermDys transgenic hearts showed similar systolic function as measured by left ventricular developed pressure (LVDP, Figure 4-8a). However, recovery of systolic function during reperfusion was significantly impaired in CtermDys hearts (Figure 4-8a, e). Additionally, recovery of diastolic function during reperfusion was also significantly impaired in CtermDys hearts as shown by elevated left ventricular end diastolic pressures (LVEDP, Figure 4-8b, e). These results show that expression of the CtermDys transgene enhances susceptibility of the heart to ischemic injury.

As mentioned above, previous studies have shown that non-muscle dystrophin isoforms that can bind dystroglycan but not actin exacerbate the dystrophic phenotype of mdx mice through competition with utrophin for binding of β-dystroglycan. To determine if expression of the CtermDys transgene enhances susceptibility to ischemic injury in mdx mice, isolated hearts of

CtermDys(mdx) and non-transgenic mdx littermate controls we subjected to ischemia and reperfusion injury. Mdx hearts were more susceptible to ischemic injury than wild-type heart as shown by impaired recovery of LVDP and LVEDP during reperfusion (Figure 4-8c, d, e). CtermDys(mdx) hearts showed recovery of LVDP and LVEDP during reperfusion which was impaired when compared with non-transgenic mice, but was similar to mdx mice (Figure 4-8c, d, e)[2]. However, because the ischemia/reperfusion protocol used here causes severe injury in mdx mice with very little recovery of function during reperfusion, future studies with a more mild ischemic injury may be useful in detecting a physiologically significant difference in recovery from ischemia between mdx and CtermDys(mdx) mice. Collectively, these findings suggest that expression of the CtermDys transgene does not dramatically alter susceptibility of mdx mice to ischemic injury. However, future studies with a less severe ischemia protocol are required to determine if the CtermDys transgene alters recovery of cardiac function following ischemia in a physiologically meaningful way.

Discussion

Previous reports have shown that the C-terminal fragment of dystrophin cleavage $2A^{pro}$ is structurally similar to those previously described as exerting a dominant negative effect on DGC function [23,24]. Based on these findings, we hypothesized that expression of the C-terminal product of $2A^{pro}$-mediated dystrophin cleavage would cause dystrophic cardiomyopathy through competition

[2] Here again, sample size is small for CtermDys(mdx) mice, with n = 3. Ongoing studies are aimed at increasing the size of this group to augment our ability to detect physiologically relevant differences in cardiac function.

with dystrophin. This study has directly tested this hypothesis by expressing both the N- and C-terminal products of dystrophin cleavage by $2A^{pro}$. We found that the C-terminal product of dystrophin cleavage by $2A^{pro}$ localizes to the sarcolemma and causes dystrophic cardiomyopathy as shown by sarcolemmal instability, cardiac fibrosis, and increased susceptibility to ischemic injury. Conversely, the N-terminal product of dystrophin cleavage by $2A^{pro}$ did not affect sarcolemmal stability or cause cardiomyopathy. Collectively, these results show that the C-terminal product of dystrophin cleavage by $2A^{pro}$ is sufficient to cause dystrophic cardiomyopathy. We hypothesize that this cardiomyopathy is due to CtermDys acting as a dominant negative competitor of dystrophin and suggest that the presence of this protein may contribute significantly to the cardiomyopathy caused by EV infection.

Using immunofluorescence, we found that the CtermDys protein localized to the sarcolemma. We also observed a ~5-10 fold increase in expression of other DGC proteins at the membranes of CtermDys mice. This suggests that the sarcolemma has a reserve capacity to accommodate DGC protein complexes which is limited by the availability of dystrophin (or other β-dystroglycan binding proteins, such as CtermDys). This assertion is also supported by previous findings which show that transgenic overexpression of sarcoglycans does not result in increased expression of other DGC proteins [46,47]. Additionally, expression the CtermDys protein caused a ~70% reduction in dystrophin. To explain these data, we hypothesize that the CtermDys protein nucleates a novel CtermDys-DGC complex which exhausts the sarcolemma's ability to

accommodate DGC proteins, then competes with the native DGC for residency at the sarcolemma. However, at the current time we cannot exclude the possibility of CtermDys competing directly with dystrophin for incorporation into already formed DGC. Additionally, we propose that this cardiomyopathy is not caused directly by expression of the CtermDys transgene, but is instead due to replacement of the DGC with a CtermDys-DGC, which is hypofunctional due to its inability to tether actin and β-dystroglycan. Interestingly, 5-10 fold increase of expression of DGC proteins in the hearts of CtermDys transgenic mice was insufficient to prevent dystrophic cardiomyopathy, strongly emphasizing the importance of dystrophin's role as mechanical tether.

Expression of the CtermDys transgene also increased susceptibility of the heart to ischemic injury as shown by reduced recovery of systolic and diastolic function during reperfusion. This finding has clinical significance in light of previous findings by Andreoletti and colleagues [1] that showed EV infection increases susceptibility of the heart to ischemic injury. Collectively, these results show that expression of the C-terminal product of dystrophin cleavage by $2A^{pro}$ is sufficient to cause dystrophic cardiomyopathy and increase susceptibility to ischemic injury. Because the products of dystrophin cleavage by $2A^{pro}$ have been observed following EV infection along with reductions in dystrophin, these findings suggest the presence of CtermDys and loss of dystrophin may contribute significantly to the pathogenesis of EV infection.

Because $2A^{pro}$ cleavage of dystrophin results in production of both N- and C-terminal dystrophin fragments, we also determined the effects of NtermDys

expression on the heart. Compared to dystrophin at the CtermDys protein, NtermDys localized diffusely throughout the myocardium, but was enriched at the sarcolemma and nucleus. This is in agreement with previous findings showing similar sarcolemmal localization of modified dystrophin proteins lacking only the dystroglycan-binding domain [48]. The mechanism by which the NtermDys protein traffics to the sarcolemma is not clear but may involve binding to cytoskeletal actin or direct interactions with membrane phospholipids [49]. The NtermDys protein also localized strongly in the nucleus of cardiac myocytes through mechanisms which are not clear and warrant further study. However, we speculate that the actin binding activity of NtermDys dictates its localization in cardiac myocytes. This explains the presence of the NtermDys protein near the sarcolemma and its striated pattern of expression. Additionally, actin is also present in the nucleus [50] which may explain the nuclear localization of NtermDys. To my knowledge, no previous study has shown nuclear localization of dystrophin or any engineered dystrophin protein. A previous report has shown that a disease-causing mutation in δ-sarcoglycan causes its retention in the nucleus, but it unclear at this time if the mechanism of nuclear localization is similar to that which occurs in NtermDys mice [46]. NtermDys mice show normal expression and localization of DGC proteins and no evidence of sarcolemmal instability (Figures 4-2,4-3, 4-6).

In order to simulate the effects of dystrophin cleavage by $2A^{pro}$ in the myocardium most accurately, we created double transgenic mice expressing both NtermDys and CtermDys in the heart. These mice show dystrophic

cardiomyopathy, as shown by enhanced sarcolemmal instability which was similar to CtermDys and mdx mice. These findings, along with those in single transgenic mice show that expression of CtermDys causes dystrophic cardiomyopathy and that expression of NtermDys has no detrimental effects on the heart. Additionally, because double transgenic mice essentially replace intact dystrophin with 2 proteins expressing all of its functional domains, but collectively lack the ability to tether actin to β-dystroglycan, this again suggests that dystrophin's primary function in the cardiac myocyte is to act as a mechanical tether. This is in agreement with a previous report showing that expression of all dystrophin functional domains *in trans* does not correct dystrophy in mdx skeletal muscle [51].

When relating the phenotype of these transgenic mice to the pathogenesis of EV infection, it is important to consider differences in the mechanism by which dystrophin expression is reduced. During EV infection, $2A^{pro}$ causes cleavage and loss of dystrophin concomitant with production of both the N- and C-terminal cleavage products. Alternatively, expression of the CtermDys transgene causes a ~70% reduction in dystrophin content at the sarcolemma likely through competition for binding with β-dystroglycan. We speculate that the CtermDys transgene is overexpressed relative to endogenous dystrophin at a molar level due to the significant increase in DGC proteins in the hearts of CtermDys mice. However, in each case, expression of dystrophin at the sarcolemma is reduced and replaced with expression of the products of dystrophin cleavage by $2A^{pro}$.

Thus, we propose that transgenic expression of NtermDys and CtermDys models the effects of $2A^{pro}$-mediated cleavage of ~70% of dystrophin on the heart.

In addition to studying the effects of dystrophin cleavage by $2A^{pro}$ on a wild-type background, we also crossed the CtermDys transgene onto the dystrophin-deficient mdx background. Previous reports have shown that expression of short, dystroglycan-binding isoforms of dystrophin exacerbate the dystrophic phenotype of mdx skeletal muscle [32,34]. The data set for this comparison is still rather nascent, but we observed a non-significant trend toward enhanced membrane instability in CtermDys(mdx) mice compared to mdx mice. However, expression of the CtermDys transgene did not enhance susceptibility to ischemic injury in mdx mice. Further study and enhancement of group sizes are ongoing to determine if there is a statistically significant and physiologically relevant effect of the CtermDys protein on the hearts of mdx mice.

In this study, we have shown that expression of the β-dystroglycan-binding CtermDys protein is sufficient to cause dystrophic cardiomyopathy. The significance of these findings lie in the identification of $2A^{pro}$-mediated dystrophin cleavage as a novel target for therapeutic intervention in EV infection, a clinically relevant disease process.

Figures

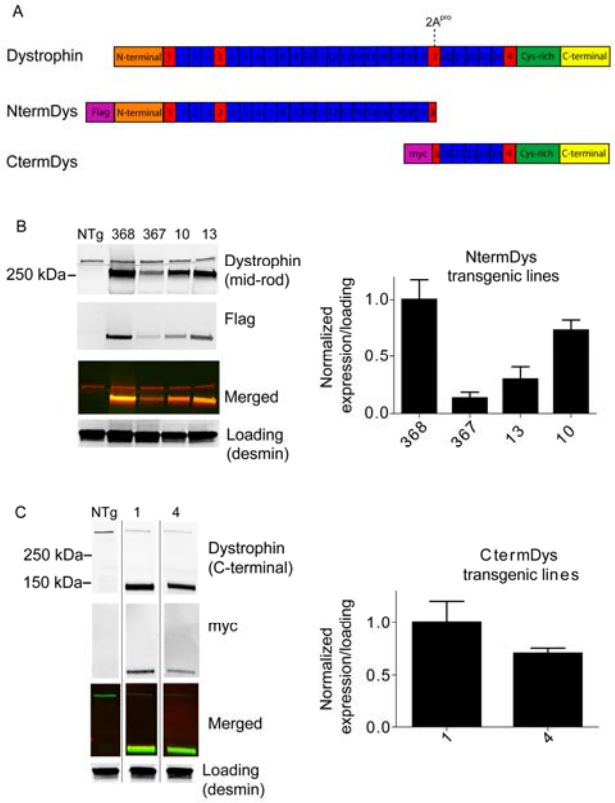

Figure 4-1. Creation of transgenic mice and transgene expression. A) Top, Schematic of dystrophin structure. Hinge domains are indicated by red boxes. Spectrin-like repeats are indicated by blue boxes, with light blue boxes constituting the rod domain actin binding region of dystrophin. Dotted line within Hinge 3 indicates $2A^{pro}$ cleavage site. Lower, Schematic of the NtermDys and CtermDys transgenes with N-terminal epitope tags. NtermDys contains an N-terminal flag epitope tag, the N-terminal domain of dystrophin, and the N-terminal portion of the central rod domain (including spectrin-like repeats 1 through 19 and hinges 1, 2, and part of hinge 3). CtermDys contains an N-terminal myc epitope tag, dystrophin's cysteine-rich domain, C-terminal domain, and C-terminal portion of the rod domain (containing part of hinge 3, hinge 4, and spectrin-like repeats 20-24). B) Left, Western blot for NtermDys protein in representative samples of total protein from non-transgenic (NTg) littermates and NtermDys transgenic lines. Predicted MW of NtermDys – 283 kDa. NtermDys protein was detected with an anti-flag antibody and an anti-dystrophin antibody (mid rod) which also detected dystrophin. Right, Quantification of transgene expression in NtermDys transgenic lines, shown as expression relative to loading normalized to line 368. C) Left, Western blot for CtermDys protein in representative samples of total protein from NTg and CtermDys transgenic lines. CtermDys protein was detected with an anti-flag antibody and an anti-dystrophin antibody (C-terminal) which also detected dystrophin. Intervening lanes of same blot removed for clarity. Right, Quantification of transgene expression in CtermDys transgenic lines, shown as expression relative to loading normalized to line 1. Data expressed as mean ± SEM. N = 4-6 per group.

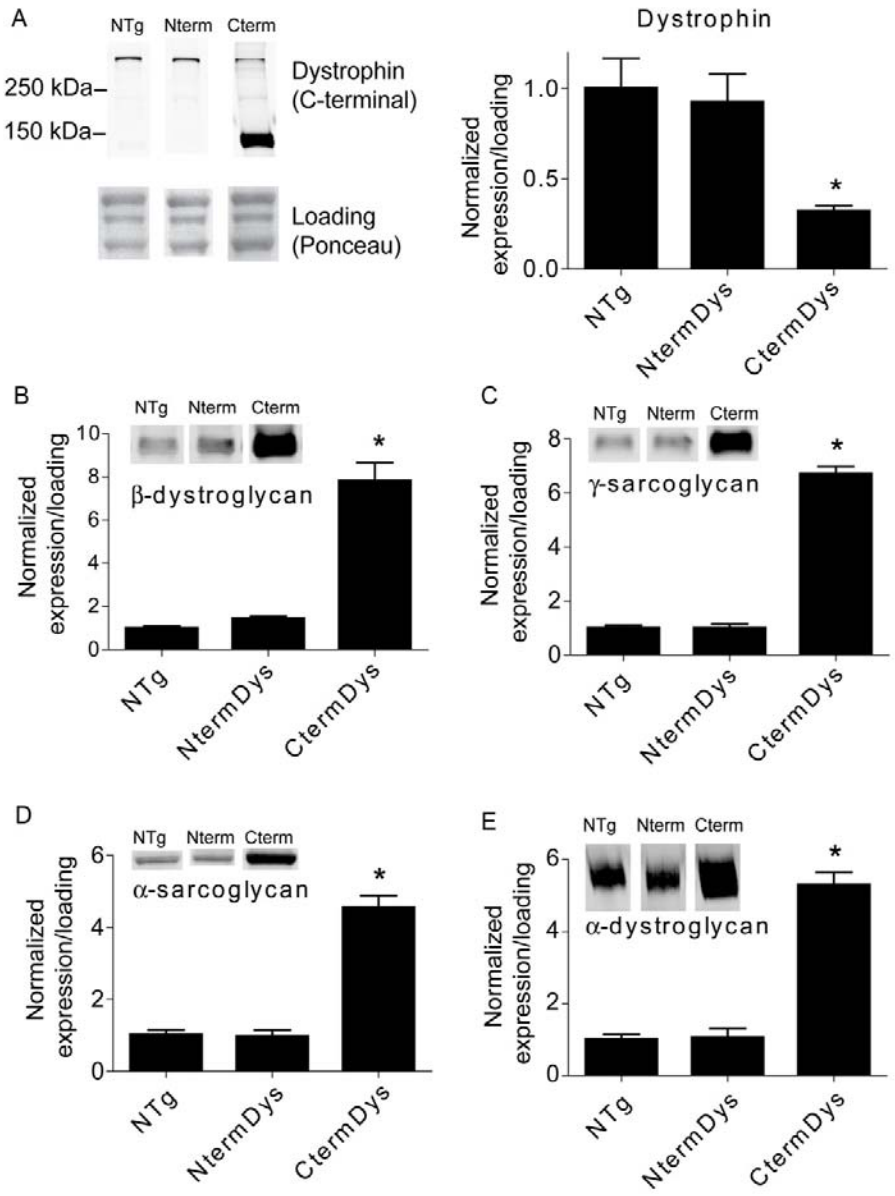

Figure 4-2. DGC protein expression at the membrane in hearts of transgenic mice. A) Left, representative Western blot for dystrophin expression in non-transgenic (NTg), CtermDys, and NtermDys mice. Right, quantification of dystrophin expression shown as expression relative to loading normalized to NTg. B) Representative western blot and quantification of β-dystroglycan expression in transgenic mice. C) Representative western blot and quantification of γ-sarcoglycan expression in transgenic mice. D) Representative western blot and quantification of α-sarcoglycan expression in transgenic mice. E) Representative western blot and quantification of α-dystroglycan expression in transgenic mice. . Intervening lanes of same blot removed for clarity. Data expressed as mean ± SEM. N = 4-7 per group. Quantification of protein expression shown as expression relative to loading normalized to NTg. * - $P < 0.05$ vs. NTg.

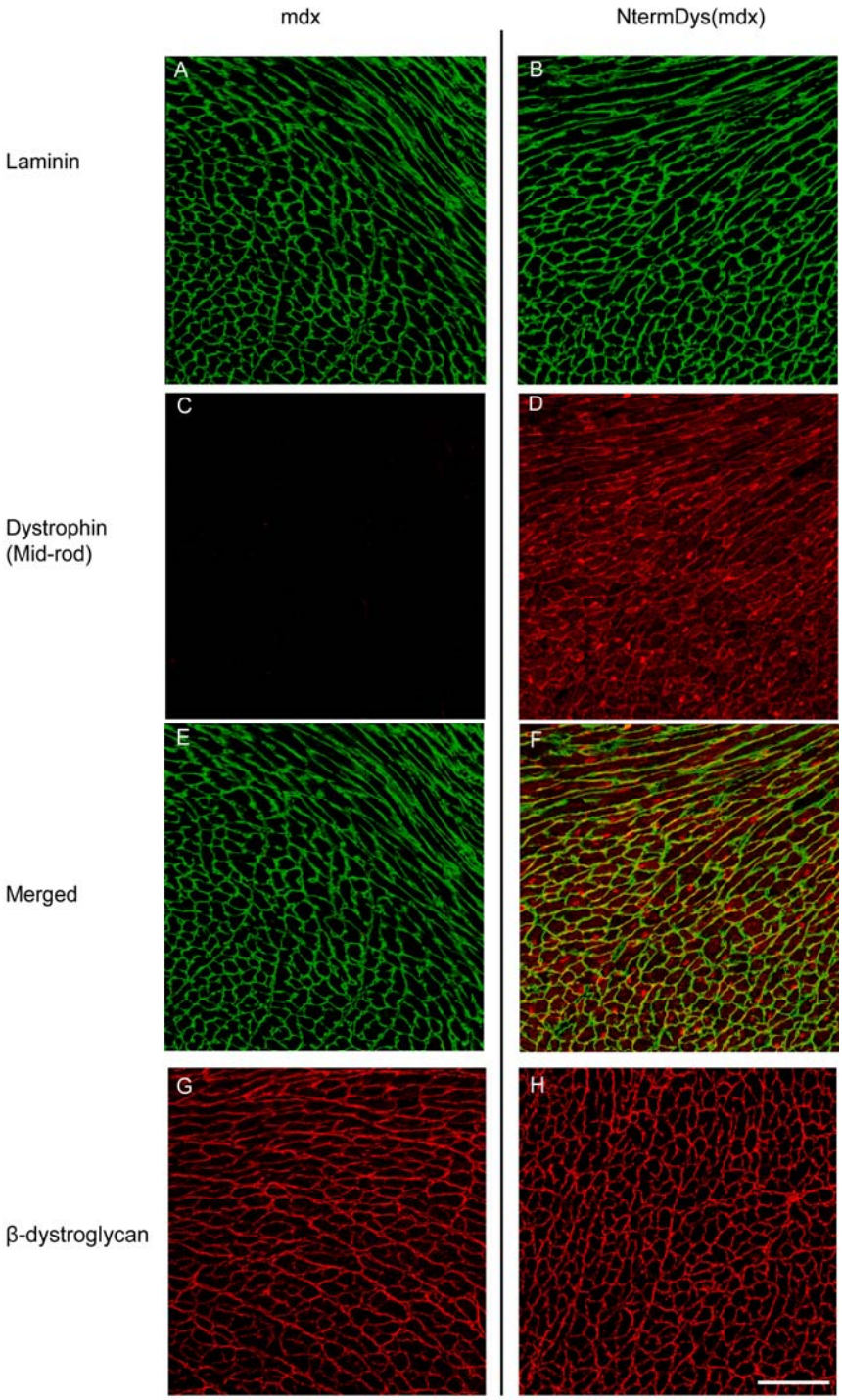

Figure 4-3. Subcellular localization the NtermDys protein and β-dystroglycan in the heart. Immunofluorescent detection of laminin (A, B) and the NtermDys protein (C, D) in non-transgenic (NTg) mdx and NtermDys(mdx) hearts. E, F - Merged images. Scale bar – 100 μm.

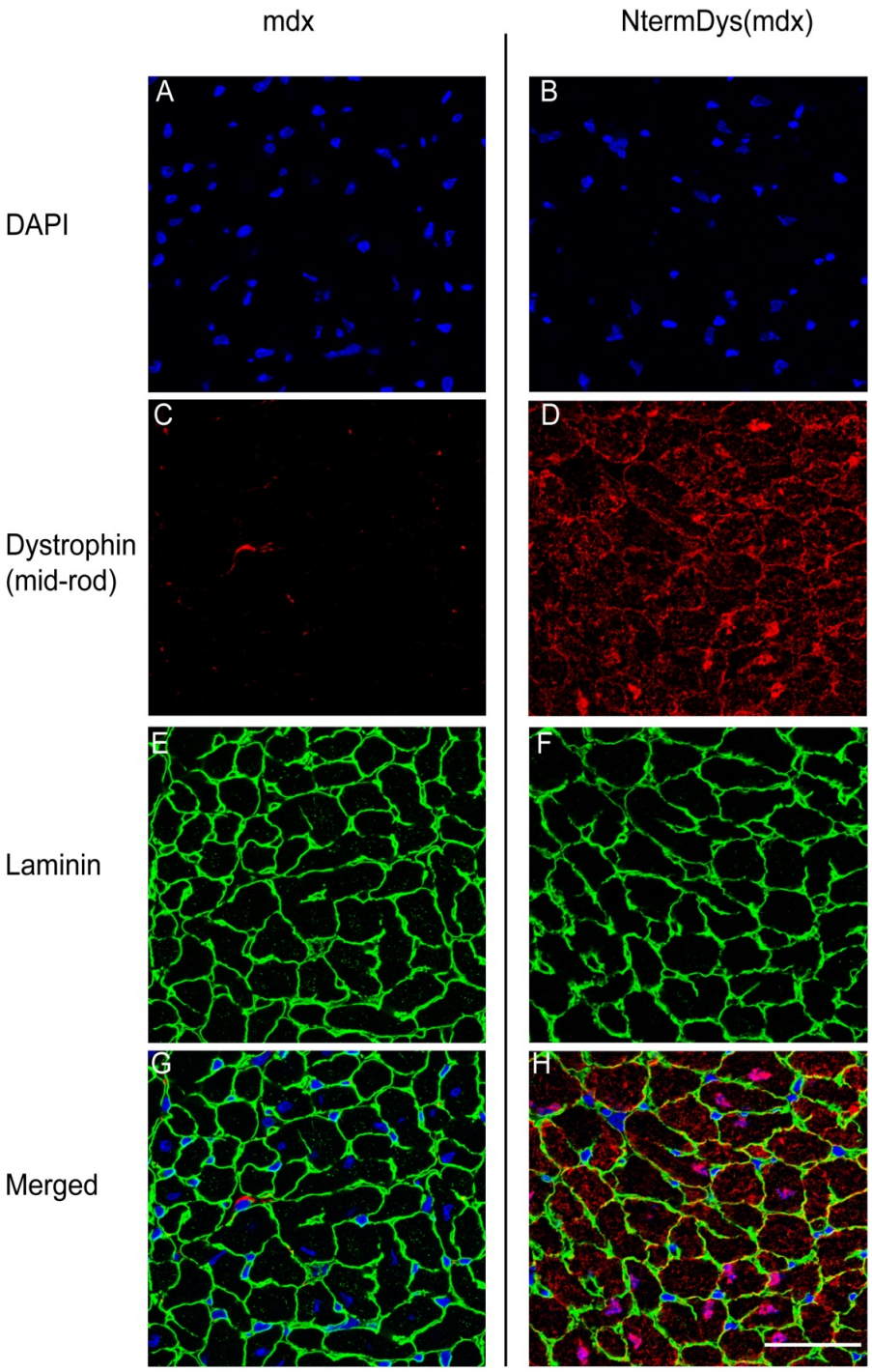

Figure 4-4. Nuclear localization of the NtermDys protein in the heart. Nuclei shown with DAPI (A, B). Immunofluorescent detection of the NtermDys protein (C, D) and laminin (E, F) in non-transgenic (NTg) mdx and NtermDys(mdx) hearts. G, H - Merged images. Subcellular localization of β-dystroglycan in mdx (G) and NtermDys(mdx) (H) hearts. Scale bar - 50 μm.

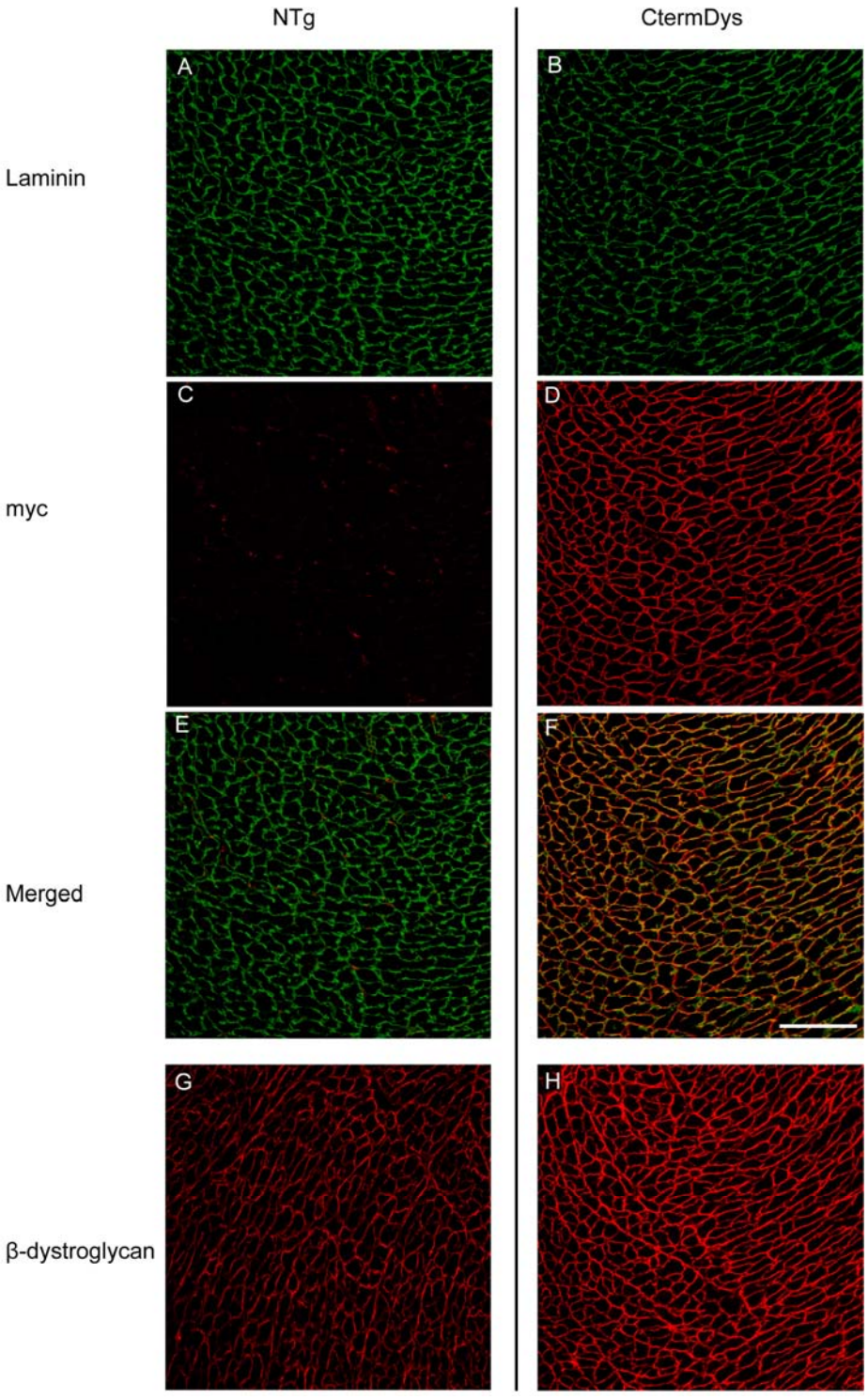

Figure 4-5. Subcellular localization the CtermDys protein and β-dystroglycan in the heart. Immunofluorescent detection of laminin (A, B) and the CtermDys protein (C, D) in non-transgenic (NTg) and CtermDys hearts. E, F - Merged images. Subcellular localization of β-dystroglycan in NTg (G) and CtermDys (H) hearts. Scale bar - 100 μm.

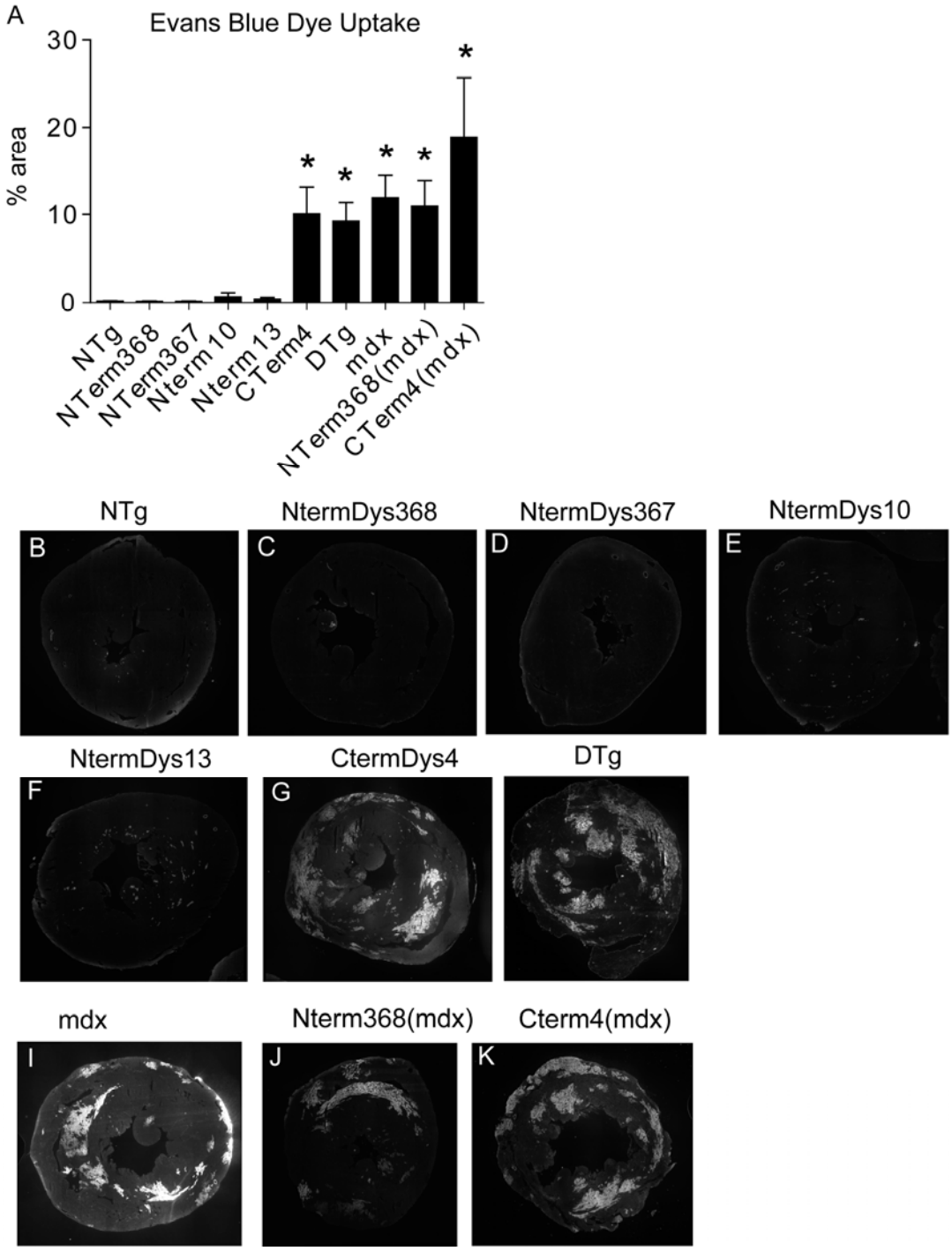

Figure 4-6. Membrane stability in hearts of transgenic mice. A) Quantification of % EBD positive area in transgenic mice and non-transgenic (NTg) littermates. Data expressed as mean ± SEM. N = 4-17 per group. * - P < 0.05 vs. NTg. B) Representative mosaic images EBD uptake in hearts of NTg (B), NtermDys368(C), NtermDys367(D), NtermDys10(E), NtermDys13(F), CtermDys4(G), double transgenic (DTg, H), non-transgenic mdx (mdx, I), NtermDys368(mdx) (J), Cterm4(mdx) (K).

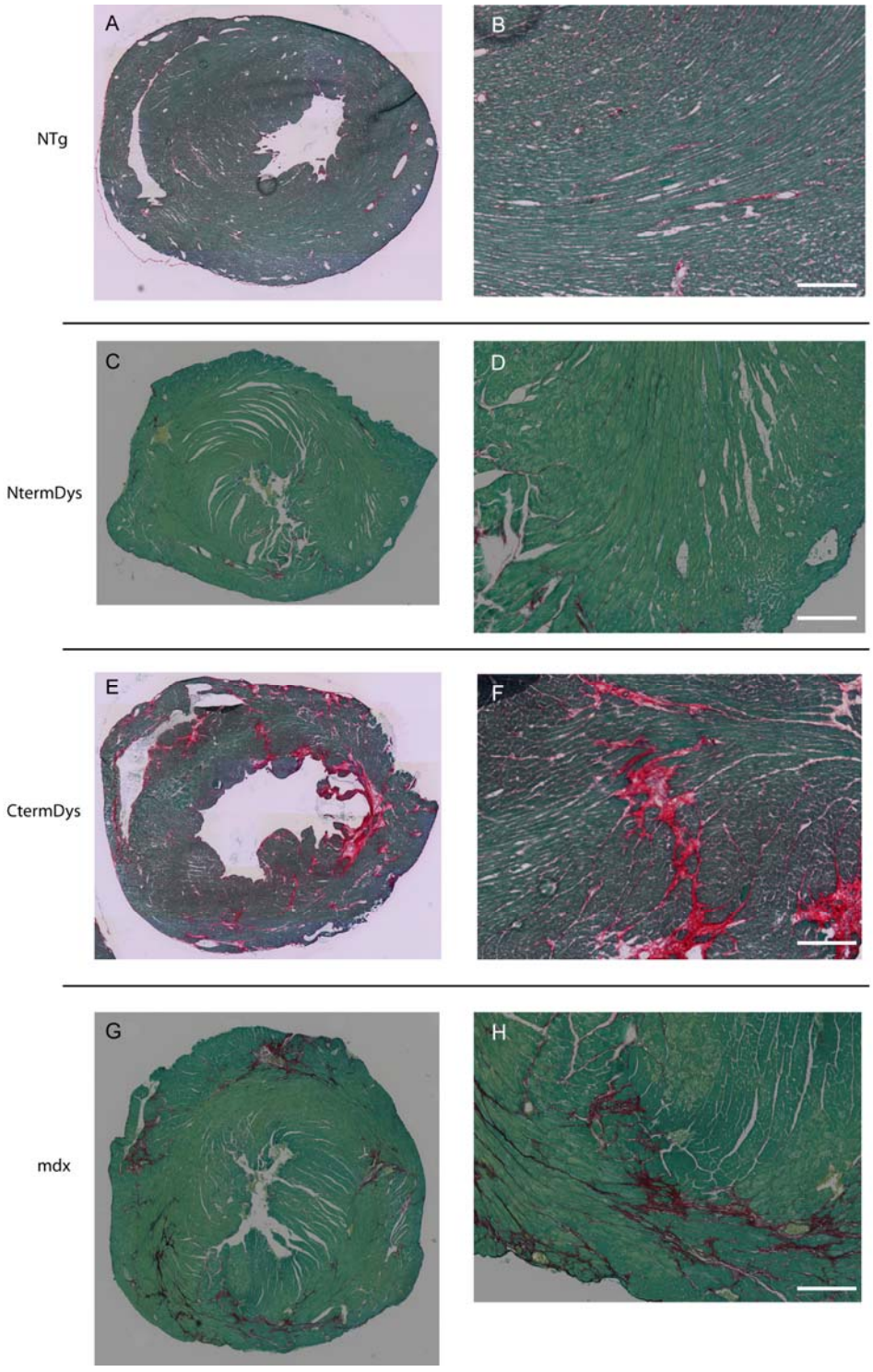

Figure 4-7. Fibrosis in hearts of transgenic mice. Sirius Red-Fast Green staining of non-transgenic (NTg), NtermDys, CtermDys hearts, and mdx hearts. Mosaic images of NTg (A), NtermDys (C), CtermDys (E), and mdx (G) hearts. Higher magnification images of NTg (B), NtermDys (D), CtermDys (D), and mdx (F) hearts. Scale bar = 200 μM.

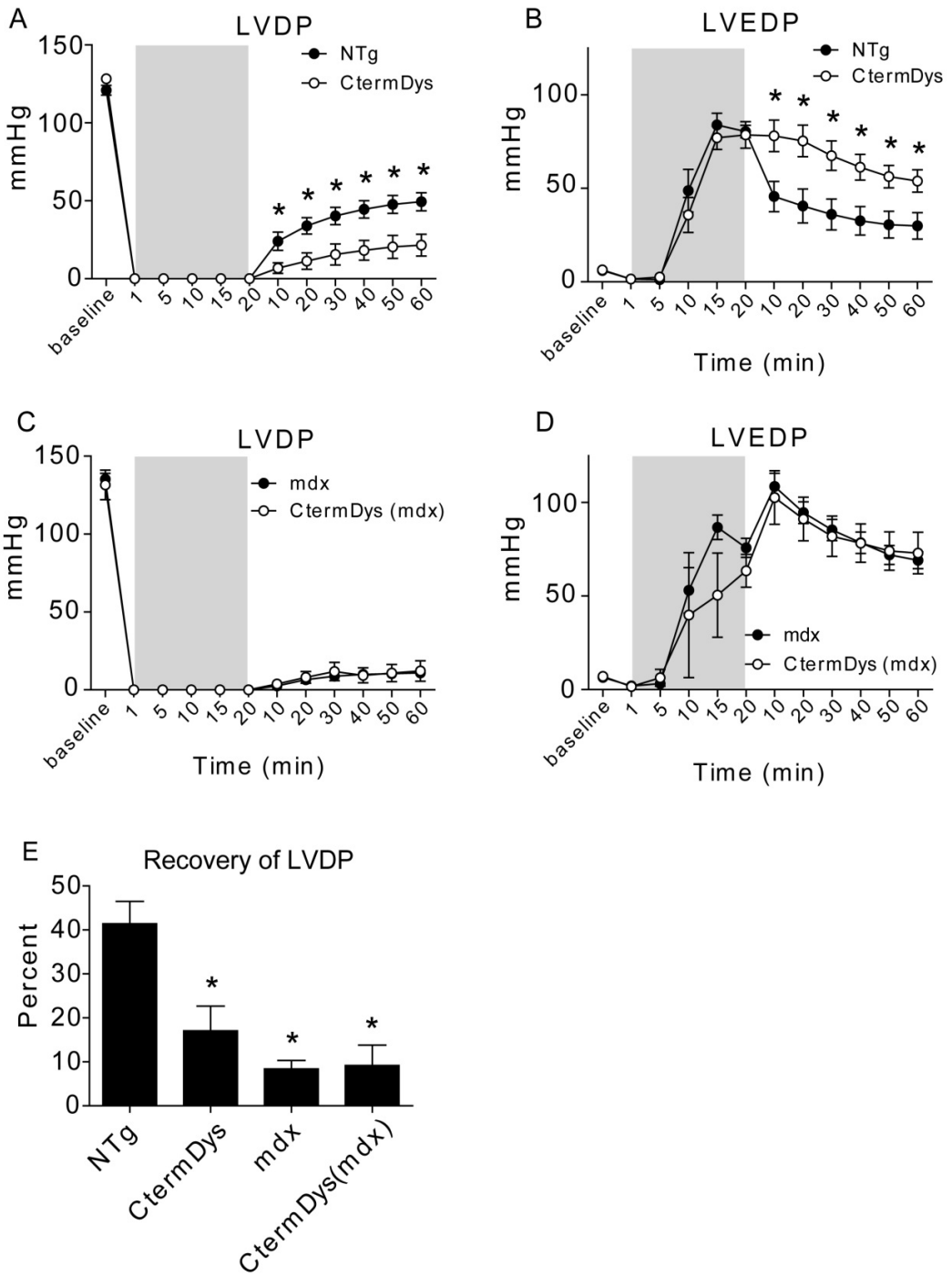

Figure 4-8. Susceptibility to ischemic injury in isolated hearts of transgenic mice. Systolic (A) and diastolic (B) function of non-transgenic (NTg) and CtermDys hearts during ischemia/reperfusion. Systolic (C) and diastolic (D) function of NTg(mdx) and CtermDys(mdx) hearts during ischemia/reperfusion. E) Recovery of systolic function in hearts of transgenic mice and non-transgenic littermates. Data expressed as mean ± SEM. N = 3-12 per group. * - $P < 0.05$ vs. NTg.

Literature cited

1. Andreoletti L, Venteo L, Douche-Aourik F, Canas F, Lorin de la Grandmaison G, et al. (2007) Active Coxsackieviral B infection is associated with disruption of dystrophin in endomyocardial tissue of patients who died suddenly of acute myocardial infarction. J Am Coll Cardiol 50: 2207-2214.

2. Stevens PJ, Ground KE (1970) Occurrence and significance of myocarditis in trauma. Aerosp Med 41: 776-780.

3. Woodruff JF (1980) Viral myocarditis. A review. Am J Pathol 101: 425-484.

4. Feldman AM, McNamara D (2000) Myocarditis. N Engl J Med 343: 1388-1398.

5. Archard LC, Khan MA, Soteriou BA, Zhang H, Why HJ, et al. (1998) Characterization of Coxsackie B virus RNA in myocardium from patients with dilated cardiomyopathy by nucleotide sequencing of reverse transcription-nested polymerase chain reaction products. Hum Pathol 29: 578-584.

6. Bowles NE, Richardson PJ, Olsen EG, Archard LC (1986) Detection of Coxsackie-B-virus-specific RNA sequences in myocardial biopsy samples from patients with myocarditis and dilated cardiomyopathy. Lancet 1: 1120-1123.

7. Fujioka S, Koide H, Kitaura Y, Deguchi H, Kawamura K, et al. (1996) Molecular detection and differentiation of enteroviruses in endomyocardial biopsies and pericardial effusions from dilated cardiomyopathy and myocarditis. Am Heart J 131: 760-765.

8. Jin O, Sole MJ, Butany JW, Chia WK, McLaughlin PR, et al. (1990) Detection of enterovirus RNA in myocardial biopsies from patients with myocarditis and cardiomyopathy using gene amplification by polymerase chain reaction. Circulation 82: 8-16.

9. Schwaiger A, Umlauft F, Weyrer K, Larcher C, Lyons J, et al. (1993) Detection of enteroviral ribonucleic acid in myocardial biopsies from patients with idiopathic dilated cardiomyopathy by polymerase chain reaction. Am Heart J 126: 406-410.

10. Ervasti JM, Ohlendieck K, Kahl SD, Gaver MG, Campbell KP (1990) Deficiency of a glycoprotein component of the dystrophin complex in dystrophic muscle. Nature 345: 315-319.

11. Yoshida M, Ozawa E (1990) Glycoprotein complex anchoring dystrophin to sarcolemma. J Biochem 108: 748-752.

12. Ervasti JM, Campbell KP (1993) A role for the dystrophin-glycoprotein complex as a transmembrane linker between laminin and actin. J Cell Biol 122: 809-823.

13. Rybakova IN, Patel JR, Ervasti JM (2000) The dystrophin complex forms a mechanically strong link between the sarcolemma and costameric actin. J Cell Biol 150: 1209-1214.

14. Way M, Pope B, Cross RA, Kendrick-Jones J, Weeds AG (1992) Expression of the N-terminal domain of dystrophin in E. coli and demonstration of binding to F-actin. FEBS Lett 301: 243-245.

15. Suzuki A, Yoshida M, Hayashi K, Mizuno Y, Hagiwara Y, et al. (1994) Molecular organization at the glycoprotein-complex-binding site of dystrophin. Three dystrophin-associated proteins bind directly to the carboxy-terminal portion of dystrophin. Eur J Biochem 220: 283-292.

16. Rosa G, Ceccarini M, Cavaldesi M, Zini M, Petrucci TC (1996) Localization of the dystrophin binding site at the carboxyl terminus of beta-dystroglycan. Biochem Biophys Res Commun 223: 272-277.

17. Stedman HH, Sweeney HL, Shrager JB, Maguire HC, Panettieri RA, et al. (1991) The mdx mouse diaphragm reproduces the degenerative changes of Duchenne muscular dystrophy. Nature 352: 536-539.

18. Van Erp C, Loch D, Laws N, Trebbin A, Hoey AJ Timeline of cardiac dystrophy in 3-18-month-old MDX mice. Muscle Nerve 42: 504-513.

19. Yasuda S, Townsend D, Michele DE, Favre EG, Day SM, et al. (2005) Dystrophic heart failure blocked by membrane sealant poloxamer. Nature 436: 1025-1029.

20. Weller B, Karpati G, Carpenter S (1990) Dystrophin-deficient mdx muscle fibers are preferentially vulnerable to necrosis induced by experimental lengthening contractions. J Neurol Sci 100: 9-13.

21. Vilquin JT, Brussee V, Asselin I, Kinoshita I, Gingras M, et al. (1998) Evidence of mdx mouse skeletal muscle fragility in vivo by eccentric running exercise. Muscle Nerve 21: 567-576.

22. Somer H, Donner M, Murros J, Konttinen A (1973) A serum isozyme study in muscular dystrophy. Particular reference to creatine kinase, aspartate aminotransferase, and lactic acid dehydrogenase isozymes. Arch Neurol 29: 343-345.

23. Badorff C, Lee GH, Lamphear BJ, Martone ME, Campbell KP, et al. (1999) Enteroviral protease 2A cleaves dystrophin: evidence of cytoskeletal disruption in an acquired cardiomyopathy. Nat Med 5: 320-326.

24. Badorff C, Berkely N, Mehrotra S, Talhouk JW, Rhoads RE, et al. (2000) Enteroviral protease 2A directly cleaves dystrophin and is inhibited by a dystrophin-based substrate analogue. J Biol Chem 275: 11191-11197.

25. Xiong D, Yajima T, Lim BK, Stenbit A, Dublin A, et al. (2007) Inducible cardiac-restricted expression of enteroviral protease 2A is sufficient to induce dilated cardiomyopathy. Circulation 115: 94-102.

26. Joachims M, Van Breugel PC, Lloyd RE (1999) Cleavage of poly(A)-binding protein by enterovirus proteases concurrent with inhibition of translation in vitro. J Virol 73: 718-727.

27. Lamphear BJ, Yan R, Yang F, Waters D, Liebig HD, et al. (1993) Mapping the cleavage site in protein synthesis initiation factor eIF-4 gamma of the 2A proteases from human Coxsackievirus and rhinovirus. J Biol Chem 268: 19200-19203.

28. Wong J, Zhang J, Yanagawa B, Luo Z, Yang X, et al. Cleavage of serum response factor mediated by enteroviral protease 2A contributes to impaired cardiac function. Cell Res.

29. Warner LE, DelloRusso C, Crawford RW, Rybakova IN, Patel JR, et al. (2002) Expression of Dp260 in muscle tethers the actin cytoskeleton to the dystrophin-glycoprotein complex and partially prevents dystrophy. Hum Mol Genet 11: 1095-1105.

30. Cox GA, Sunada Y, Campbell KP, Chamberlain JS (1994) Dp71 can restore the dystrophin-associated glycoprotein complex in muscle but fails to prevent dystrophy. Nat Genet 8: 333-339.

31. Greenberg DS, Sunada Y, Campbell KP, Yaffe D, Nudel U (1994) Exogenous Dp71 restores the levels of dystrophin associated proteins but does not alleviate muscle damage in mdx mice. Nat Genet 8: 340-344.

32. Judge LM, Haraguchiln M, Chamberlain JS (2006) Dissecting the signaling and mechanical functions of the dystrophin-glycoprotein complex. J Cell Sci 119: 1537-1546.

33. Wieneke S, Heimann P, Leibovitz S, Nudel U, Jockusch H (2003) Acute pathophysiological effects of muscle-expressed Dp71 transgene on normal and dystrophic mouse muscle. J Appl Physiol 95: 1861-1866.

34. Leibovitz S, Meshorer A, Fridman Y, Wieneke S, Jockusch H, et al. (2002) Exogenous Dp71 is a dominant negative competitor of dystrophin in skeletal muscle. Neuromuscul Disord 12: 836-844.

35. Subramaniam A, Jones WK, Gulick J, Wert S, Neumann J, et al. (1991) Tissue-specific regulation of the alpha-myosin heavy chain gene promoter in transgenic mice. J Biol Chem 266: 24613-24620.

36. Bunnell TM, Jaeger MA, Fitzsimons DP, Prins KW, Ervasti JM (2008) Destabilization of the dystrophin-glycoprotein complex without functional deficits in alpha-dystrobrevin null muscle. PLoS One 3: e2604.

37. Townsend D, Blankinship MJ, Allen JM, Gregorevic P, Chamberlain JS, et al. (2007) Systemic administration of micro-dystrophin restores cardiac geometry and prevents dobutamine-induced cardiac pump failure. Mol Ther 15: 1086-1092.

38. Bostick B, Yue Y, Long C, Marschalk N, Fine DM, et al. (2009) Cardiac expression of a mini-dystrophin that normalizes skeletal muscle force only partially restores heart function in aged Mdx mice. Mol Ther 17: 253-261.

39. Day SM, Westfall MV, Fomicheva EV, Hoyer K, Yasuda S, et al. (2006) Histidine button engineered into cardiac troponin I protects the ischemic and failing heart. Nat Med 12: 181-189.

40. Hemmings L, Kuhlman PA, Critchley DR (1992) Analysis of the actin-binding domain of alpha-actinin by mutagenesis and demonstration that dystrophin contains a functionally homologous domain. J Cell Biol 116: 1369-1380.

41. Amann KJ, Renley BA, Ervasti JM (1998) A cluster of basic repeats in the dystrophin rod domain binds F-actin through an electrostatic interaction. J Biol Chem 273: 28419-28423.

42. Henderson DM, Lee A, Ervasti JM Disease-causing missense mutations in actin binding domain 1 of dystrophin induce thermodynamic instability and protein aggregation. Proc Natl Acad Sci U S A 107: 9632-9637.

43. Rybakova IN, Humston JL, Sonnemann KJ, Ervasti JM (2006) Dystrophin and utrophin bind actin through distinct modes of contact. J Biol Chem 281: 9996-10001.

44. Rybakova IN, Amann KJ, Ervasti JM (1996) A new model for the interaction of dystrophin with F-actin. J Cell Biol 135: 661-672.

45. Albesa M, Ogrodnik J, Rougier JS, Abriel H Regulation of the cardiac sodium channel Nav1.5 by utrophin in dystrophin-deficient mice. Cardiovasc Res 89: 320-328.

46. Heydemann A, Demonbreun A, Hadhazy M, Earley JU, McNally EM (2007) Nuclear sequestration of delta-sarcoglycan disrupts the nuclear

localization of lamin A/C and emerin in cardiomyocytes. Hum Mol Genet 16: 355-363.

47. Imamura M, Mochizuki Y, Engvall E, Takeda S (2005) Epsilon-sarcoglycan compensates for lack of alpha-sarcoglycan in a mouse model of limb-girdle muscular dystrophy. Hum Mol Genet 14: 775-783.

48. Rafael JA, Cox GA, Corrado K, Jung D, Campbell KP, et al. (1996) Forced expression of dystrophin deletion constructs reveals structure-function correlations. J Cell Biol 134: 93-102.

49. DeWolf C, McCauley P, Sikorski AF, Winlove CP, Bailey AI, et al. (1997) Interaction of dystrophin fragments with model membranes. Biophys J 72: 2599-2604.

50. Pederson T, Aebi U (2002) Actin in the nucleus: what form and what for? J Struct Biol 140: 3-9.

51. Gardner KL, Kearney JA, Edwards JD, Rafael-Fortney JA (2006) Restoration of all dystrophin protein interactions by functional domains in trans does not rescue dystrophy. Gene Ther 13: 744-751.

Chapter 5

Discussion

In this dissertation I have made significant new findings regarding the role of dystrophin in the heart. Specifically, I have carried out studies characterizing novel mechanisms by which loss of functional dystrophin in the heart causes disease in DMD and non-inherited heart diseases. Summarized below are the major findings of these studies and their relevance to the field.

Summary of significant results

Inbred mouse strains show significant divergence in cardiac function. Inbred mouse strains are extremely common in modern biomedical research. The genetic homogeneity of these mice allows for exquisite control and reproducibility experiments. However, because many different strains of inbred mouse are commonly used (over 450 inbred mouse strains have been described), comparing studies in which different inbred strains have been utilized can be challenging. Numerous previous reports have shown that inbred strains show significant divergence in various measures of physiological function. In chapter 2, I have described strain-specific differences in cardiac function of

several commonly used inbred mouse strains using 2 commonly utilized techniques: the *ex vivo* perfused heart preparation and *in vivo* hemodynamic analysis using conductance micromanometry. I assessed cardiac performance using these techniques at baseline and during physiologically relevant stress and found significant divergence between enormous inbred strains. These differences were not consistent between the *ex vivo* and *in vivo* techniques, suggesting that researchers should consider both the strain of inbred mice and the technique used to assess function when designing experiments. Additionally, the findings of this study shed light on the mild dystrophic phenotype of mdx mice when compared to DMD patients. Mdx mice are bred onto the C57BL/10SnJ genetic background, which showed no marked resistance to cardiac stress and injury compared to other common inbred strains. This suggests that the mild phenotype of mdx mice is not due genetic background effects and is more likely caused by fundamental physiologically difference between mice and humans. Upregulation of utrophin, which has not been convincingly shown to occur in humans, is commonly believed to contribute to the mild phenotype of mdx mice [1,2,3]. More recently, loss of function mutations of CMAH in humans have also been identified which worsen dystrophy when knocked into the counterpart mouse locus [4].

The DGC is a critical determinant of whole-organ cardiac compliance. Previously, our lab and others have demonstrated that mechanical instability of the sarcolemma is a primary cellular defect in DMD [5]. Additionally, our lab has

previously shown that instability of the membrane causes reduced mechanical compliance in isolated cardiac myocytes through aberrant influx of calcium across the sarcolemma [5]. To expand upon and translate these findings from single cells to whole organs, I subjected isolated dystrophin-deficient (mdx) hearts to whole-organ stretch *ex vivo*. Unexpectedly, I found that mdx hearts show increased whole-organ compliance compared to normal hearts as shown by blunted increases in LVEDP as LV volume increases above 8 mmHg. In previous studies, influx of extracellular calcium through sarcolemmal "micro-tears" was identified as a key moderator of increased single cell compliance in isolated mdx myocytes, which could be rescued using the membrane sealant poloxamer 188 (P188) [5]. To determine the role of membrane damage and extracellular calcium influx on the increased compliance observed in isolated mdx hearts, whole-organ compliance was determined at varying perfusate calcium concentrations and in the presence of P188. From these studies I found that the increased whole-organ compliance of mdx hearts was independent of perfusate calcium concentration and was not affected by perfusion with P188. I also found that increased whole-organ compliance in isolated hearts was not associated with greater excursions in sarcomere length of mdx hearts. This suggests that the determinants of whole-organ compliance are not a simple extrapolation of findings in single cells.

Based upon these findings, I proposed a novel model for ventricular dilation in the dystrophin-deficient heart through side-to-side translation, or slippage, of myocytes past each other during mechanical distention. In this

model, slippage is caused by disruption of the DGC-mediated linkage between cardiac myocytes and the extracellular matrix. Additional studies in other genetic models of dystrophy showed similar findings in models where the DGC or its extracellular binding partner laminin were disrupted, suggesting that alterations in cell-extracellular matrix contacts may be a common mechanism for pathological left ventricular dilation in multiple forms of muscular dystrophy. Mice lacking the membrane repair protein dysferlin showed normal compliance. These findings are consistent with the proposed model of enhanced myocardial compliance caused by myocyte slippage and suggest that the mechanical linkage provided by the DGC is a crucial determinant of the whole-organ mechanical properties of the heart.

These findings provide insight into a novel mechanism of heart disease in muscular dystrophy. Many forms of muscular dystrophy are associated with cardiomyopathy with some showing increased propensity to develop DCM. Since many muscular dystrophies are hypothesized to be caused by fundamental defects in mechanical membrane stability, it unclear why certain dystrophies cause DCM at a higher rate than others. Here, I suggest a novel mechanism for the pathological dilation of the ventricular during dystrophy through disruption of the DGC. Clinical data support this hypothesis, as mutations in dystrophin, laminin-α_2, and β-sarcoglycan frequently cause dilated cardiomyopathy whereas mutations in dysferlin do not [6,7,8,9,10,11]. This provides strong evidence that the measurements made in Chapter 3 provide direct insight into the mechanisms of pathological LV dilation. With regard to alternative mechanisms for the

reduced compliance observed in dystrophic hearts, dystrophy often causes fibrosis within the myocardium which may alter passive compliance. However, previous reports have shown that enhanced cardiac collagen content, as observed in the tight-skin mouse, does not alter the passive compliance of the myocardium [12]. Additionally, studies in our lab have shown that individual, membrane-permeabilized cardiac myocytes from mdx mice show no differences in passive compliance, suggesting that altered compliance is not caused by the sarcomeric protein titin [13].

C-terminal product of 2A^{pro}-mediated dystrophin cleavage is sufficient to cause dystrophic cardiomyopathy. As described in Chapters 1 and 4 of this thesis, cardiac enterovirus infection is a clinically relevant disease process which is involved in both acute and chronic cardiac dysfunction [14,15,16,17,18,19]. The precise mechanisms by which enterovirus infection causes cardiomyopathy are still being investigated. Previously, it has been shown that 2A^{pro}, a protease expressed by enteroviruses, cleaves dystrophin within the hinge 3 domain [20,21]. The putative C-terminal product of 2A^{pro}-mediated cleavage of dystrophin is structurally similar to some naturally occurring non-muscle isoforms of dystrophin, including Dp71 and Dp116 [22,23]. These proteins contain dystrophin's dystroglycan-binding domains, but lack its actin-binding domains. Previously, it has been shown that expression of these short isoforms of dystrophin cause dystrophic myopathy when transgenically expressed in normal skeletal muscle [24,25,26,27]. These studies suggested that the short isoforms

of dystrophin act as a dominant negative to full-length dystrophin, competing for incorporation into the DGC at the sarcolemma and essentially replacing dystrophin with a less functional protein. Based on these findings, I hypothesized that the C-terminal product of dystrophin cleavage by $2A^{pro}$ would act in a similar dominant negative fashion in the heart and cause dystrophic cardiomyopathy. To test this hypothesis, I created transgenic mice which transgenically express the putative C-terminal fragment of dystrophin cleavage by $2A^{pro}$.

The C-terminal dystrophin transgene (CtermDys) localized to the sarcolemma, as shown by immunofluorescence, and the CtermDys protein can also be purified with integral and peripheral membrane proteins, including the DGC. Expression of the CtermDys transgene causes a 70% reduction in expression of full-length dystrophin at the membrane. Additionally, expression of CtermDys causes a ~5-10 fold increase in expression of other DGC proteins. The elevation in DGC proteins above normal levels in CtermDys transgenic mice suggests that the content of dystrophin is the rate-limiting step in incorporation of DGC complexes into the sarcolemma. Collectively, these findings support the hypothesis that CtermDys exerts a dominant negative effect on DGC function. It is not currently clear whether CtermDys competes directly with dystrophin for binding to β-dystroglycan at the already formed DGC or if the CtermDys-DGC competes with native DGC for residency at the sarcolemma.

Since enterovirus infection has been associated with dilated cardiomyopathy and increased susceptibility to death following acute myocardial infarction at a very high rate (20-40%), I tested the response of CtermDys

transgenic mice to ischemic injury using an *ex vivo* ischemia and reperfusion injury. Expression of the CtermDys transgene is sufficient to cause increased susceptibility to ischemic injury. Since the putative products of dystrophin cleavage by $2A^{pro}$ have been observed following cardiac enterovirus infection [20], this is a clinically relevant finding suggesting that loss of functional dystrophin through $2A^{pro}$ cleavage contributes to heightened risk of cardiac dysfunction following ischemic injury.

The N-terminal product of $2A^{pro}$-mediated dystrophin cleavage (NtermDys) does not contain the DGC binding domain of dystrophin and thus was not predicted to interact with the DGC or cause dystrophic cardiomyopathy. However, previous reports have shown that modified dystrophin proteins which lack its dystroglycan-binding domains still localize to the sarcolemma, but do not correct muscular dystrophy when expressed in dystrophin deficient muscle [28,29,30]. The localization of these proteins at the sarcolemma in the absence of dystroglycan binding is hypothesized to be due to direct interactions between dystrophin and membrane phospholipids [31]. In agreement with these previous results, I found that the NtermDys protein localized to the sarcolemma and was found in the membrane fraction. However, unlike CtermDys, expression of NtermDys did not affect expression of dystrophin or other DGC proteins. Curiously, the NtermDys protein also trafficked to the nucleus through mechanisms which are not clear but may involve its actin binding activity.

NtermDys transgenic mice did not show dystrophic cardiomyopathy as shown by normal EBD uptake. This is in agreement with our hypothesis that

expression of a truncated dystrophin protein does not, per se, cause cardiomyopathy. However, as in the case of the CtermDys transgenic mice, truncated dystrophin proteins that can bind β-dystroglycan have the potential to cause dystrophic cardiomyopathy if they also lack actin binding function.

Since cleavage of dystrophin by $2A^{pro}$ during enterovirus infection causes the creation of both N- and C-terminal cleavage products, I crossed CtermDys and NtermDys mice together to generate double transgenic mice. These mice showed dystrophic cardiomyopathy as shown by increased EBD uptake which was similar to both mdx and CtermDys mice. This supports my hypothesis that expression of the CtermDys protein causes dystrophic cardiomyopathy which is not contributed to by the NtermDys protein.

In addition to studying the effects of the CtermDys and NtermDys proteins on the normal myocardium, I also crossed these transgenic mice onto the dystrophin-deficient mdx mouse line. Although these studies do not have direct relevance to the cardiomyopathy of cardiac enterovirus infection, no previous studies have expressed truncated dystrophin fragments structurally similar to the NtermDys and CtermDys transgenes in the heart. Therefore, crossing these lines onto the mdx background provides insight into the structural basis for dystrophin function in the heart. This information could then be used in the design of truncated, functional dystrophin isoforms for delivery and treatment of DMD

CtermDys mice crossed onto an mdx background (CtermDys(mdx)) showed membrane instability as shown by increased EBD uptake. The level of

EBD uptake was higher than non-transgenic, but similar to mdx mice. Additionally, CtermDys(mdx) hearts showed impaired recovery of function following *ex vivo* ischemic injury compared to wild-type mice, but were similar to mdx hearts. These results suggest that the CtermDys protein does not act as a dominant negative to utrophin by competing for occupancy the DGC. Additionally, since CtermDys(mdx) mice show a similar phenotype to mdx mice despite increased expression of DGC proteins at the sarcolemma, this provides further evidence that the non-mechanical function of dystrophin plays a relatively minor role in the prevention of dystrophy and maintenance of heart function.

NtermDys(mdx) mice showed dystrophic cardiomyopathy as shown by increased EBD which was significantly greater than wild-type mice but equivalent to mdx mice. This finding is in agreement with our hypothesis that the NtermDys protein does not affect membrane stability.

Future directions

Investigating the mechanisms of pathological LV dilation in muscular dystrophy. As discussed above, I have proposed a novel mechanism for the pathological dilation of the LV in some forms of muscular dystrophy. Specifically, in this thesis I have shown increased compliance of the dystrophin-deficient myocardium which when correlated with our measurements of sarcomere length suggest that changes in sarcomere length do not track with changes in LV volume. Using these data I hypothesized that disruption of the DGC causes myocytes to translate or "slip" past each other, providing a mechanism by which

greater excursions in LV volume occur without greater changes in LV volume of mdx hearts. However, sarcomere length was not measured directly during stretch due to technical limitations. Instead, hearts were pressure-clamped at given LV pressures, fixed and sectioned for the measurement of sarcomere length by immunofluorescence. Although the data generated support this model of LV dilation, it has not been shown ***directly*** that mechanical stretch causes slippage of cardiac myocytes past each other to a greater degree in the dystrophin-deficient myocardium. Currently, the technical capability exists to carry out experiments to answer this question. Specifically, applying mechanical stretch to isolated trabeculae while visualizing sarcomeres utilizing confocal microscopy would allow for direct visualization of adjacent myocytes during stretch. From these recordings, the contribution of myocyte slippage during mechanical stretch of the myocardium could be determined. Carrying out this experiment on wild-type and mdx trabeculae would provide invaluable data to directly determine if myocyte slippage is enhanced in the absence of dystrophin.

Although previous reports have shown that mdx mice show no evidence of enhanced fibrosis in the myocardium at the ages tested in Chapter 3 [32], we cannot exclude that alteration in the micro- or macrostructure of collagen within the extracellular matrix did not contribute to the enhanced compliance of isolated dystrophic hearts. To directly probe the mechanical properties of the exctracellular matrix, I propose to decellularize the heart using SDS as previously described by Ott and colleagues [33]. The decellularized matrix lacks all cells but retains extracellular collagen [33]. Performing a stress-strain analysis will then

determine if alterations in collagen may contribute to altered compliance of dystrophic hearts.

Determination of whole-organ compliance in other genetic models of DCM. As discussed above, chapter 3 of this thesis characterizes whole-organ cardiac compliance in various genetic models of muscular dystrophy. From these data, I hypothesized that cell-cell slippage of cardiac myocytes contributes to the pathological dilation of the LV that occurs in many forms of muscular dystrophy. The common mechanistic link between increased whole-organ compliance and LV dilation is disruption of the DGC or other proteins which facilitate cell-extracellular matrix linkages. However, not all forms of DCM are caused by mutations which directly affect cell-extracellular matrix interactions. For instance, it has previously been shown that DCM can be caused by mutations in sarcomeric proteins, specifically cardiac troponin I, cardiac troponin C, cardiac troponin T, and α-tropomyosin [34,35,36,37,38]. Since sarcomeric proteins are not directly involved in cell-extracellular matrix contacts, I do not expect them to show enhanced slippage. If this is the case, these studies would still be of value in identifying divergent mechanisms for the development of DCM. However, a finding of similar changes in whole-organ compliance between dystrophic and sarcomeric mutant hearts could reveal myocyte slippage to be a potential common pathway for the development of DCM in numerous disease states. To determine if myocyte slippage contributes to LV dilation in these mice, I propose that similar studies to those described in Chapter 3 be carried out on transgenic mice that express these sarcomeric DCM proteins to determine

whole-organ cardiac compliance and to track sarcomere length during whole-organ stretch. At least one transgenic mouse expressing a sarcomeric DCM mutant protein exists [39].

Investigating the mechanisms of cardiomyopathy caused by enterovirus infection. As discussed in the first chapter, a significant body of research suggests that enterovirus infection causes cardiomyopathy through cleavage of dystrophin by $2A^{pro}$. Specifically, previous studies have shown that enterovirus infection causes fragmentation of dystrophin *in vitro* and *in vivo* [20,21]. Dystrophin was identified as a substrate for $2A^{pro}$, providing a mechanistic explanation for its cleavage [20] with further studies identifying the putative site within the hinge 3 domain [21]. Additionally, expression of the entire coxsackievirus genome or the $2A^{pro}$ gene alone causes cardiomyopathy [40,41]. However, it should be mentioned that although it is clear that expression $2A^{pro}$ causes cardiomyopathy, it is not totally clear whether this is due to cleavage of dystrophin. In the study referenced above by Xiong et al, transgenic expression of $2A^{pro}$ causes cardiomyopathy, but no evidence of dystrophin cleavage (by Western blot) was shown [40]. Additionally, the authors assert that expression of $2A^{pro}$ causes dystrophic cardiomyopathy as shown by increased Evans blue dye uptake [40]. However, the data published shows only a handful of cardiac myocytes by immunofluorescence and it should be noted when interpreting this data that $2A^{pro}$ cleaves numerous substrates which are essential to cell function [42,43,44]. Collectively, these results highlight a gap in knowledge regarding the

cleavage of dystrophin by $2A^{pro}$ and its effects on cardiac function during enterovirus. Specifically, although dystrophin fragmentation occurs following enterovirus infection and $2A^{pro}$ cleaves dystrophin *in vitro*, evidence of dystrophin cleavage has not been observed following expression of $2A^{pro}$ *in vivo*. Although the reason for this obvious omission is not clear, I speculate that prolonged inhibition of protein translation through $2A^{pro}$-mediated cleavage of eIF4-G precludes detection of dystrophin and its cleavage products. In previous *in vivo* studies of $2A^{pro}$ activity, the protease is expressed for days or weeks prior to tissue harvest which may have led to loss of dystrophin through inhibition of protein translation rather than proteolytic cleavage [40,41]. To "catch" the cleavage of dystrophin by 2Apro before wholesale inhibition of protein translation precludes its detection, I propose studies involving acute treatment of isolated hearts with recombinant $2A^{pro}$ conjugated to the TAT cell penetrating peptide to avoid long-term suppression of translation. Previously, it has been shown that proteins conjugated to TAT are effectively able to cross the cell membrane and incorporate into the cytoplasm [45]. This study would allow for enhanced temporal control of dystrophin cleavage by $2A^{pro}$ and could potentially document, for the first time, the presence of the putative products of $2A^{pro}$-mediated cleavage of dystrophin in intact cardiac myocytes.

The pathogenesis of enterovirus infection is a complex process caused by the detrimental functions of the viral proteins expressed during viral replication [46]. An aim of this thesis is to determine the contribution of dystrophin cleavage by $2A^{pro}$ to the pathogenesis of enterovirus infection. In Chapter 4, I have shown

that expression of the CtermDys protein is sufficient to cause cardiomyopathy when transgenically expressed. However, because $2A^{pro}$ cleaves numerous host substrates, the **specific** effect of dystrophin cleavage (distinguished from the effects of $2A^{pro}$ cleaving other substrates) in the pathogenesis of cardiac enterovirus expression is not clear. To determine the specific effects of dystrophin cleavage on the pathogenesis of enterovirus infection, I propose studies involving transgenic expression of a $2A^{pro}$-resistant micro-dystrophin during enterovirus infection. Specifically, I propose to create transgenic mice expressing either normal hinge 3 microdystrophin or a modified hinge 3 microdystrophin containing a point mutation within the hinge 3 domain which has previously been shown to confer resistance to $2A^{pro}$ cleavage [21]. These mice would be crossed on an mdx background then infected with enterovirus as previously described [20] or could be delivered $2A^{pro}$ by AAV-mediated gene transfer [47]. If the transgenic mice expressing $2A^{pro}$-resistant microdystrophin show improved cardiac function following enterovirus infection or $2A^{pro}$ expression, this will show for the first time the specific role of dystrophin cleavage by $2A^{pro}$ in the pathogenesis of enterovirus infection in the heart.

Determining the requirement for dystrophin in the heart. Currently, there is a significant gap in knowledge regarding the level of dystrophin required to prevent dystrophy in skeletal and cardiac muscle. Previous reports suggests that ~30% of normal dystrophin can protect skeletal muscle from dystrophy [48,49]. However, a more thorough study aimed at titrating in dystrophin to striated

muscle would help to clearly define the quantitative need for dystrophin and inform therapeutic goals for treatment of DMD. This could be accomplished through several different approaches. Previously, a group led by Dr. George Dickson created a short hairpin RNA (shRNA) construct which, when packaged into an adeno-associated virus (AAV) vector, is capable of knocking down dystrophin expression in skeletal muscle [50]. By delivering this vector to the heart using recombinant AAV as previously described [47,50], it would be possible to monitor dystrophin expression and the development of sarcolemmal instability (believed to be the fundamental defect in DMD) as dystrophin expression wanes. I have acquired this reagent from Dr. Dickson and attempted *in vivo* gene knockdown of dystrophin. However, my attempts were not successful due to technical problems in generating effective AAV vectors. Experiments are ongoing to make a second attempt at *in vivo* knockdown of dystrophin. Alternatively, titrating dystrophin expression in the heart could be achieved through the use of transgenic mice expressing dystrophin by inducible promoters. Using this approach, transgenic expression of dystrophin could be controlled using an inducible promoter such as the tetracycline-inducible promoter or the thyroid-responsive and cardiac-specific alpha myosin heavy chain promoter. Treatment with 6-propyl 2-thiouracil has been shown to suppress expression from the alpha myosin heavy chain promoter and could be used to suppress transgene expression [51].

Assessing the non-mechanical function of dystrophin in the heart. As cited above, it has previously been shown that the non-muscle dystrophin isoform Dp116 exacerbates the dystrophic phenotype in skeletal muscle of mdx mice by exerting a dominant negative effect on the utrophin-glycoprotein complex present in mdx skeletal muscle [24]. However, a more recent study has shown that Dp116 can increase lifespan and improve histological signs of muscle wasting in skeletal muscle of dystrophin/utrophin double knockout (DKO) mouse [52]. This suggests that despite the inability of Dp116 to mechanically tether actin and β-dystroglycan, the signaling/scaffolding functions of dystrophin play a modest, yet significant role in maintaining the viability and function of skeletal muscle. The mechanism of dystrophin's non-mechanical function may be related to its role in localizing numerous functionally significant proteins to the sarcolemma, including nNOS, diacylglycerol kinase-ζ, sodium channels, and TRPC channels [53,54,55,56,57,58]. The individual contributions each of these proteins hasn't been defined in most cases. However, nNOS has been shown to play an important role in regulating vasoconstriction and blood flow to striated muscle during exercise [59]. The CtermDys transgene is structurally very similar to Dp116 and although its expression does not improve the phenotype of CtermDys(mdx) mice, it is possible that compensatory utrophin expression may be concealing some potentially beneficial effects of CtermDys expression. Therefore, I propose to cross the CtermDys transgene onto a dystrophin/utrophin double knockout background to determine if the non-mechanical functions of dystrophin improve cardiac function in a physiologically meaningful way.

Effects of altering gap junction conductance on DMD cardiomyopathy. As shown by myself in Chapter 4 and others [60], membrane instability in mdx hearts, as shown by EBD intake, occurs in focal lesions. The reasons for this pattern of membrane instability are not clear, but have been hypothesized to occur through disruption of the myocardium entirely through regional mechanical stress. Alternatively, it has been hypothesized that these focal lesions arise due to pathological extracellular calcium influx which is propagated to neighboring myocytes via gap junctions. Previously, our lab has shown that membrane instability of isolated dystrophin-deficient cardiac myocytes predisposes them to catastrophic influx of extracellular calcium [5]. Normally, ionic conductance at gap junctions aids in propagating action potentials and synchronizing contraction of the myocardium. However, in the dystrophin-deficient heart pathological calcium influx due to membrane instability may be propagated via gap junctions to neighboring cells and cause membrane instability in many more myocytes through mechanical stress brought on by calcium-induced hypercontracture. In this model the initiating event is mechanical disruption of the membrane, but the propagation of myocardial damage occurs via conductance of calcium through gap junctions. Therefore, limiting conductance through gap junctions may improve membrane stability in the dystrophic heart. The central ion channel present in the gap junctions of cardiac myocytes is connexin43. Connexin43-null mice are neonatal-lethal, but mice heterozygous for the knockout allele are viable, grossly indistinguishable from wild-type mice, and express ~50% of

normal connexin43 in the ventricles (expression of connexin40 and connexin45 are unchanged in these mice) [61,62]. Although there is some controversy regarding the phenotype of connexin43 heterozygous mice, numerous reports have shown reduced conduction velocity in these mice [61,62,63,64]. Therefore, I propose crossing connexin43 heterozygous mice onto the dystrophin-deficient mdx background with the hypothesis that reduced conduction of calcium in gap junctions of connexin43 heterozygous(mdx) mice will reduce the size, but not the number, of EBD-positive lesions by inhibiting the spread of calcium from damaged cells to their neighbors. The therapeutic value of these studies is questionable, since altering connexin43 content in the myocardium may be arrythmogenic. However, from a basic science perspective, this study has the potential to enhance understanding the physiological processes by which loss of dystrophin causes focal membrane instability in the heart and ultimately leads to cardiomyopathy.

DMD-floxed exon mice to explore tissue-specific effects of dystrophin function. Genetically modified mice have changed the way modern research is carried out. These model organisms have permeated every field of biomedical research and allow for the study of individual genes in complex biological systems. The development of inducible and tissue specific-promoter elements have allowed for further control of gene expression in genetically modified mice. This has been exploited thoroughly through the creation tissue-specific and inducible Cre recombinase expressing mice. The Jackson Lab alone maintains

300 distinct Cre-expressing lines (http://jaxmice.jax.org/). Investigators have exploited this technology thoroughly by using these Cre mice to modify gene expression in a spatio-temporal manner [65]. Despite the prevalence of this technology, it has not been applied with any vigor to the study of dystrophin and other products of the DMD gene. Previously, a knockin mouse was created in which the entire DMD gene was floxed [66]. Our lab acquired these mice and I crossed them with multiple Cre-expressing lines [67,68] in an attempt to achieve efficient excision of the DMD gene *in vivo*. I found that *in vivo* excision of the DMD gene was extremely inefficient, presumably due to the large size of the DMD gene. The lack of an effective conditional-null model for products of the DMD gene is a gaping gap in the field. I propose the creation of a knockin mouse harboring loxP sites around a rationally chosen exon of the DMD gene. This mouse would allow for spatio-temporal knockout of DMD gene expression dictated by Cre recombinase activity. Choosing the appropriate exon is obviously crucial to the success of this mouse model, since not all exon deletions result in frameshift mutations and because compensatory splicing has been observed to avert or lessen disease caused by mutations in the DMD gene [69]. Exon 66 is a suitable candidate exon to excise using this model. Exon 66 is 86 base pairs which, based on previous studies [67], should allow for high efficiency Cre-mediated recombination *in vivo.* Deletion of exon 66 is predicted to cause a frameshift mutation leading to premature truncation of DMD proteins in the functionally crucial cysteine-rich domain. Deletion of exon 66 causes DMD in human patients [70,71], although it is not clear if disease is caused by total loss

of dystrophin or by rendering dystrophin non-functional. However, a similar mutation occurs in mdx^{3cv} mice, a DMD mouse model created by ENU mutagenesis [72,73,74]. Importantly, deletion of this exon is predicted to disrupt all isoforms of the DMD gene (Figure 1-1). However, the mdx^{3cv} mouse does express ~5% of normal dystrophin despite the nonsense mutation it harbors in the DMD gene, suggesting some ability for compensatory splicing of dystrophin which may also be interesting to study [73]. Interestingly, a previous report described DMD with severe mental retardation in patients from 2 discrete families with mutations resulting in skipping of exon 66 from the dystrophin transcript [71]. This suggests that mice with a floxed exon 66 may be used to study the neural aspects of DMD. Therefore, when used in combination with tissue-specific Cre-expressing mice this mouse could be used to study the functional effects of dystrophin expression in a range of different tissues. This has clinical relevance since DMD is often associated with mental retardation which has been linked to loss of the "short" dystrophin isoforms Dp71 and Dp140 [75]. Previous studies comparing mdx (which express Dp260, Dp140, and Dp71) and mdx^{3cv} mice found phenotypic differences in behavior between these two DMD mouse models, supporting the role of the short isoforms of dystrophin in physiological function of the brain [76]. However, these mice lack the temporal and tissue-specific control of dystrophin isoform expression required for more mechanistic studies of cognitive defects.

Collectively, a DMD-floxed-exon mouse along with modern Cre-expressing lines could be used to study the products of the DMD gene in ways

that are currently not possible. This mouse would be of great interest to researchers studying DMD, but also to others interested in dystrophin function in a broader sense.

Literature Cited

1. Pons F, Robert A, Fabbrizio E, Hugon G, Califano JC, et al. (1994) Utrophin localization in normal and dystrophin-deficient heart. Circulation 90: 369-374.

2. Nguyen TM, Ellis JM, Love DR, Davies KE, Gatter KC, et al. (1991) Localization of the DMDL gene-encoded dystrophin-related protein using a panel of nineteen monoclonal antibodies: presence at neuromuscular junctions, in the sarcolemma of dystrophic skeletal muscle, in vascular and other smooth muscles, and in proliferating brain cell lines. J Cell Biol 115: 1695-1700.

3. Mizuno Y, Nonaka I, Hirai S, Ozawa E (1993) Reciprocal expression of dystrophin and utrophin in muscles of Duchenne muscular dystrophy patients, female DMD-carriers and control subjects. J Neurol Sci 119: 43-52.

4. Chandrasekharan K, Yoon JH, Xu Y, deVries S, Camboni M, et al. A human-specific deletion in mouse Cmah increases disease severity in the mdx model of Duchenne muscular dystrophy. Sci Transl Med 2: 42ra54.

5. Yasuda S, Townsend D, Michele DE, Favre EG, Day SM, et al. (2005) Dystrophic heart failure blocked by membrane sealant poloxamer. Nature 436: 1025-1029.

6. Durbeej M, Cohn RD, Hrstka RF, Moore SA, Allamand V, et al. (2000) Disruption of the beta-sarcoglycan gene reveals pathogenetic complexity of limb-girdle muscular dystrophy type 2E. Mol Cell 5: 141-151.

7. Xu H, Wu XR, Wewer UM, Engvall E (1994) Murine muscular dystrophy caused by a mutation in the laminin alpha 2 (Lama2) gene. Nat Genet 8: 297-302.

8. Araishi K, Sasaoka T, Imamura M, Noguchi S, Hama H, et al. (1999) Loss of the sarcoglycan complex and sarcospan leads to muscular dystrophy in beta-sarcoglycan-deficient mice. Hum Mol Genet 8: 1589-1598.

9. Barresi R, Di Blasi C, Negri T, Brugnoni R, Vitali A, et al. (2000) Disruption of heart sarcoglycan complex and severe cardiomyopathy caused by beta sarcoglycan mutations. J Med Genet 37: 102-107.

10. Spyrou N, Philpot J, Foale R, Camici PG, Muntoni F (1998) Evidence of left ventricular dysfunction in children with merosin-deficient congenital muscular dystrophy. Am Heart J 136: 474-476.

11. Wenzel K, Geier C, Qadri F, Hubner N, Schulz H, et al. (2007) Dysfunction of dysferlin-deficient hearts. J Mol Med (Berl) 85: 1203-1214.

12. Omens JH, Rockman HA, Covell JW (1994) Passive ventricular mechanics in tight-skin mice. Am J Physiol 266: H1169-1176.

13. Townsend D, Turner I, Yasuda S, Martindale J, Davis J, et al. Chronic administration of membrane sealant prevents severe cardiac injury and ventricular dilatation in dystrophic dogs. J Clin Invest 120: 1140-1150.

14. Jin O, Sole MJ, Butany JW, Chia WK, McLaughlin PR, et al. (1990) Detection of enterovirus RNA in myocardial biopsies from patients with myocarditis and cardiomyopathy using gene amplification by polymerase chain reaction. Circulation 82: 8-16.

15. Andreoletti L, Venteo L, Douche-Aourik F, Canas F, Lorin de la Grandmaison G, et al. (2007) Active Coxsackieviral B infection is associated with disruption of dystrophin in endomyocardial tissue of patients who died suddenly of acute myocardial infarction. J Am Coll Cardiol 50: 2207-2214.

16. Bandt CM, Staley NA, Noren GR (1979) Acute viral myocarditis. Clinical and histologic changes. Minn Med 62: 234-237.

17. Archard LC, Khan MA, Soteriou BA, Zhang H, Why HJ, et al. (1998) Characterization of Coxsackie B virus RNA in myocardium from patients with dilated cardiomyopathy by nucleotide sequencing of reverse transcription-nested polymerase chain reaction products. Hum Pathol 29: 578-584.

18. Fujioka S, Koide H, Kitaura Y, Deguchi H, Kawamura K, et al. (1996) Molecular detection and differentiation of enteroviruses in endomyocardial biopsies and pericardial effusions from dilated cardiomyopathy and myocarditis. Am Heart J 131: 760-765.

19. Bowles NE, Richardson PJ, Olsen EG, Archard LC (1986) Detection of Coxsackie-B-virus-specific RNA sequences in myocardial biopsy samples from patients with myocarditis and dilated cardiomyopathy. Lancet 1: 1120-1123.

20. Badorff C, Lee GH, Lamphear BJ, Martone ME, Campbell KP, et al. (1999) Enteroviral protease 2A cleaves dystrophin: evidence of cytoskeletal disruption in an acquired cardiomyopathy. Nat Med 5: 320-326.

21. Badorff C, Berkely N, Mehrotra S, Talhouk JW, Rhoads RE, et al. (2000) Enteroviral protease 2A directly cleaves dystrophin and is inhibited by a dystrophin-based substrate analogue. J Biol Chem 275: 11191-11197.

22. Byers TJ, Lidov HG, Kunkel LM (1993) An alternative dystrophin transcript specific to peripheral nerve. Nat Genet 4: 77-81.

23. Bar S, Barnea E, Levy Z, Neuman S, Yaffe D, et al. (1990) A novel product of the Duchenne muscular dystrophy gene which greatly differs from the known isoforms in its structure and tissue distribution. Biochem J 272: 557-560.

24. Judge LM, Haraguchiln M, Chamberlain JS (2006) Dissecting the signaling and mechanical functions of the dystrophin-glycoprotein complex. J Cell Sci 119: 1537-1546.

25. Warner LE, DelloRusso C, Crawford RW, Rybakova IN, Patel JR, et al. (2002) Expression of Dp260 in muscle tethers the actin cytoskeleton to the dystrophin-glycoprotein complex and partially prevents dystrophy. Hum Mol Genet 11: 1095-1105.

26. Leibovitz S, Meshorer A, Fridman Y, Wieneke S, Jockusch H, et al. (2002) Exogenous Dp71 is a dominant negative competitor of dystrophin in skeletal muscle. Neuromuscul Disord 12: 836-844.

27. Wieneke S, Heimann P, Leibovitz S, Nudel U, Jockusch H (2003) Acute pathophysiological effects of muscle-expressed Dp71 transgene on normal and dystrophic mouse muscle. J Appl Physiol 95: 1861-1866.

28. Dunckley MG, Wells KE, Piper TA, Wells DJ, Dickson G (1994) Independent localization of dystrophin N- and C-terminal regions to the sarcolemma of mdx mouse myofibres in vivo. J Cell Sci 107 (Pt 6): 1469-1475.

29. Helliwell TR, Ellis JM, Mountford RC, Appleton RE, Morris GE (1992) A truncated dystrophin lacking the C-terminal domains is localized at the muscle membrane. Am J Hum Genet 50: 508-514.

30. Rafael JA, Cox GA, Corrado K, Jung D, Campbell KP, et al. (1996) Forced expression of dystrophin deletion constructs reveals structure-function correlations. J Cell Biol 134: 93-102.

31. DeWolf C, McCauley P, Sikorski AF, Winlove CP, Bailey AI, et al. (1997) Interaction of dystrophin fragments with model membranes. Biophys J 72: 2599-2604.

32. Van Erp C, Loch D, Laws N, Trebbin A, Hoey AJ Timeline of cardiac dystrophy in 3-18-month-old MDX mice. Muscle Nerve 42: 504-513.

33. Ott HC, Matthiesen TS, Goh SK, Black LD, Kren SM, et al. (2008) Perfusion-decellularized matrix: using nature's platform to engineer a bioartificial heart. Nat Med 14: 213-221.

34. Murphy RT, Mogensen J, Shaw A, Kubo T, Hughes S, et al. (2004) Novel mutation in cardiac troponin I in recessive idiopathic dilated cardiomyopathy. Lancet 363: 371-372.

35. Carballo S, Robinson P, Otway R, Fatkin D, Jongbloed JD, et al. (2009) Identification and functional characterization of cardiac troponin I as a novel disease gene in autosomal dominant dilated cardiomyopathy. Circ Res 105: 375-382.

36. Mirza M, Marston S, Willott R, Ashley C, Mogensen J, et al. (2005) Dilated cardiomyopathy mutations in three thin filament regulatory proteins result in a common functional phenotype. J Biol Chem 280: 28498-28506.

37. Li D, Czernuszewicz GZ, Gonzalez O, Tapscott T, Karibe A, et al. (2001) Novel cardiac troponin T mutation as a cause of familial dilated cardiomyopathy. Circulation 104: 2188-2193.

38. Morimoto S, Lu QW, Harada K, Takahashi-Yanaga F, Minakami R, et al. (2002) Ca(2+)-desensitizing effect of a deletion mutation Delta K210 in cardiac troponin T that causes familial dilated cardiomyopathy. Proc Natl Acad Sci U S A 99: 913-918.

39. Du CK, Morimoto S, Nishii K, Minakami R, Ohta M, et al. (2007) Knock-in mouse model of dilated cardiomyopathy caused by troponin mutation. Circ Res 101: 185-194.

40. Xiong D, Yajima T, Lim BK, Stenbit A, Dublin A, et al. (2007) Inducible cardiac-restricted expression of enteroviral protease 2A is sufficient to induce dilated cardiomyopathy. Circulation 115: 94-102.

41. Wessely R, Klingel K, Santana LF, Dalton N, Hongo M, et al. (1998) Transgenic expression of replication-restricted enteroviral genomes in heart muscle induces defective excitation-contraction coupling and dilated cardiomyopathy. J Clin Invest 102: 1444-1453.

42. Wong J, Zhang J, Yanagawa B, Luo Z, Yang X, et al. Cleavage of serum response factor mediated by enteroviral protease 2A contributes to impaired cardiac function. Cell Res.

43. Joachims M, Van Breugel PC, Lloyd RE (1999) Cleavage of poly(A)-binding protein by enterovirus proteases concurrent with inhibition of translation in vitro. J Virol 73: 718-727.

44. Lamphear BJ, Yan R, Yang F, Waters D, Liebig HD, et al. (1993) Mapping the cleavage site in protein synthesis initiation factor eIF-4 gamma of the 2A proteases from human Coxsackievirus and rhinovirus. J Biol Chem 268: 19200-19203.

45. Sonnemann KJ, Heun-Johnson H, Turner AJ, Baltgalvis KA, Lowe DA, et al. (2009) Functional substitution by TAT-utrophin in dystrophin-deficient mice. PLoS Med 6: e1000083.

46. Whitton JL, Cornell CT, Feuer R (2005) Host and virus determinants of picornavirus pathogenesis and tropism. Nat Rev Microbiol 3: 765-776.

47. Townsend D, Blankinship MJ, Allen JM, Gregorevic P, Chamberlain JS, et al. (2007) Systemic administration of micro-dystrophin restores cardiac geometry and prevents dobutamine-induced cardiac pump failure. Mol Ther 15: 1086-1092.

48. Ferlini A, Galie N, Merlini L, Sewry C, Branzi A, et al. (1998) A novel Alu-like element rearranged in the dystrophin gene causes a splicing mutation in a family with X-linked dilated cardiomyopathy. Am J Hum Genet 63: 436-446.

49. Neri M, Torelli S, Brown S, Ugo I, Sabatelli P, et al. (2007) Dystrophin levels as low as 30% are sufficient to avoid muscular dystrophy in the human. Neuromuscul Disord 17: 913-918.

50. Ghahramani Seno MM, Graham IR, Athanasopoulos T, Trollet C, Pohlschmidt M, et al. (2008) RNAi-mediated knockdown of dystrophin expression in adult mice does not lead to overt muscular dystrophy pathology. Hum Mol Genet 17: 2622-2632.

51. Ng WA, Grupp IL, Subramaniam A, Robbins J (1991) Cardiac myosin heavy chain mRNA expression and myocardial function in the mouse heart. Circ Res 68: 1742-1750.

52. Judge LM, Arnett AL, Banks GB, Chamberlain JS Expression of the dystrophin isoform Dp116 preserves functional muscle mass and extends lifespan without preventing dystrophy in severely dystrophic mice. Hum Mol Genet.

53. Adams ME, Mueller HA, Froehner SC (2001) In vivo requirement of the alpha-syntrophin PDZ domain for the sarcolemmal localization of nNOS and aquaporin-4. J Cell Biol 155: 113-122.

54. Gee SH, Madhavan R, Levinson SR, Caldwell JH, Sealock R, et al. (1998) Interaction of muscle and brain sodium channels with multiple members of the syntrophin family of dystrophin-associated proteins. J Neurosci 18: 128-137.

55. Brenman JE, Chao DS, Gee SH, McGee AW, Craven SE, et al. (1996) Interaction of nitric oxide synthase with the postsynaptic density protein PSD-95 and alpha1-syntrophin mediated by PDZ domains. Cell 84: 757-767.

56. Abramovici H, Hogan AB, Obagi C, Topham MK, Gee SH (2003) Diacylglycerol kinase-zeta localization in skeletal muscle is regulated by

phosphorylation and interaction with syntrophins. Mol Biol Cell 14: 4499-4511.

57. Hogan A, Shepherd L, Chabot J, Quenneville S, Prescott SM, et al. (2001) Interaction of gamma 1-syntrophin with diacylglycerol kinase-zeta. Regulation of nuclear localization by PDZ interactions. J Biol Chem 276: 26526-26533.

58. Kameya S, Miyagoe Y, Nonaka I, Ikemoto T, Endo M, et al. (1999) alpha1-syntrophin gene disruption results in the absence of neuronal-type nitric-oxide synthase at the sarcolemma but does not induce muscle degeneration. J Biol Chem 274: 2193-2200.

59. Kobayashi YM, Rader EP, Crawford RW, Iyengar NK, Thedens DR, et al. (2008) Sarcolemma-localized nNOS is required to maintain activity after mild exercise. Nature 456: 511-515.

60. Bostick B, Yue Y, Long C, Marschalk N, Fine DM, et al. (2009) Cardiac expression of a mini-dystrophin that normalizes skeletal muscle force only partially restores heart function in aged Mdx mice. Mol Ther 17: 253-261.

61. Guerrero PA, Schuessler RB, Davis LM, Beyer EC, Johnson CM, et al. (1997) Slow ventricular conduction in mice heterozygous for a connexin43 null mutation. J Clin Invest 99: 1991-1998.

62. Thomas SA, Schuessler RB, Berul CI, Beardslee MA, Beyer EC, et al. (1998) Disparate effects of deficient expression of connexin43 on atrial and ventricular conduction: evidence for chamber-specific molecular determinants of conduction. Circulation 97: 686-691.

63. Ya J, Erdtsieck-Ernste EB, de Boer PA, van Kempen MJ, Jongsma H, et al. (1998) Heart defects in connexin43-deficient mice. Circ Res 82: 360-366.

64. Kirchhoff S, Kim JS, Hagendorff A, Thonnissen E, Kruger O, et al. (2000) Abnormal cardiac conduction and morphogenesis in connexin40 and connexin43 double-deficient mice. Circ Res 87: 399-405.

65. Ryding AD, Sharp MG, Mullins JJ (2001) Conditional transgenic technologies. J Endocrinol 171: 1-14.

66. Kudoh H, Ikeda H, Kakitani M, Ueda A, Hayasaka M, et al. (2005) A new model mouse for Duchenne muscular dystrophy produced by 2.4 Mb deletion of dystrophin gene using Cre-loxP recombination system. Biochem Biophys Res Commun 328: 507-516.

67. Sohal DS, Nghiem M, Crackower MA, Witt SA, Kimball TR, et al. (2001) Temporally regulated and tissue-specific gene manipulations in the adult

and embryonic heart using a tamoxifen-inducible Cre protein. Circ Res 89: 20-25.

68. Bruning JC, Michael MD, Winnay JN, Hayashi T, Horsch D, et al. (1998) A muscle-specific insulin receptor knockout exhibits features of the metabolic syndrome of NIDDM without altering glucose tolerance. Mol Cell 2: 559-569.

69. Aartsma-Rus A, Van Deutekom JC, Fokkema IF, Van Ommen GJ, Den Dunnen JT (2006) Entries in the Leiden Duchenne muscular dystrophy mutation database: an overview of mutation types and paradoxical cases that confirm the reading-frame rule. Muscle Nerve 34: 135-144.

70. Tuffery-Giraud S, Beroud C, Leturcq F, Yaou RB, Hamroun D, et al. (2009) Genotype-phenotype analysis in 2,405 patients with a dystrophinopathy using the UMD-DMD database: a model of nationwide knowledgebase. Hum Mutat 30: 934-945.

71. Wibawa T, Takeshima Y, Mitsuyoshi I, Wada H, Surono A, et al. (2000) Complete skipping of exon 66 due to novel mutations of the dystrophin gene was identified in two Japanese families of Duchenne muscular dystrophy with severe mental retardation. Brain Dev 22: 107-112.

72. Chapman VM, Miller DR, Armstrong D, Caskey CT (1989) Recovery of induced mutations for X chromosome-linked muscular dystrophy in mice. Proc Natl Acad Sci U S A 86: 1292-1296.

73. Li D, Yue Y, Duan D Marginal level dystrophin expression improves clinical outcome in a strain of dystrophin/utrophin double knockout mice. PLoS One 5: e15286.

74. Cox GA, Phelps SF, Chapman VM, Chamberlain JS (1993) New mdx mutation disrupts expression of muscle and nonmuscle isoforms of dystrophin. Nat Genet 4: 87-93.

75. Taylor PJ, Betts GA, Maroulis S, Gilissen C, Pedersen RL, et al. Dystrophin gene mutation location and the risk of cognitive impairment in Duchenne muscular dystrophy. PLoS One 5: e8803.

76. Vaillend C, Ungerer A (1999) Behavioral characterization of mdx3cv mice deficient in C-terminal dystrophins. Neuromuscul Disord 9: 296-304.